MICROCOPY RESOLUTION TEST CHART

NATIONAL BUREAU OF STANDARDS-1963-A

NAVAL POSTGRADUATE SCHOOL
Monterey, California

THESIS

HEAT TRANSFER TO VERTICAL FLAT PLATES
IN A RECTANGULAR GAS-FLUIDIZED BED

by

David Carter Neily

June 1984

Thesis Advisor: P. F. Pucci

85 02 19 075

REPORT DOCUMENTATION PAGE		READ INSTRUCTIONS BEFORE COMPLETING FORM
1. REPORT NUMBER	2. GOVT ACCESSION NO.	3. RECIPIENT'S CATALOG NUMBER
4. TITLE (and Subtitle) Heat Transfer to Vertical Flat Plates in a Rectangular Gas-Fluidized Bed		5. TYPE OF REPORT & PERIOD COVERED Master's Thesis; June 1984
		6. PERFORMING ORG. REPORT NUMBER
7. AUTHOR(s) David Carter Neily		8. CONTRACT OR GRANT NUMBER(s)
9. PERFORMING ORGANIZATION NAME AND ADDRESS Naval Postgraduate School Monterey, California 93943		10. PROGRAM ELEMENT, PROJECT, TASK AREA & WORK UNIT NUMBERS
11. CONTROLLING OFFICE NAME AND ADDRESS Naval Postgraduate School Monterey, California 93943		12. REPORT DATE June 1984
		13. NUMBER OF PAGES 207
14. MONITORING AGENCY NAME & ADDRESS(if different from Controlling Office)		15. SECURITY CLASS. (of this report) Unclassified
		15a. DECLASSIFICATION/DOWNGRADING SCHEDULE

16. DISTRIBUTION STATEMENT (of this Report)

Approved for public release; distribution unlimited.

17. DISTRIBUTION STATEMENT (of the abstract entered in Block 20, if different from Report)

18. SUPPLEMENTARY NOTES

f-on next pg

19. KEY WORDS (Continue on reverse side if necessary and identify by block number)

Gas-fluidization,
Heat Transfer,
Flat Plate,
Thesis.

20. ABSTRACT (Continue on reverse side if necessary and identify by block number)

This experimental study was conducted at the Naval Postgraduate School to investigate the heat transfer characteristics of flat vertical plates in a rectangular gas-fluidized bed. The primary objective was to determine what effect variations in the bed width-to-height ratio had on heat transfer to the vertical flat plates forming the container walls. The experiment was conducted using a specially

heated and instrumented fluidized bed equipped with a movable side wall which permitted modification of the bed geometry. As the width of the bed was adjusted, the settled bed height was maintained at a constant level by the addition or removal of bed material.

A secondary objective of the study was to determine the effect of variations in the fluidization gas flow rate on heat transfer to the bed walls. Flow rates ranging from fixed bed fluidization to pneumatic conveying were studied.

Pressure drop measurements as well as visual observations were used to determine minimum fluidization flow rates for each configuration. Heat transfer coefficients were calculated for each flow rate and bed geometry using temperature data obtained from a computer controlled thermocouple network. In addition, a study was made of variations in wall temperature with changes in vertical position.

aspirator supplied key a code included. 2/5t page

Accession For		
NTIS GRA&I		☒
DTIC TAB		☐
Unannounced		☐
Justification		
By		
Distribution/		
Availability Codes		
Dist	Avail and/or Special	
A-1		

Heat Transfer to Vertical Flat Plates
in a Rectangular Gas-Fluidized Bed

by

David Carter Neily
Lieutenant, United States Navy
B.S., University of Colorado, 1975

Submitted in partial fulfillment of the
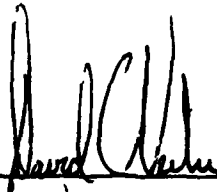requirements for the degree of

MASTER OF SCIENCE IN MECHANICAL ENGINEERING
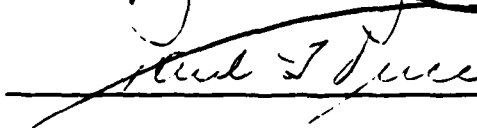
from the

NAVAL POSTGRADUATE SCHOOL
June 1984

Author: _____

Approved by: _____
                                              Thesis Advisor

_____
                                              Second Reader

_____
Chairman, Department of Mechanical Engineering

_____
           Dean of Science and Engineering

3

ABSTRACT

This experimental study was conducted at the Naval Post-graduate School to investigate the heat transfer characteristics of flat vertical plates in a rectangular gas-fluidized bed. The primary objective was to determine what effect variations in the bed width-to-height ratio had on heat transfer to the vertical flat plates forming the container walls. The experiment was conducted using a specially heated and instrumented fluidized bed equipped with a movable side wall which permitted modification of the bed geometry. As the width of the bed was adjusted, the settled bed height was maintained at a constant level by the addition or removal of bed material.

A secondary objective of the study was to determine the effect of variations in the fluidization gas flow rate on heat transfer to the bed walls. Flow rates ranging from fixed bed fluidization to pneumatic conveying were studied.

Pressure drop measurements as well as visual observations were used to determine minimum fluidization flow rates for each configuration. Heat transfer coefficients were calculated for each flow rate and bed geometry using temperature data obtained from a computer controlled thermocouple network. In addition, a study was made of variations in wall temperature with changes in vertical position.

4

TABLE OF CONTENTS

LIST OF TABLES

LIST OF FIGURES

9

10

NOMENCLATURE

ENGLISH LETTER SYMBOLS

A	Ammeter - Figure 19
A_b	Heater Wall Bottom Section Surface Area (in^2)
A_c	Copper Plate Surface Area (in^2)
A_d	Distributor Surface Area (in^2)
A_{fr}	Front/Rear Wall Surface Area (in^2)
A_i	Heater Insulation Surface Area (in^2)
A_{mb}	Heater Mounting Block Surface Area (in^2)
A_s	Heater Wall Side Section Surface Area (in^2)
A_t	Heater Wall Top Section Surface (in^2)
C_p	Specific Heat (Btu/Lbm-$^{\circ}$F)
D_p	Particle Diameter (in)
E	Heater Voltage (Volts)
G	Superficial Gas Mass Velocity (Lbm/Hr-Ft^2)
g_c	Proportionality Constant in Newton's Second Law of Motion (Lbm-Ft/Lbf-Sec^2)
G_{mf}	Superficial Mass Velocity at Minimum Fluidization (Lbm/Hr-Ft^2)
G_{opt}	Optimum Superficial Mass Velocity (Lbm/Hr-Ft^2)
H	Fluidized Bed Height (in)
h	Heat Transfer Coefficient (Btu/Hr-Ft^2-$^{\circ}$F).
h_{cb}	Heat Transfer Coefficient Copper Plate to Bed (Btu/Hr-Ft^2-$^{\circ}$F)
h_{max}	Maximum Heat Transfer Coefficient (Btu/Hr-Ft^2-$^{\circ}$F)

11

h_{mba} Heat Transfer Coefficient Heater Mounting Block to Atmosphere (Btu/Hr-Ft^2 -^{o}F)

H_e Expanded Bed Height (in)

I Heater Current (Amps)

k_c Thermal Conductivity of Copper Plate (Btu/Hr-Ft-^{o}F)

k_{fr} Thermal Conductivity of Front/Rear Walls (Btu/Hr-Ft-^{o}F)

k_i Thermal Conductivity of Heater Insulation (Btu/Hr-Ft-^{o}F)

k_{mb} Thermal Conductivity of Heater Mounting Block (Btu/Hr-Ft-^{o}F)

L_c Thickness of Copper Plate (in)

L_{fr} Thickness of Front/Rear Walls (in)

L_i Thickness of Heater Insulation (in)

L_{mb} Thickness of Heater Mounting Block (in)

$\dot{m}$ Air Mass Flow Rate (Lbm/Hr)

P_a Atmospheric Pressure (in. Hg absolute)

q_a Total Thermal Energy (Heat Flux) Losses to Atmosphere (Btu/Hr)

q_{ao} Thermal Energy Carried Out of Bed by Outgoing Airstream (Btu/Hr)

q_b Total Heat Flux Entering Bed from All Sources (Btu/Hr)

q_{ba} Thermal Energy Lost to Atmosphere from Wall Section Below Heater (Btu/Hr)

q_{bb} Thermal Energy Entering Bed from Wall Section Below Heater (Btu/Hr)

q_{br} Total Heat Flux Entering Bed from All Right Hand Sources (Btu/Hr)

q_{bl} Total Heat Flux Entering Bed from All Left Hand Sources (Btu/Hr)

12

q_{cb} Heat Flux into Bed from Copper Plate (Btu/Hr)

q_{fra} Thermal Energy Lost to Atmosphere through Front/ Rear Walls (Btu/Hr)

q_{ie} Electrical Energy into Heater (Btu/Hr)

q_o Total Heat Flux Leaving Bed (Btu/Hr)

q_{ob} Total Heat Flux into Bed from Sources Other than the Copper Plate (Btu/Hr)

q_{mb} Thermal Energy Lost through Heater Mounting Block (Btu/Hr)

q_{sa} Thermal Energy Lost to Atmosphere from Wall Sections Adjacent to Heater (Btu/Hr)

q_{sb} Thermal Energy Entering Bed from Wall Sections Adjacent to Heater (Btu/Hr)

q_{ta} Thermal Energy Lost to Atmosphere from Wall Section Above Heater (Btu/Hr)

q_{tb} Thermal Energy Entering Bed from Wall Section Above Heater (Btu/Hr)

$R(N)$ Average Heater Row Temperature (^{O}F) (N indicates row number)

R_e Particle Reynolds Number

R_{emf} Particle Reynolds Number at Minimum Fluidization

$T(N)$ Thermocouple Temperature Reading (^{O}F) (N indicates thermocouple number)

T_a Ambient Temperature (^{O}F)

T_{ai} Temperature of Air Entering Bed (^{O}F)

T_{ao} Temperature of Air Leaving Bed (^{O}F)

T_b Average Bed Temperature (^{O}F)

T_h Average Heater Temperature (^{O}F)

T_{mb} Average Temperature of Heater Mounting Block Outer Surface (^{O}F)

T_p Average Temperature of Copper Plate Outer Surface (^{O}F)

13

. U	Superficial Gas Velocity (Ft/Sec)
V	Voltmeter - Figure 19
V	Air Volumetric Flow Rate (Ft^3/Hr)
W	Bed Width (in.)
X	Highest Number Thermocouple Probe

GREEK LETTER SYMBOLS

ΔP	Pressure Drop
ΔP_{mf}	Pressure Drop at Minimum Fluidization
ε	Particle Voidage
ε_{mf}	Particle Voidage at Minimum Fluidization
μ	Dynamic Viscosity ($Lbf\text{-}Sec/Ft^3$)
ρ_a	Air Density (Lbm/Ft^3)
ρ_p	Particle Density (Lbm/Ft^3)

ACKNOWLEDGEMENT

I. INTRODUCTION

A fluidization bed in its simplest form consists of a container filled with small particles which are subjected to an upward flow of fluid emerging from the bottom of the container. When the upward viscous force (drag) exerted on the particles by the moving fluid balances or exceeds the downward force of gravity, the particles become suspended and begin to move about the container in a fluid-like manner, hence the term "fluidization." This churning mixture of particles and gas is often referred to as the "emulsion phase." When the velocity of the fluid is increased to the point that the particles are carried out of the container, a transition is made to a different form of fluidization known variously as pneumatic conveying, entrained flow fluidization, or carryover. When the velocity of the fluid is too low to counteract the gravitational force and cause fluidization, the bed is referred to as being "packed" or "fixed" and the process is known as flow through a porous medium or fixed bed fluidization.

Distinctly different modes of behavior are observed depending on whether the fluid passing through the container is a liquid or a gas. Liquid fluidized beds are often referred to as homogeneous or particulately fluidized beds. This type of bed tends to display a very smooth transition through the various stages of fluidization from fixed to fluidized to

16

carryover. Concurrently a very smooth transition in heat transfer characteristics and hydrodynamic behavior is observed. On the other hand, gas fluidized beds tend to display a more erratic performance. Most researchers attribute the difference in behavior to the differing particle to fluid density ratios. Gas fluidized beds are known as "aggregate" or "bubbling fluidized beds." In this type of bed, once fluidization has begun, the gas usually forms into bubbles which displace the bed particles as the bubbles rise. The appearance of a bubbling bed is remarkably similar to that of a boiling liquid, as shown in Figure 1. During conditions of very active fluidization the bubbles sometimes form together or coalesce to create a large bubble whose diameter approaches the width of the bed, as shown in Figure 2. This condition is known as "slugging" or "heaving" and can significantly effect bed performance. Another phenomenon of gas fluidized beds is shown in Figure 3. It is a condition known as "channelling." When this occurs, the gas travels through a fairly confined area forming a gas filled tube within the bed rather than passing evenly throughout the cross section. This behavior is believed to be caused by poor distributor design and, like slugging, can strongly effect the heat transfer characteristics of the bed.

Fluidized beds offer a wide variety of beneficial characteristics such as high rates of heat transfer, high thermal inertia, large solid to fluid contact area, and isothermal

17
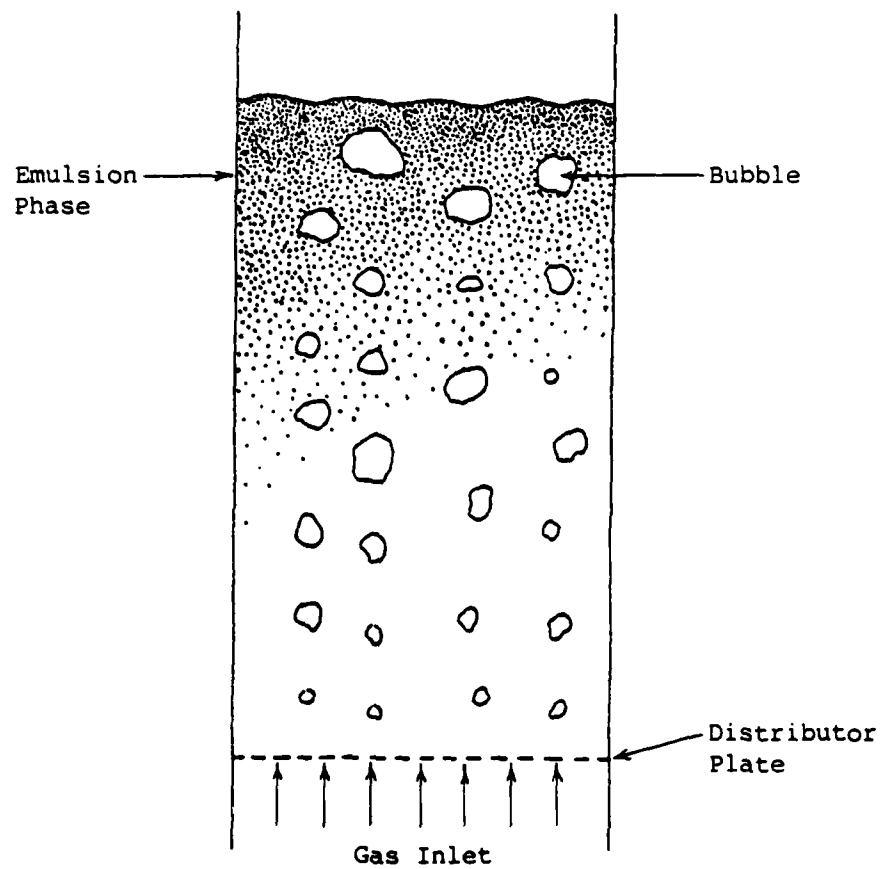
Figure 1.   Bubbling Bed Cross Section

18
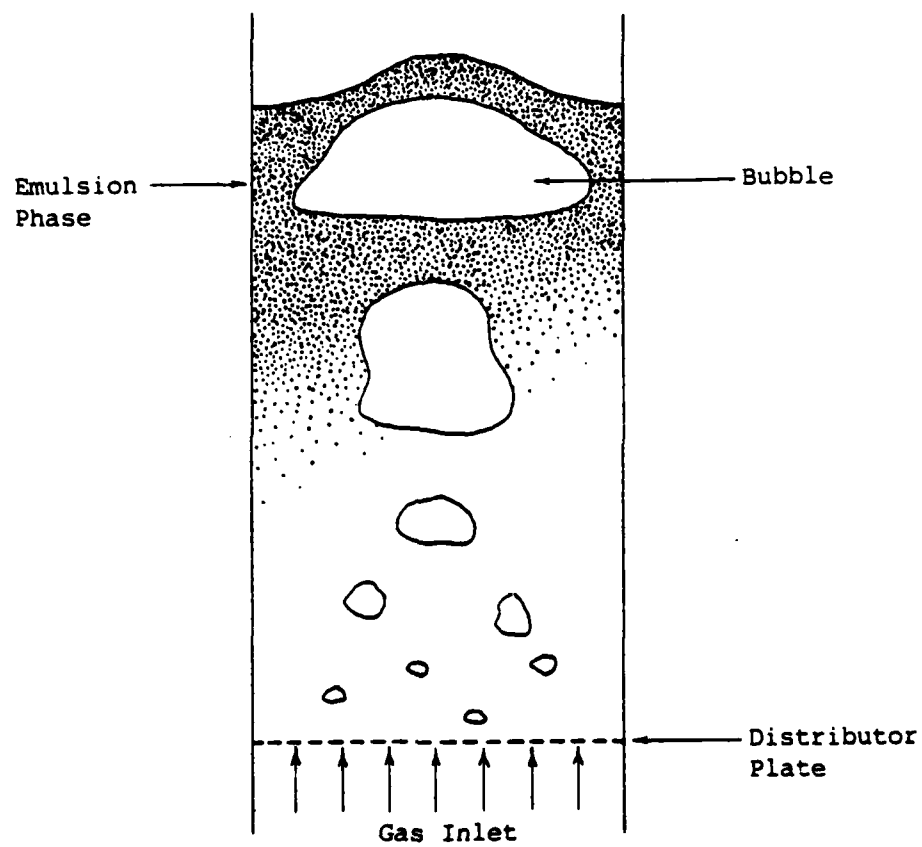
Figure 2. Slugging Bed Cross Section

19
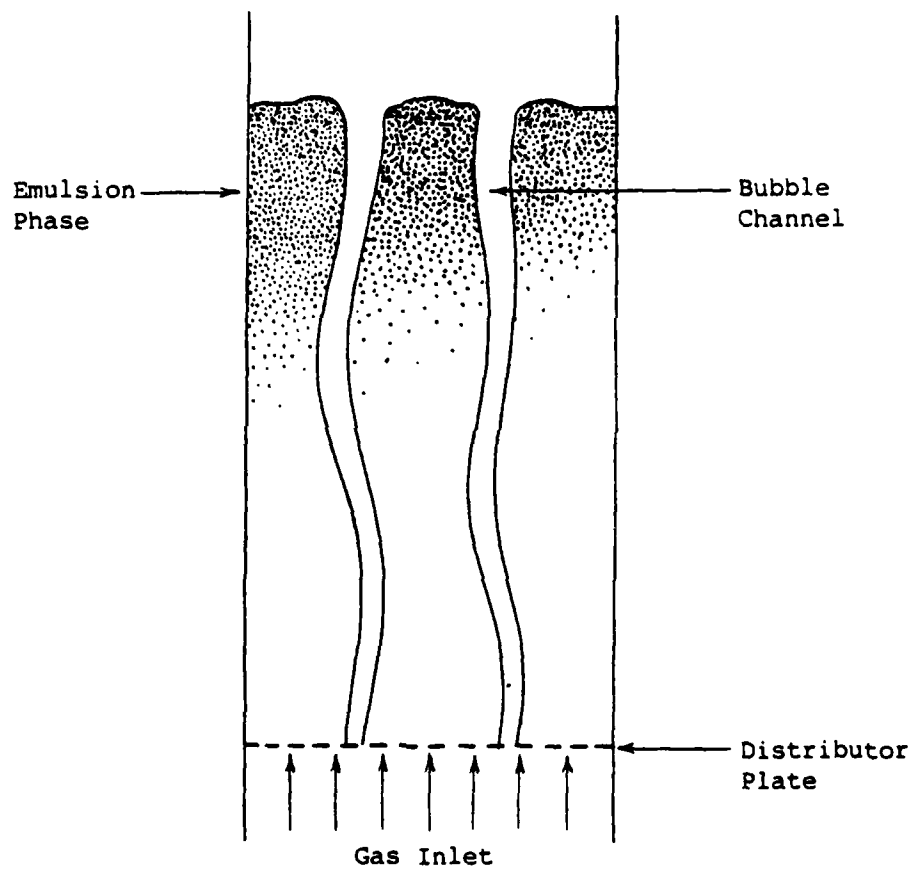
Figure 3. Channelling Bed Cross Section

20

bed temperatures. In addition, once fluidized, the pressure drop across a bed remains relatively constant despite variations in fluid flow rate. The pressure drop is a function of bed height and particle density and is independent of particle size. [Ref. 1] This permits increasing the surface area by using smaller particles without paying a penalty in increased pressure loss.

Fluidized beds also suffer from certain limitations. The size of particles which can be fluidized is limited to a specific range extending from approximately 0.001 inch in diameter to about 0.25 inch diameter, depending on the density of the particles and the fluid. [Ref. 2] In addition, some materials cannot be fluidized regardless of size because of their tendency to clump together and form particles too large to fluidize, or because of their tendency to break down into particles which are so small that they become entrained in the fluidizing medium and are carried from the bed. Another disadvantage is that fluidization requires the expenditure of energy to force the fluidizing medium through the bed at the required velocity.

In general the beneficial aspects of fluidized beds far exceed the limitations and as a result, fluidized bed principles have been utilized in many diverse applications over the years. Early mining engineers used fluidization to separate solids of different densities by suspending them in rising streams of water. [Ref. 1] Prior to World

21

War II, chemical engineers discovered that fluidized beds
made outstanding chemical reactors because of the extremely
large contact area between the particles and the fluid.
For example, a container measuring one foot by one foot by
one foot, filled with 0.01 inch diameter spherical particles
yields approximately 4,000 squares feet of surface area.
This characteristic of fluidized beds has been utilized to
great advantage in a wide number of chemical processes, most
notable the catalytic cracking of petroleum. [Ref. 3]
Because the particles within a fluidized bed are constantly
churning about and mixing, the temperature at one point in
the bed is usually in very close agreement with the tempera-
ture at any other point. Industry has capitalized on this
isothermal property by using fluidized beds to improve the
heat treatment of metals in such processes as quenching,
tempering, and carburizing. As a combined result of the
large surface area and the thorough mixing of the particles,
fluidized beds possess impressive heat transfer capabilities.
Consequently, the power generation industry has begun utiliz-
ing this technology to create a new generation of heat
transfer devices such as steam generators which efficiently
burn poor quality fuels while simultaneously yielding very
low levels of harmful emissions. These devices are capable
of burning high sulfur coal, pelletized garbage, and even
raw crushed shale, just as it comes from the ground. Another
application is seen in waste heat recovery units which are

22

fluidized by the exhaust gases from conventional boilers or gas turbines. The thermal energy which would otherwise have been wasted is transferred to a secondary fluid circulating through tubes emersed within the bed. This recovered energy is then utilized to increase overall plant efficiency. [Ref. 4]

The use of fluidized bed technology has expanded greatly in recent years as hundreds of new applications have been discovered, ranging from advanced ship propulsion plants to sophisticated solar energy conversion and storage devices. As the utilization of these devices increases so does the quest for a better understanding of the many complex phenomenon associated with fluidization.

Fluidized bed research has been conducted throughout the world and more has been written about fluidization than can be read in a lifetime, however much remains to be learned in order to unlock the full potential of this fascinating process. This thesis represents a modest attempt to add to the knowledge of fluidization in the area of heat transfer to vertical flat plates in gas fluidized beds.

II. OBJECTIVES AND METHOD OF APPROACH

A. GENERAL STATEMENT OF THE PROBLEM

The bulk of fluidized bed heat transfer research conducted to date has been related to the study of heat transfer to or from objects immersed within the bed, particularly tubes and tube bundles. Comparatively little research has been done on the study of heat transfer to the walls of the containing vessel itself. In addition, a large majority of the test apparatus utilized thus far to collect experimental data have been cylindrical in configuration. Very few studies have been conducted on heat transfer within rectangular fluidized beds; a geometry which is being used with increasing frequency in a wide variety of applications.

The principle objective of this thesis was to gain a greater understanding of the heat transfer to the flat vertical plates which form the walls of a rectangular gas fluidized bed and to determine what effects, if any, variations in bed geometry had on heat transfer performance.

A secondary objective was to study the variations in heat transfer which occurred as the fluidization gas flow rate was adjusted over a wide range.

B. METHOD OF APPROACH

This investigation was primarily experimental in nature with limited utilization of analytical methods for comparison

24

purposes. To acquire the necessary data for this study, a computerized data acquisition system was linked to a network of up to 75 copper-constantan thermocouples installed in a specially instrumented and heated fluidized bed. This system was used to obtain a thermal "snapshot" of the test apparatus which showed the temperature at numerous key locations at a specific point in time. This data was then combined with measured values of input power and incoming air flow rates to produce a calculated heat transfer coefficient. Experimental data was obtained for a number of different air flow rates and bed conditions beginning with fixed bed fluidization and progressing through to the onset of entrained flow fluidization. Once data had been collected for the entire range of flow rates, the bed geometry was altered by moving an adjustable side wall within the test apparatus so that the width of the rectangular bed was increased. Additional particles were then added to the bed so that the bed depth remained at the same level as in the previous configuration.

The data collection process was then repeated in its entirety for the new configuration. A total of four different bed geometries were studied in the course of this work. Over 5,700 temperature readings were recorded for eighty different test runs. All experimental data, including narrative comments regarding observed bed behavior were recorded on magnetic disks. The recorded data was automatically processed by computer and then printed out in such a manner

25

that bed performance for a particular test run was readily apparent. The calculated results for the individual runs were then analyzed to determine overall trends.

In addition to the heat transfer investigation, an experimental study of bed pressure drop characteristics was conducted for each geometric configuration in order to establish the point of fluidization onset and to confirm proper operation of the fluidizing apparatus.

III. EXPERIMENTAL APPARATUS AND PROCEDURES

A. DESCRIPTION OF FLUIDIZATION APPARATUS

The fluidization apparatus consisted of a rectangular plexiglas box filled with 0.012 inch diameter silica glass beads as shown in Figure 4. The box was equipped with a movable side wall which permitted the inside dimensions of the bed to be varied from 6.25 inches wide by 6 inches deep by 18 inches high to 24 inches wide by 6 inches deep by 18 inches high. The movable wall was equipped with felt gaskets which prevented the escape of beads through the gap between the movable side wall and the fixed front and rear walls. 0.5 inch thick clear plexiglas (grade GM) was used throughout the construction and all components were assembled using plastic laminating cement with wood screw reinforcements. The floor of the apparatus also served as the distributor plate whose function was to evenly distribute the flow of incoming air over the entire cross section of the bed. The distributor plate was constructed from a plexiglas sheet with 0.125 inch diameter holes drilled 0.25 inches on center. Secured over this plate was a 140 mesh stainless steel wire screen to prevent the beads from falling down into the holes and to provide an even finer distribution of air.

. Located beneath the distributor plate was an air chamber or plenum which served to ensure that the air pressure on

27
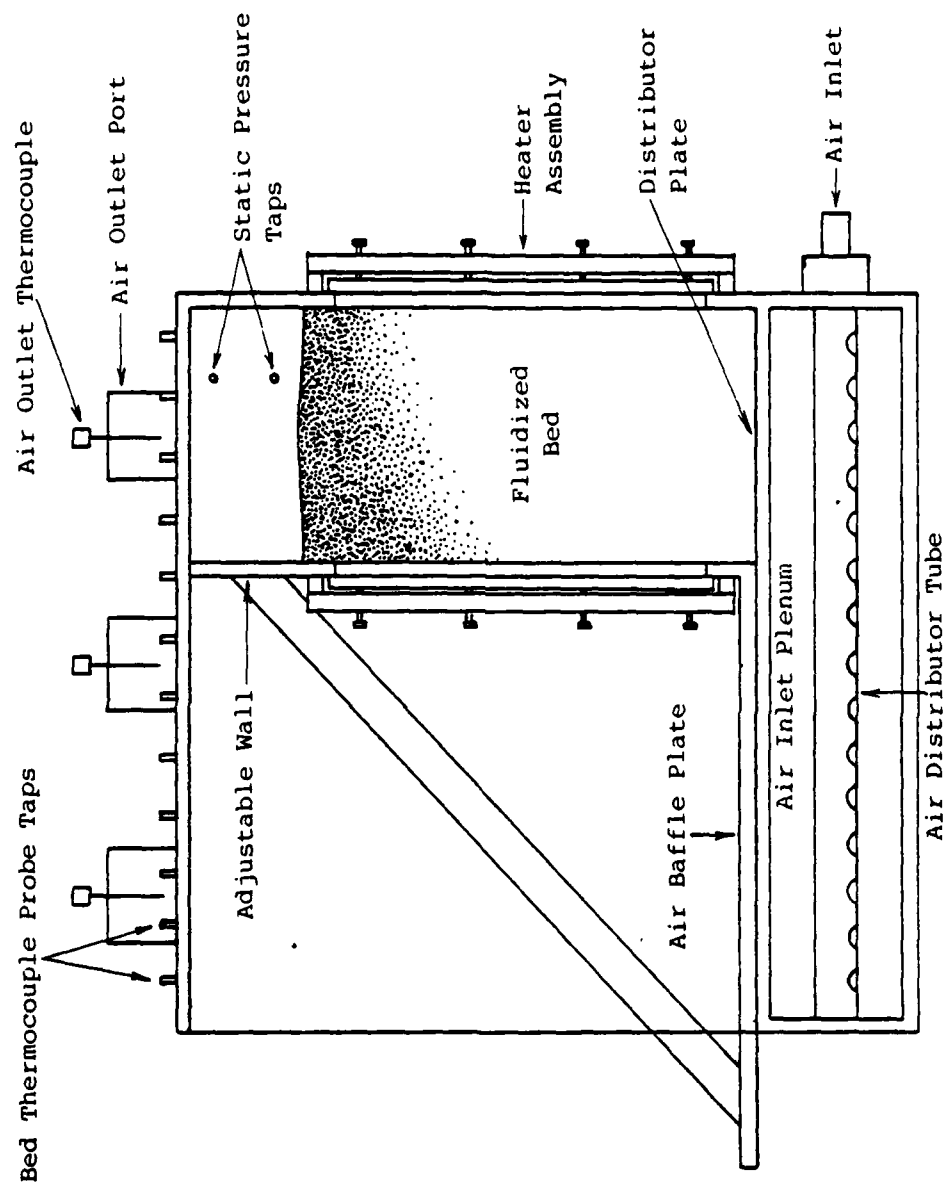
Figure 4. Fluidized Bed Apparatus

28

the underside of the distributor plate was the same at any point. This was accomplished by first directing the incoming air through a 2.5 inch inside diameter plexiglas distribution tube centered lengthwise within the 24 inch by 6 inch by 6 inch plenum. This tube had 0.5 inch diameter holes drilled on 1 inch centers on its underside and served to evenly direct the incoming air downward over the entire length of the plenum. In order to prevent the escape of air when the bed was configured to a width less than the 24 inch width of the distributor plate, the movable side wall was equipped with a horizontal baffle plate which laid flat over the top of the unused portion of the distributor plate. Once the desired position of the movable wall was set, the baffle plate was securely clamped to the distributor plate and the edges were sealed with silicon caulking. After passing through the distributor plate and finally the bed itself, the fluidizing air escaped from the apparatus via one or more of three plexiglas exhaust tubes positioned on the top of the apparatus. These tubes were quipped with wire mesh covers to prevent the loss of glass beads due to carryover.

In order to measure the air pressure at various depths the apparatus was equipped with static pressure taps positioned along the rear wall with 2 inch vertical spacing between centers. Additionally taps were installed just below the distributor plate and immediately above it. These taps were connected by flexible plastic tubing to a manifold

29

which permitted selective connection of the taps to a
Meriam Model 33KA35 30 inch water manometer as shown in
Figure 5.

The fluidizing apparatus was supplied with air from a
Spencer axial flow turbo compressor rated at 500 SCFM.
The fluidizing air was not filtered or dehydrated prior
to entry. The volumetric flow rate of air entering the
apparatus was measured by a calibrated Fisher and Porter
flowmeter rated at 34 CFM.

B. DESCRIPTION OF HEAT TRANSFER APPARATUS

The test apparatus was equipped with two instrumented
flat plate heater assemblies each measuring 5 inches wide
by 10 inches high. These assemblies were mounted flush with
the inside surface of both the movable side wall and the
fixed side wall opposite it. Each heater assembly was
powered by a Watlow strip heater rated at 250 watts. The
heater consisted of a grid of nickel alloy resistance wire
embedded in a thin sheet of rubberized supporting material
and backed by a 0.5 inch thick sheet of silicone sponge
rubber insulation. This insulation was in turn bonded to
a 0.5 inch thick clear plexiglas mounting block. The face
of the assembly consisted of a 0.25 inch thick copper plate
mounted flush with the heating surface of the strip heater.
In order to avoid the use of screws or other conventional
attachment methods which may have altered or impeded the
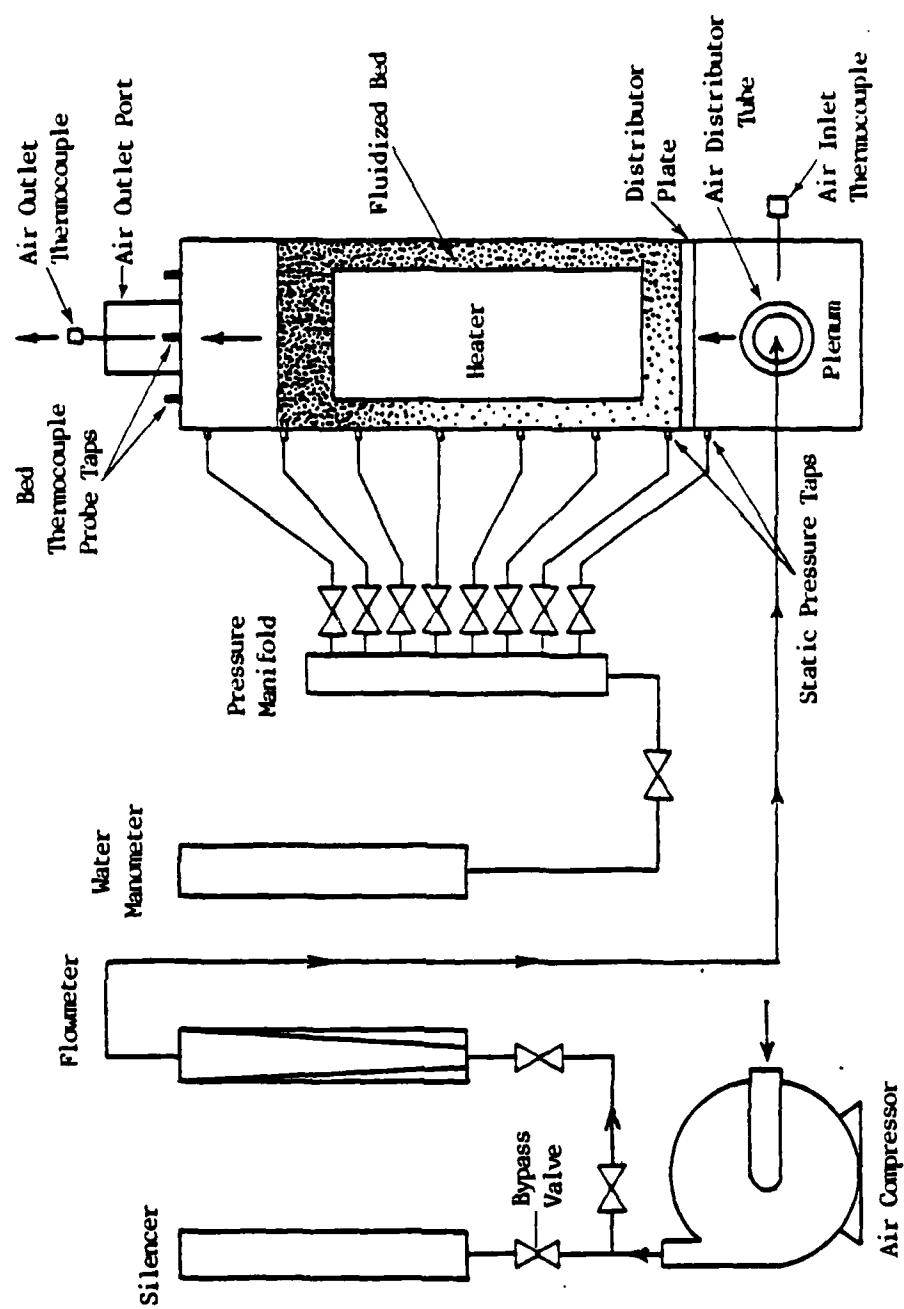
Figure 5. Fluidization System Diagram

31

heat flow from the strip heater to the copper plate, the two were held together using a strongback arrangement as shown in Figures 6 and 7. This mounting method ensured that the strip heater was held firmly against the copper plate, thus helping to minimize thermal contact resistance between the two. To further reduce this resistance, a thermally conductive paste was applied to the heating surface of the strip heater prior to positioning the copper plate over it. Power was supplied to the left hand heater by a Lambda regulated DC power supply model LK345A, while the right hand heater was supplied by a Hewlett Packard DC power supply Model 6296A. Both power supplies were rated at 60 Volts and 2 Amps and were each equipped with an individual voltmeter and ammeter.

All thermocouples used in this apparatus were 10 gauge, ANSI Type T, copper-constantan, exposed junction type. Each heater assembly was equipped with twenty thermocouples arranged in five rows of four thermocouples each as shown in Figures 8 and 9. These thermocouples were mounted to the copper plate in such a manner so as to be least disruptive of the heat distribution patterns within the plate. The thermocouple junctions were soldered into small shallow holes drilled into the back of the plates so that the top of the junction was flush with the plate surface. The thermocouple leads were then routed straight back through holes drilled into the strip heater and its mounting block. Figure 10

32
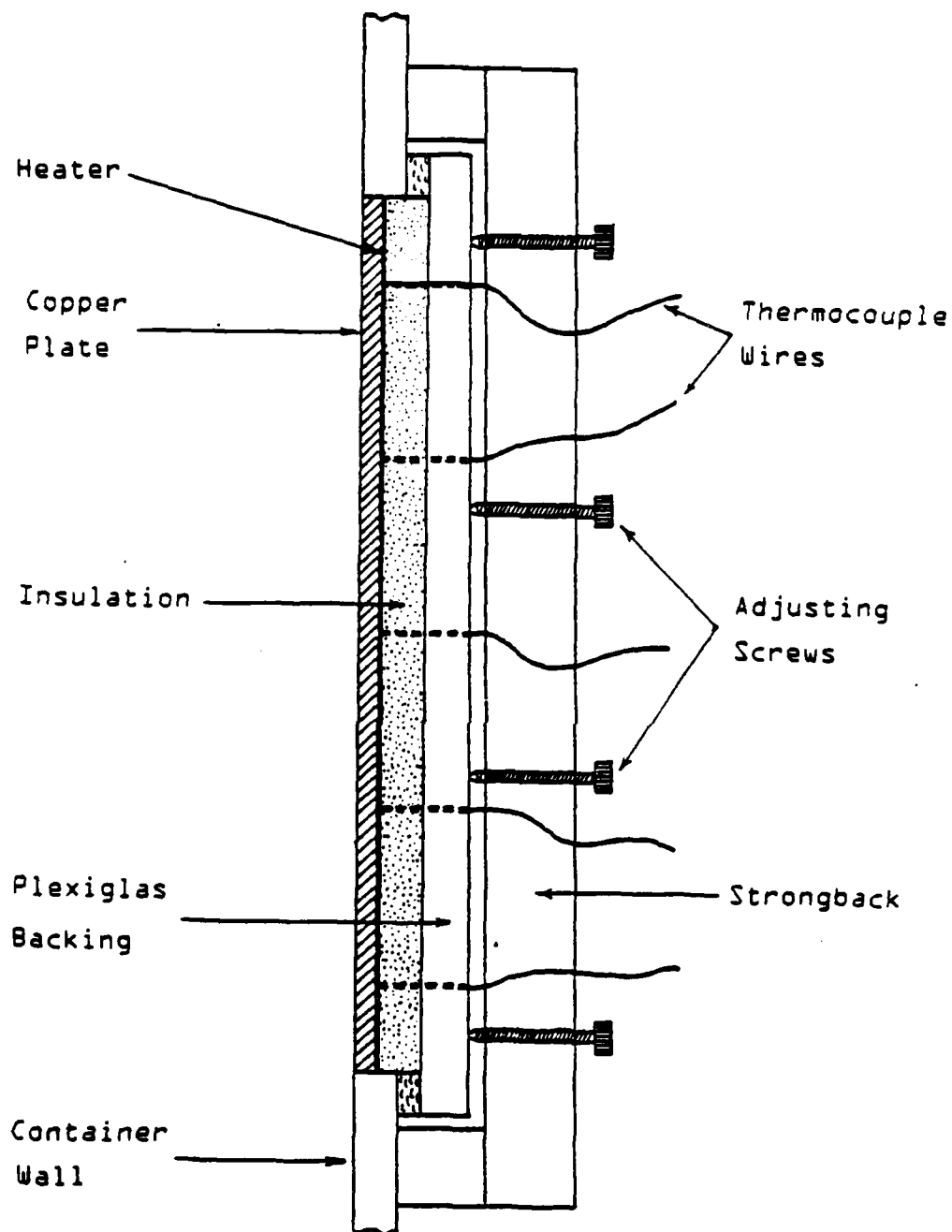
Figure 6. Heater Assembly Mounting Diagram; Side View

33
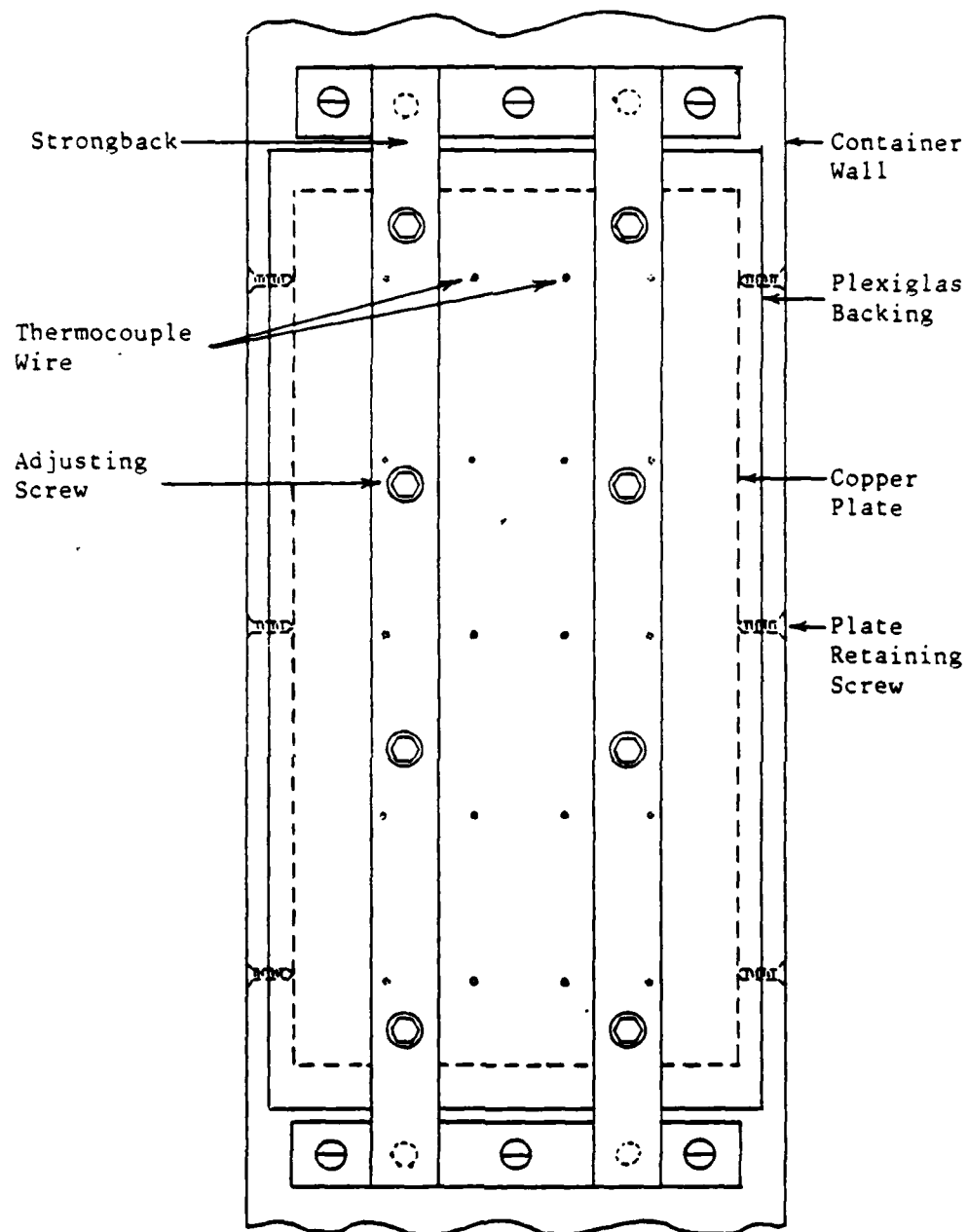
Figure 7. Heater Assembly Mounting Diagram; Rear View

34

```
         T(1)    T(2)    T(3)    T(4)
          .       .       .       .


         T(5)    T(6)    T(7)    T(8)
          .       .       .       o


         T(9)   T(10)   T(11)   T(12)
      '   .       o       .       .


        T(13)   T(14)   T(15)   T(16)
          .       .       .       .


        T(17)  T(18)    T(19)   T(20)
          .       .       .       .
```
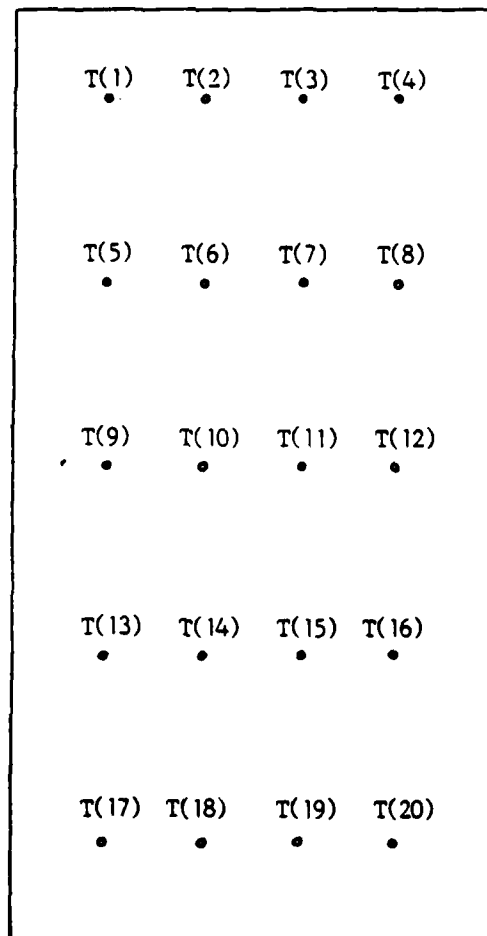
NOTE: Arrangement is as seen from within the
        bed (front view).

Figure 8.   Right Hand Heater Thermocouple Arrangement

35
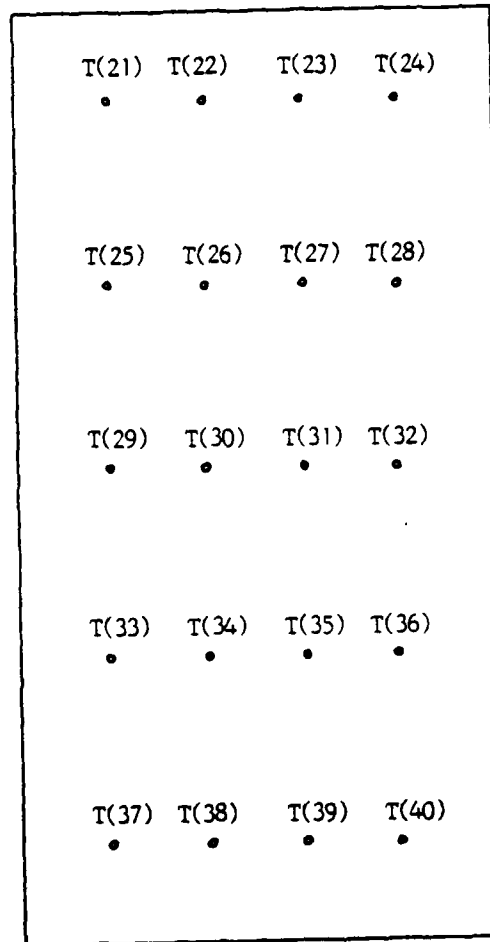
NOTE: Arrangement is as seen from within the
bed (front view).

Figure 9.   Left Hand Heater Thermocouple Arrangement
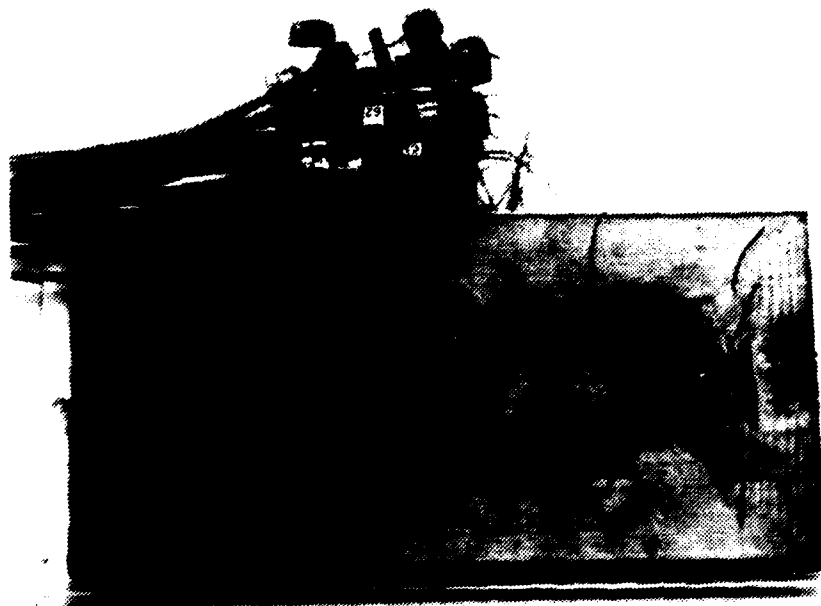
Figure 10. Photograph of Heater Thermocouple Mounting Procedure

shows the thermocouple mounting procedure. X-ray photographs
were used to determine the exact location of the resistance
wires embedded within the heaters so as to avoid striking
them while drilling the holes. This thermocouple arrangement
made it possible to read the plate inside surface temperature
immediately adjacent to the surface of the strip heater while
causing minimum disruption of the heat flux patterns within
the plate itself. A determination of the plate outside
surface temperature as seen by the bed was then accomplished
by means of simple calculations as shown in section IIIE.

The temperatures within the bed itself were monitored by
15 retractable, 24 inch, stainless steel sheathed, exposed
junction, Omega Engineering Type T thermocouple probes. The
position of these probes was held fixed at a bed depth of
7 inches above the distributor plate for all data runs. The
number of bed probes actually utilized depended on the geo-
metric configuration being studied, as shown in Figure 11.

Incoming air temperature was monitored by 3 retractable,
4 inch, stainless steel, sheathed thermocouple probes posi-
tioned within the air plenum as shown in Figure 12. Out-
going air temperature was monitored by 3 similar probes
mounted one each in the center of the 3 air exhaust tubes,
as shown in Figure 13. Because of the positioning of these
tubes with respect to the movable side wall only one thermo-
couple was used to read the air outlet temperature for all
data runs.

38
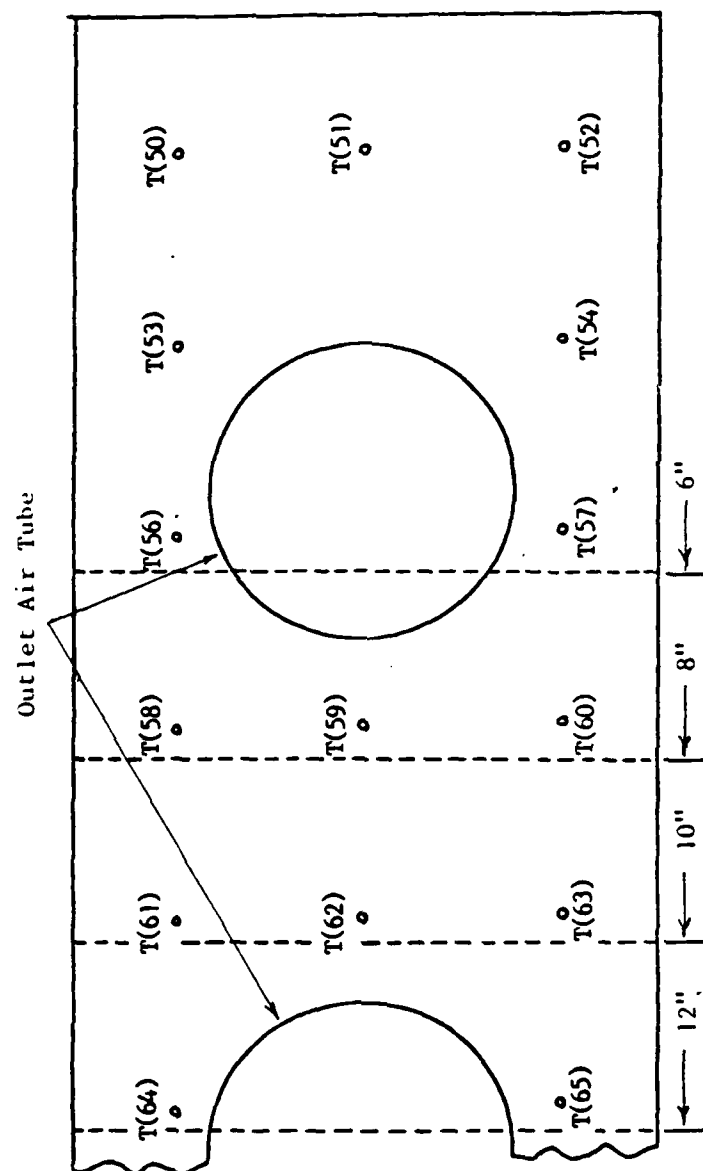
NOTE: Arrangement is as viewed from top front.

Figure 11. Bed Thermocouple Probe Arrangement

39
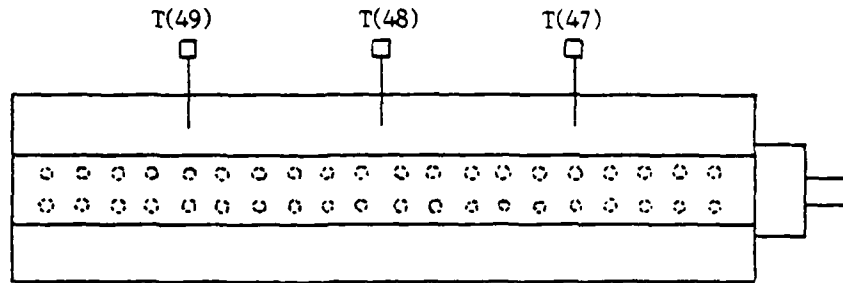
NOTE: Arrangement is as viewed from top front.

Figure 12. Air Inlet Thermocouple Probe Arrangement
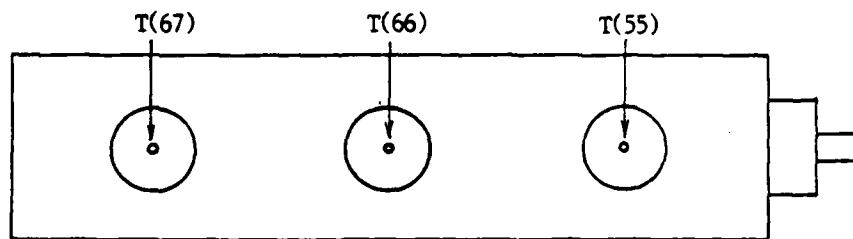
NOTE: Arrangement is as viewed from top front.

Figure 13. Air Outlet Thermocouple Probe Arrangement

40
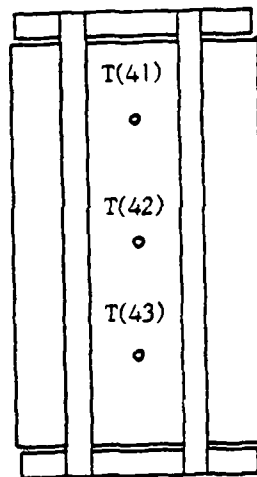
Figure 14.   Right Hand Heater Mounting Block Thermocouple
Arrangment
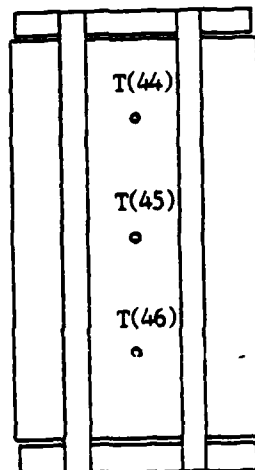
Figure 15.   Left Hand Heater Mounting Block Thermocouple
Arrangment

41
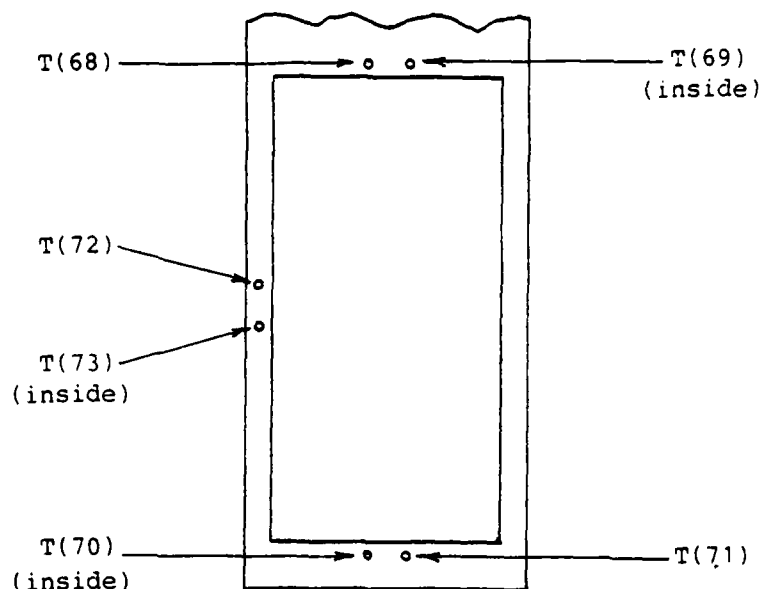
Figure 16. Right Hand Heater Sidewall Thermocouple Arrangement;
Rear View
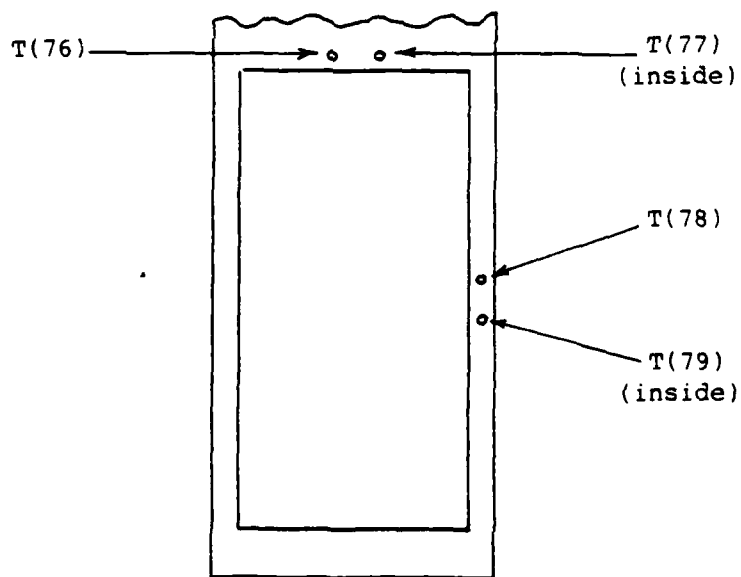
Figure 17. Left Hand Heater Sidewall Thermocouple Arrangement;
Rear View

42

Three insulated thermocouples were mounted to the outside surface of each of the plexiglas heater mounting blocks, as shown in Figures 14 and 15, in order to determine the mounting block outer surface temperatures. These temperatures were used to estimate the amount of heat lost through the back of the heater assemblies as explained in section IIIE. Thermocouples were also mounted on the inside and outside surfaces of the plexiglas sidewalls, as shown in Figures 16 and 17, in order to estimate the losses to the atmosphere and to the bed itself from the thin plexiglas wall strips adjacent to the edges of the heater assemblies. A final set of thermocouples was mounted to the inside and outside surfaces of the container rear wall, as shown in Figure 18, in order to obtain an estimate of losses through the rear wall. Because of symmetry it was assumed that the losses through the front wall were identical to the rear wall losses.

All thermocouples used in the test apparatus were sampled by an HP 3497A data acquisition system controlled by an HP 85 desk top computer. This system was capable of sampling and storing the output of seventy five thermocouples within seven seconds. Because of the steady state conditions in existance during each of data runs, the seven second sampling time was considered brief enough to treat the thermocouple readings as through they had all been taken simultaneously.

Once all of the thermocouples had been sampled, the HP 85 retrieved the stored thermocouple voltages and converted them

to temperature values using equations previously developed. These temperature values, along with other stored parameters, were then recorded on magnetic disks using a Hewlett Packard Model HP 82901M dual flexible disk drive. This recorded data was later processed and permanently displayed using an HP 82905B printer and an HP 7225A plotter.

Computer programs used to control data acquisition and data processing are shown in Appendixes J and K, respectively. The arrangement of the heat transfer data collection and processing system is shown in Figure 19 while Figures 20 and 21 show photographic views of the entire experimental system.

C. EXPERIMENTAL APPARATUS CALIBRATION

The inlet air flowmeter was calibrated using an ASME Herschel-type venturi with an inlet diameter of 4.26 inches and a throat diameter of 2.13 inches. Experimental data (shown in Appendix B) was collected for nine different data points and from this data, volumetric air flow rates were calculated using equations shown in Appendix H. A plot of air flowrate vs flowmeter reading is shown in Figure 22. A least squares curve fit was applied to the data points to obtain a linear equation which converts flowmeter readings to air flow rates in CFM. This equation was then incorporated into the data reduction computer program shown in Appendix K. The rotameter calibration data shows that a 100% flowmeter reading equates to 34.0 CFM.

T(74)

T(75)
(inside)
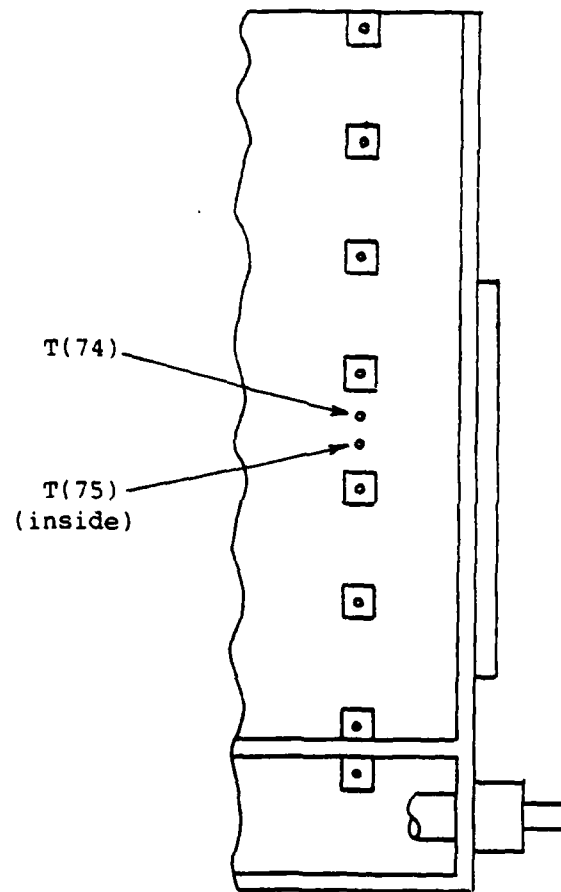
Figure 18. Rear Wall Thermocouple Arrangement

45
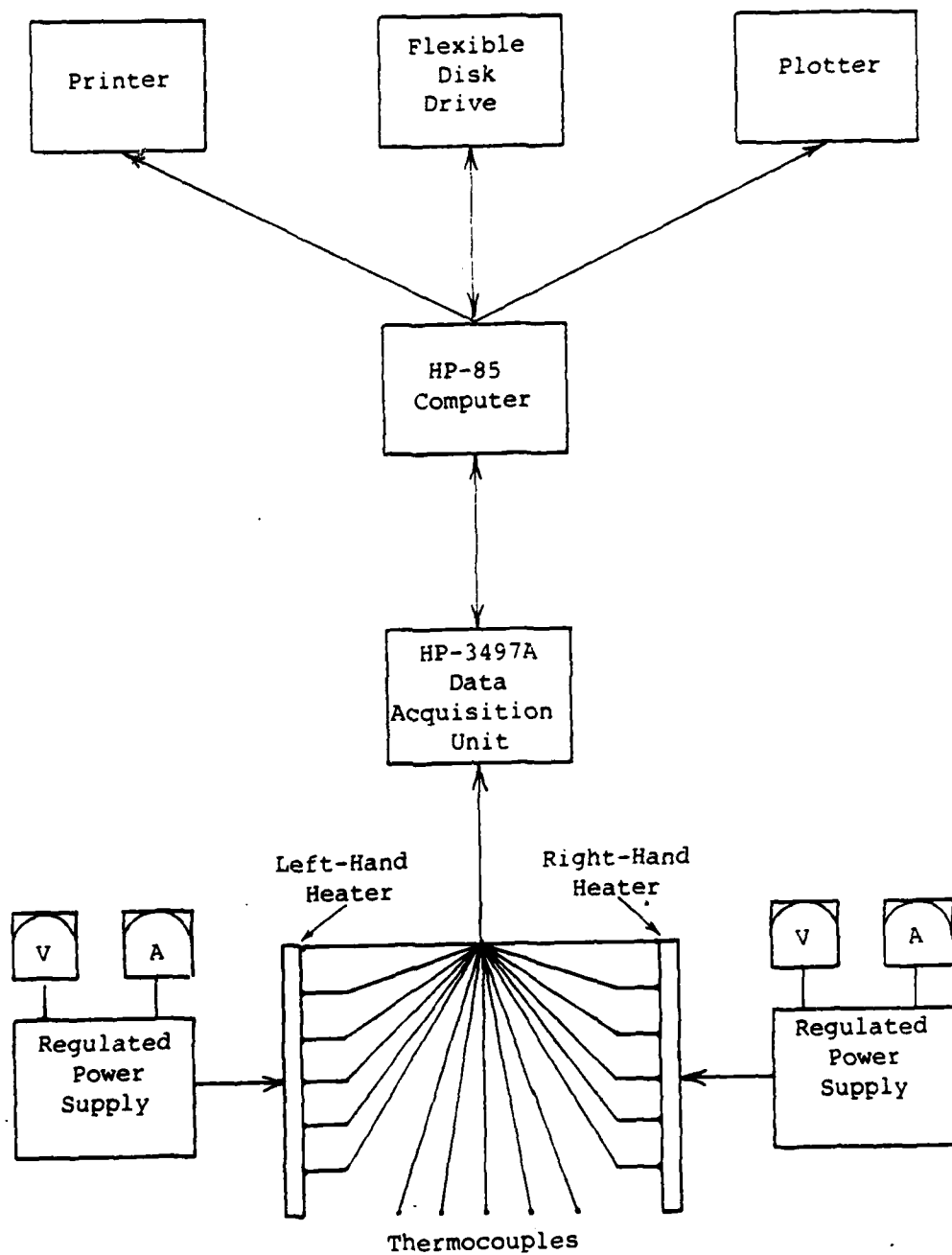
Figure 19. Heat Transfer Data Collection System Diagram
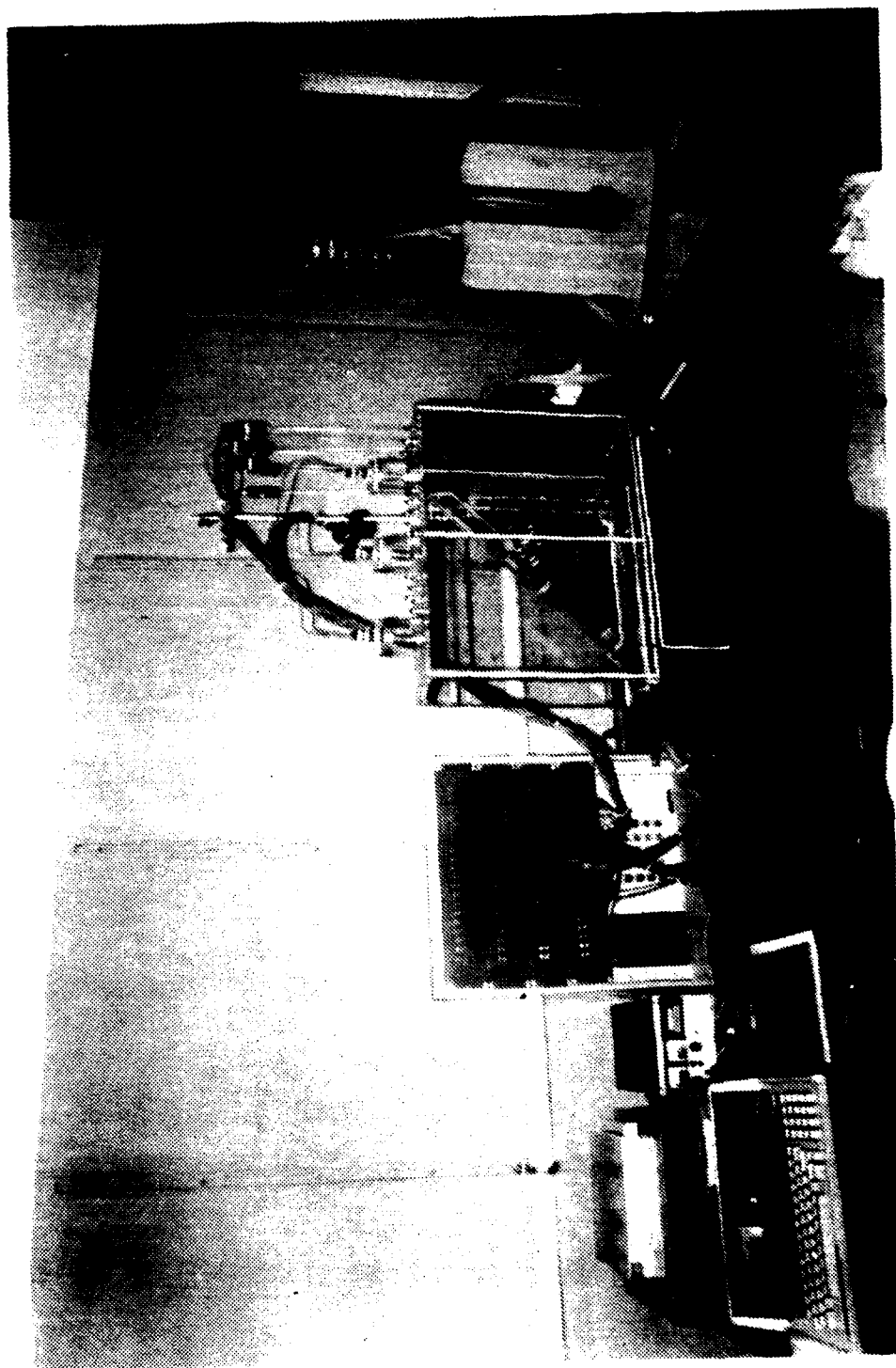
Figure 20. Photograph of Experimental Apparatus

47
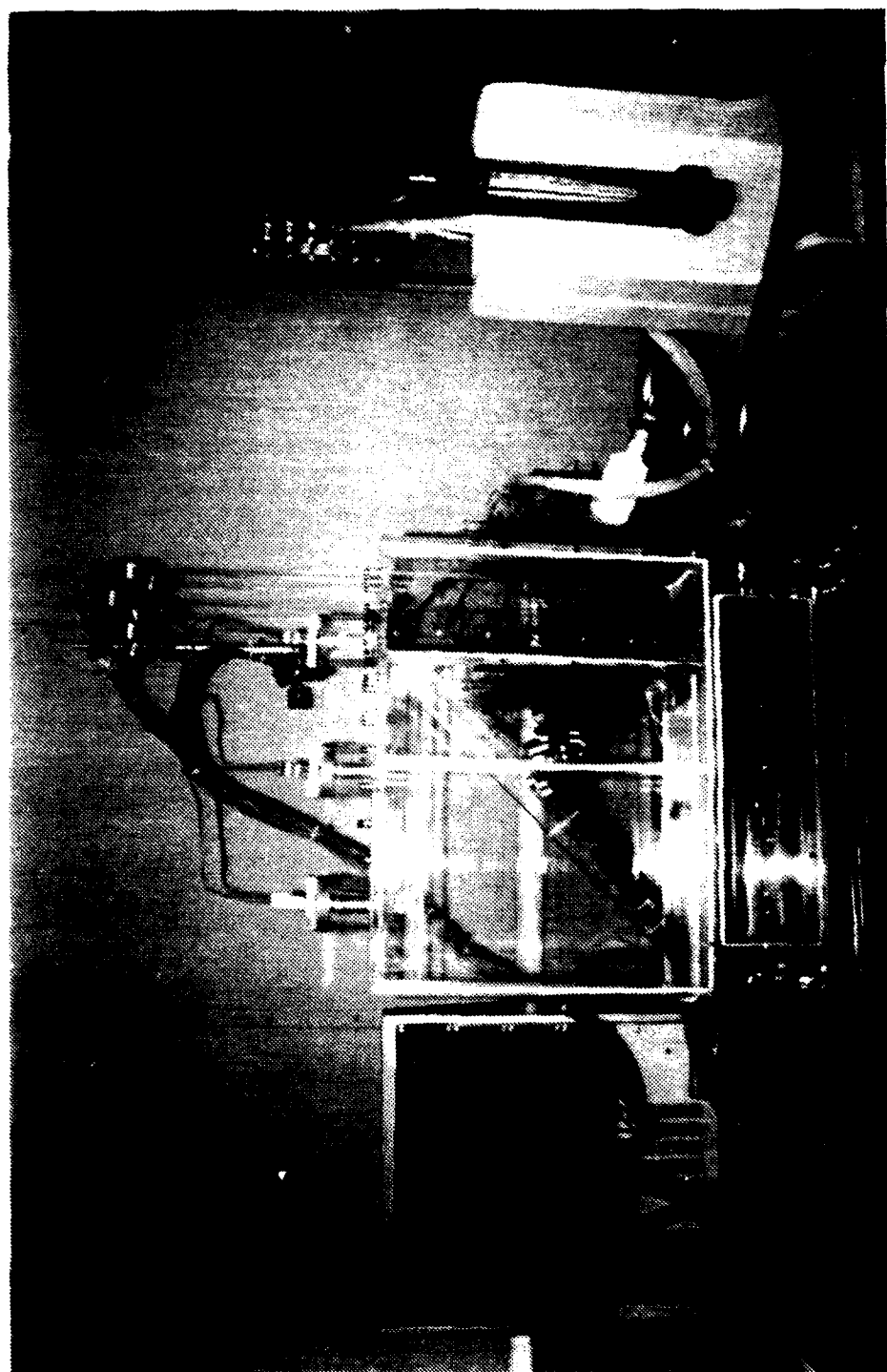
Figure 21. Photograph of Experimental Apparatus

48
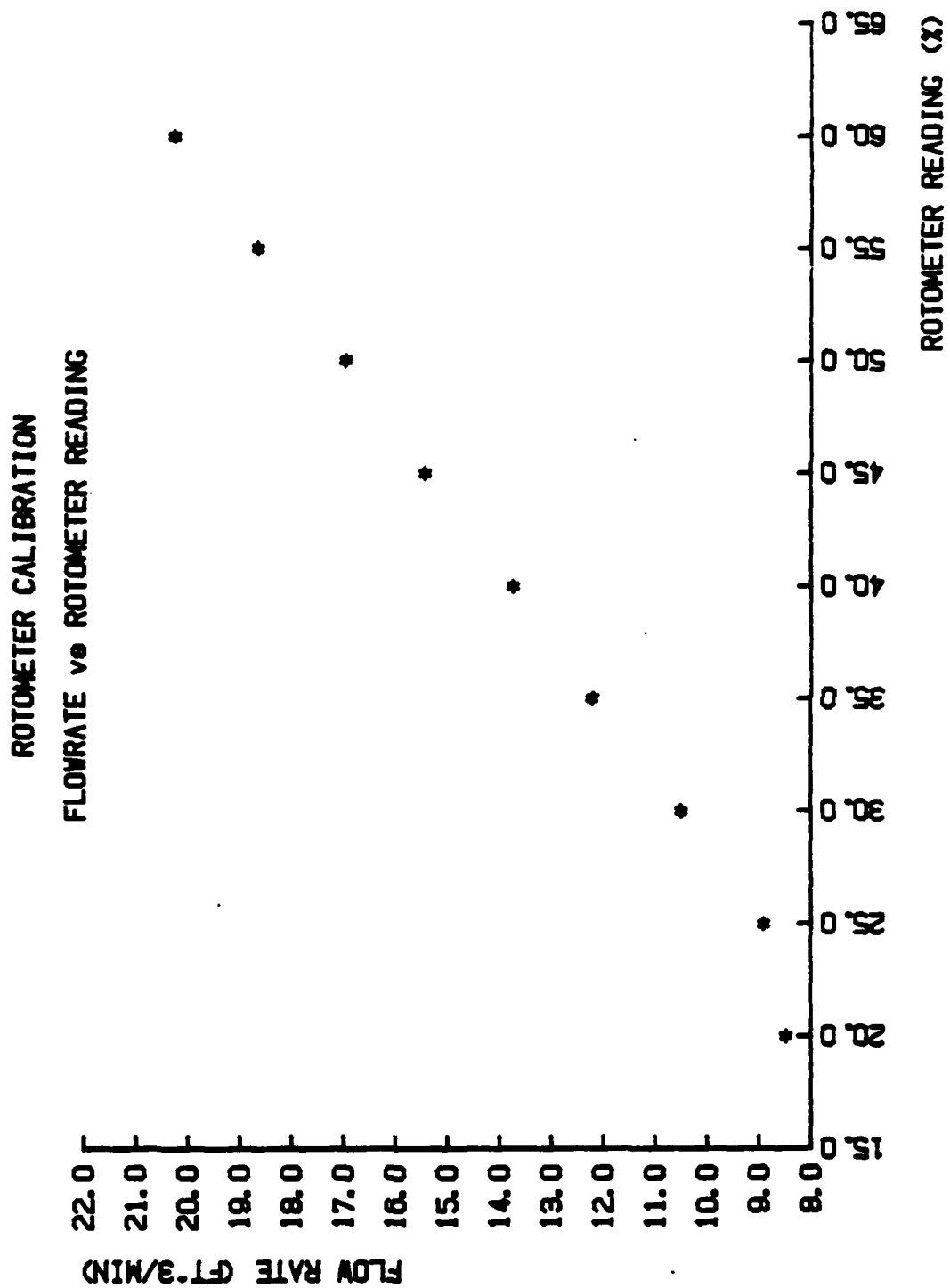
Figure 22. Air Flowrate vs Rotometer Reading

49
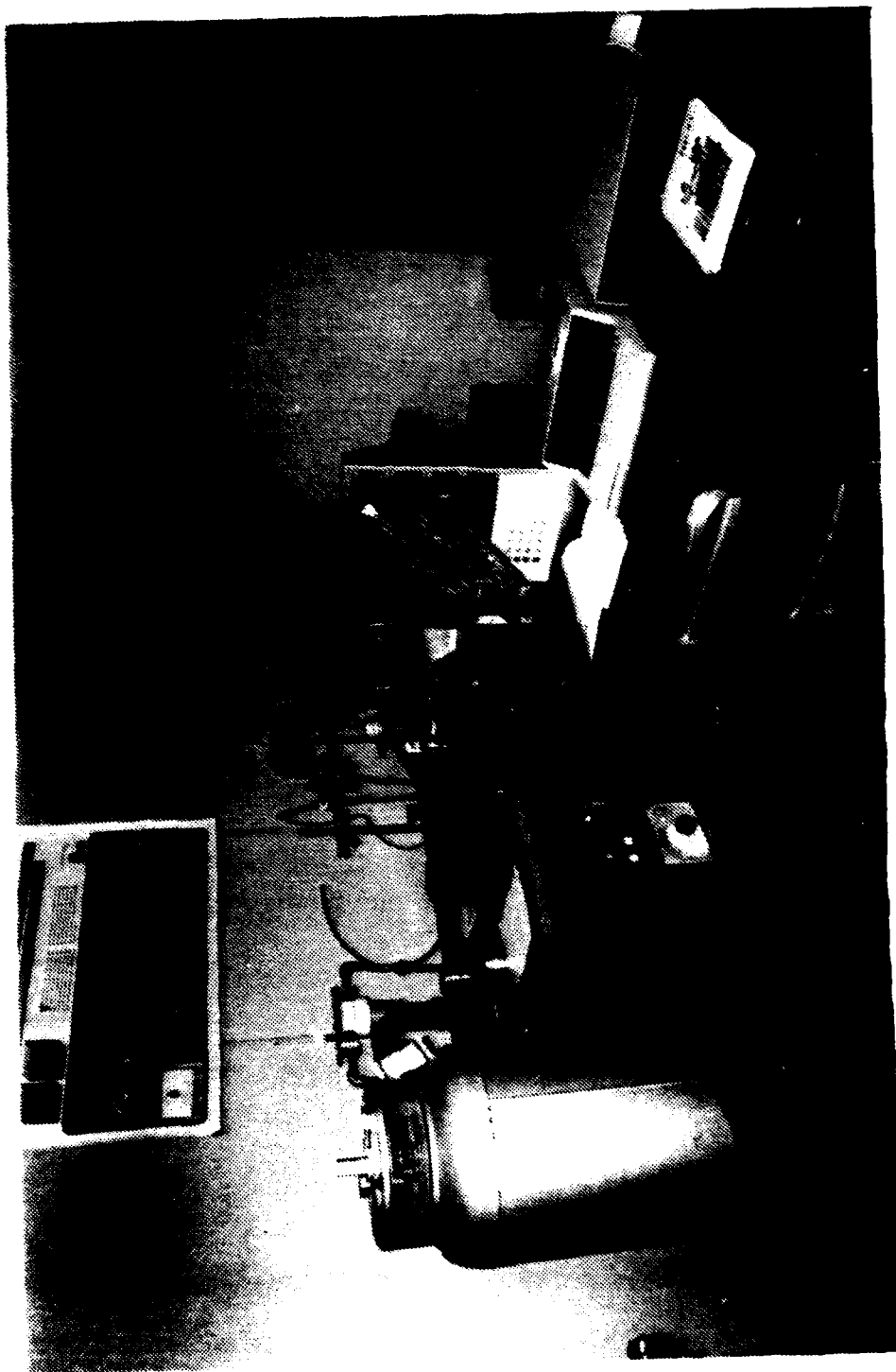
Figure 23. Photograph of Calibration Apparatus

Thermocouples number 1 through 67 were calibrated using a Rosemount Commutating Bridge Model 920A and a Rosemount Calibration Bath Model 913A using liquid nitrogen and water. The HP 3497A and the HP 85 were included in the system during calibration, as shown in Figure 23. Data was collected for twenty different bath temperatures and a least squares curve fit was applied to the data to obtain a fourth order polynomial function for each of the thermocouples. The constants from these functions were then incorporated into the data acquisition computer program shown in Appendix J to allow automatic conversion of thermocouple output voltage to temperature, in degrees Fahrenheit. A sample of the calibration data in shown in Appendix D.

Thermocouples number 68 through 79 were not calibrated but were instead assigned constants from the standard power expansion for Type T thermocouples. [Ref. 5] They were then compared in a water bath of known temperature to confirm proper operation.

The water manometer used to determine static pressure drop within the bed was regularly rechecked for zero readings and was readjusted as necessary.

D. EXPERIMENTAL PROCEDURE

Preparation for the taking of heat transfer data was accomplished by adjusting the movable side wall to the proper position for the geometry to be studied. The baffle plate

51

was then clamped into position and the joints were sealed with silicone rubber caulking. This caulking was allowed to harden for a minimum of twenty four hours to ensure a leak tight seal. Carefully weighed quantities of glass beads were then added to the bed through the right hand air exhaust tube until the depth of the bed reached 12.5 inches above the distributor plate. The air supply turbo compressor was then lined up and energized. Following this, the air inlet control valve was opened and adjusted until the desired air flow rate registered on the flowmeter. The heater power supplies were then energized and adjusted to the desired level.

The power supply controls were set so that the voltage going to each of the heaters was the same. Current into the heaters was determined by the resistance of the nickel-heating element which was in turn determined by the temperature of the heaters. Once the voltage was equilized, the bed was allowed to come to steady state conditions. Prior to the taking of data, the system was checked for thermal equilibrium by monitoring the temperature at specific points using a special computer program which sampled thermocouples at five-second intervals. Once it was confirmed that the heater assemblies and the bed itself were at a steady temperature, the data acquisition program was initiated. At the beginning of the program the computer requested that the operator provide certain information regarding the data

52

run to be recorded. The first item of information requested
was the run number. This number was structured so as to be
as informative as possible. The first two digits represented
the bed width in inches. These two digits were followed by
a letter indicating which of the heaters was energized; "L"
designated left, "R" stood for right, and "B" designated both.
This letter was followed by two digits indicating the air
flowmeter reading. Finally, a single letter was used for
special purpose designations such as a repeated run without
a change in configuration or flow rate. The next item of
information requested by the program was the date and time.
This was followed by requests for bed width and height, air
flow rate, ambient temperature (read on a mercury in glass
thermometer positioned near the test apparatus), voltage
and current readings from the two power supplies to each of
the heaters, the number of bed thermocouple probes in use,
and the amount of bed expansion, if any. Finally, general
comments concerning observed bed behavior were entered.
As the push of a button, all of the thermocouples were
then sampled and the corresponding temperatures were then
recorded on disc along with the other data entered from the
keyboard. Once the recording process was completed, the
system was ready to begin another data run. If the next
run to be studied was for the same bed configuration, all
that had to be done was adjust the air flow rate to the new
reading and wait for the temperatures to stabilize. In

some cases, the power supplied to the heaters was also adjusted in order to maintain as large a temperature differential as possible between the incoming air and the heaters. In order to avoid excessive softening of the plexiglas adjacent to the heaters, the maximum heater temperature was limited to approximately one hundred eighty degrees Fahrenheit.

After data was collected over the entire range of flow rates for a given geometry, the caulking was removed and the movable wall was repositioned for the next configuration. The entire data collection process was then repeated. In all, four different geometric configurations were studied. Bed widths of 6.25 inches, 8 inches, 10 inches, and 12 inches were used. In addition, data runs were taken in the 6.25 inch configuration with the bed empty. Data was also collected with the underside of the distributor to the left of the movable wall masked off as a check to see if the baffle plate was performing effectively. A total of eighty data runs were completed during this study. Experimental heat transfer data as well as calculated results are shown in Appendix C.

Pressure drop data was collected for each bed configuration by aligning the valve manifold (shown in Figure 5) so that the static pressure tap immediately above the distributor plate was connected to the 30 inch water manometer. The fluidizing air flow rate was then adjusted to the desired level and the pressure reading at the base of the bed was read

54

on the manometer and recorded. The manifold was then re-
aligned so that the static pressure tap near the top of
the bed housing was connected to the manometer. This read-
ing was then read and recorded. By substracting this read-
ing from that obtained at the base of the bed, the bed
pressure drop was determined. Pressure drop data was ob-
tained in this fashion over the entire flow range for each
of the bed configurations. During the pressure drop data
runs, the power to each of the heaters was secured.

E. EXPERIMENTAL DATA PROCESSING

All raw data was processed using an HP 85 desk top
computer. The final results consisted of six pages of
printed data for each run. The first page was a listing of
experimental conditions and comments recorded during the
data acquisition phase of the study.

The second page was a listing of all thermocouple out-
puts and their corresponding temperatures.

The third page showed a temperature profile of the right
hand heater surface as seen from within the bed. In addition,
an average value of the thermocouple readings in each hori-
zontal row was calculated and displayed. Thermocouple number
four was found to be malfunctioning; therefore it's output
was disregarded. In a separate display, the average row
temperatures were plotted against bed depth to show how the
heater temperatures varied from top to bottom.

The fourth page of the results printout showed the left hand heater temperature profile in a format identical to that of page three.

The fifth page showed the temperature profile of the bed itself, as measured by the thermocouple probes immersed within it. The profile is arranged as seen from above the bed.

The sixth and final page contained the calculated results. The first value displayed on this page was the average heater temperature (T_h). This value was a simple arithmetic average of the five horizontal row temperatures previously calculated.

$$T_h = \{R(1) + R(2) + R(3) + R(4) + R(5)\}/5 \qquad (3.1)$$

The average bed temperature (T_b) was similarly calculated using the temperatures displayed on page five of the printout.

$$T_b = \{T(50) + T(51) + T(52) + T(53) + T(54) + T(56)$$
$$+ \ldots + T(X)\}/(X-50) \qquad (3.2)$$

    X = Highest number bed probe

The electrical energy into the heater (q_{ie}) was calculated from the voltage and current measurements read off. The heater power supplies as shown below:

$$q_{ie} = I \times E \times 0.0569 \ (\frac{Btu}{Watt\text{-}Min}) \times 60 \ (\frac{Min}{Hr}) \qquad (3.3)$$

An estimate of the heat less from the heater to the atmosphere, through the heater mounting block (q_{mb}) was obtained as follows: First an average temperature (T_{mb}) was calculated for the three thermocouples attached to the outer surface of the heater mounting block.

$$T_{mb} = \{T(41) + T(42) + T(43)\}/3 \qquad (3.4)$$

Next it was assumed that the thermal contact resistance between the copper plate and the strip heater was negligible, therefore the temperature of the strip heater surface was equal to T_h. The contact resistance between the strip heater and the insulation was also assumed to be negligible.

The heater insulation and mounting block was then considered to be a composite wall as shown in Figure 24. Fourier's Law of Conduction was then utilized to calculate the heat flux through the mounting block.

$$q_{mb} = \frac{T_h - T_{mb}}{(\frac{L_i}{k_i A_i}) + (\frac{L_{mb}}{k_{mb} A_{mb}})} \qquad (3.5)$$
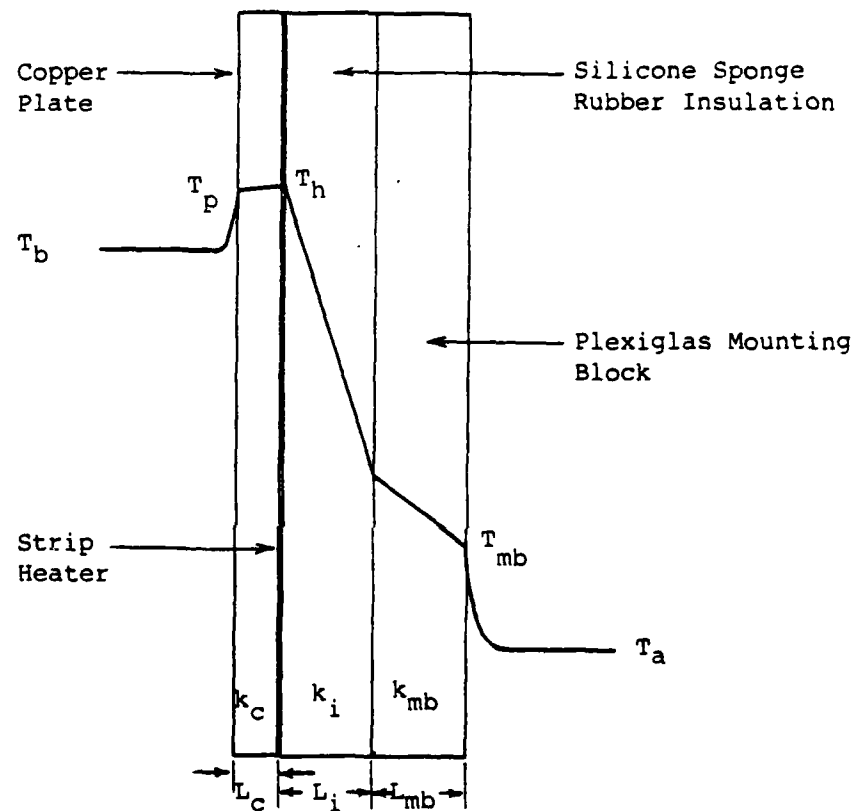
Figure 24. Heater Assembly Temperature Profile

$$L_i = L_{mb} = 0.5 \text{ inches}$$

$$A_i = A_{mb} = 5 \text{ in.} \times 10 \text{ in.} = 50 \text{ in}^2$$

$$k_i = 0.025 \frac{Btu}{Hr\text{-}Ft\text{-}^{o}F}$$

$$k_{mb} = 0.112 \frac{Btu}{Hr\text{-}Ft\text{-}^{o}F}$$

Next a convection heat transfer coefficient (h_{mba}) from the mounting block to the atmosphere was calculated using Newton's Law of Cooling.

$$h_{mba} = \frac{q_{mb}}{A_{mb}(T_{mb} - T_a)} \qquad (3.6)$$

Then an estimate was made of the heat lost to the atmosphere from the hot plexiglas side wall sections adjacent to the side edges of the heater (q_{sa}). This estimate was based on the side wall outer surface temperature and used Newtons Law of Cooling and the convection heat transfer coefficient previously calculated for the heater mounting block. Since the side wall sections and the mounting block were in such close proximity it was assumed that the coefficients would be in close agreement with one another.

$$q_{sa} = h_{mba} \times A_s \times \{T(72) - T_a\} \qquad (3.7)$$

$$A_s = 0.5 \text{ in.} \times 10 \text{ in.} \times \frac{1 \text{ Ft}^2}{144 \text{ in}^2} \times 2$$

(one strip on each side of heater)

A similar loss estimate was then calculated for the heat flux to the atmosphere from the side wall sections adjacent to the top edge of the heater (q_{ta}).

$$q_{ta} = h_{mba} \times A_t \times \{T(68) - T_a\} \qquad (3.8)$$

$$A_t = 0.5 \text{ in.} \times 6 \text{ in.} \times \frac{1 \text{ Ft}^2}{144 \text{ in}^2}$$

Yet another estimate was then calculated for the loss to the atmosphere from the side wall section adjacent to the bottom edge of the heater (q_{ba}).

$$q_{ba} = h_{mba} \times A_b \times \{T(71) - T_a\} \qquad (3.9)$$

$$A_b = 0.5 \text{ in.} \times 6 \text{ in.} \times \frac{1 \text{ Ft}^2}{144 \text{ in}^2}$$

All atmospheric losses were then totaled.

$$q_a = q_{mb} + q_{sa} + q_{ta} + q_{ba} \qquad (3.10)$$

The difference between the electrical power input, q_{ei}, and losses from the heater to the atmosphere, q_a, is the heat flux transferred to the bed. In order to identify that portion transferred directly from the heated copper plate to the bed, an estimate of the heat flux from the heated plastic strip surrounding the copper plate to the bed must be made. This is done by assuming that same heat transfer coefficient applies

60

to both the copper plate and to the plastic strip. The method
selected was an iterative; wherein it was first assumed that
the heat flux passed through the copper plate, from which the
heat transfer coefficient was calculated. Using this coeffi-
cient, the heat flux from the heated plastic strip was cal-
culated which in turn yielded a new heat flux from the copper
plate. The process was repeated until the heat flux values
did not change significantly. Thus following this procedure
the heat flux into the bed from the heater q_{cb} was assumed
to be equal to the incoming electrical power q_{ed} minus the
losses from the heater to the atmosphere q_a.

$$q_{cb} = q_{ei} - q_a \tag{3.11}$$

Once the heat flux through the copper plate q_{cb} was known,
the plate outside surface temperature T_p seen by the bed
could be calculated.

$$T_p = T_h - (\frac{q_{cb} \times L_c}{k_c \times A_c}) \tag{3.12}$$

$$L_c = 0.25 \text{ in.} \times (\frac{1 \text{ Ft}}{12 \text{ in}})$$

$$k_c = 232 - \{0.032 \times (T_h - 70)\} \text{ Btu/Hr-Ft-}^\circ\text{F}$$

$$A_c = 5 \text{ in.} \times 10 \text{ in.} \times (\frac{1 \text{ Ft}^2}{144 \text{ in}^2})$$

61

Once the outside plate surface temperature was known, the convection heat transfer coefficient from the plate to the bed (h_{cb}) could be calculated.

$$h_{cb} = \frac{q_{cb}}{A_c(T_p - T_b)} \tag{3.13}$$

Using the plate to bed heat transfer coefficient (h_{cb}) just determined, an estimate was made of the heat flux which reached the bed from the hot plexiglas strips adjacent to the heater sides (q_{sb}).

$$q_{sb} = h_{cb} \times A_s \times \{T(73) - T_b\} \tag{3.14}$$

Similar estimates were then prepared for the flux entering the bed from the hot sidewall section adjacent to the top edge of the heater (q_{tb}) as well as the section adjacent to the bottom edge of the heater (q_{bb}).

$$q_{tb} = h_{cb} \times A_t \times \{T(69) - T_b\} \tag{3.15}$$

$$q_{bb} = h_{cb} \times A_b \times \{T(70) - T_b\} \tag{3.16}$$

The heat flux into the bed from all sources other than the heater plate itself were then added to obtain a total value (q_{ob}).

62

$$q_{ob} = q_{sb} + q_{tb} + q_{bb} \qquad (3.17)$$

The original copper plate heat flux value was then cor-
rected to allow for that amount (q_{ob}) which did not pass
through the plates.

$$q_{cb} = q_{ei} - q_a - q_{ob} \qquad (3.18)$$

It was then necessary to recalculate all of the parameters
dependent on this value. This process was repeated in an iter-
ative fashion until the calculated flux through the plate did
not change signficiantly. Once the iterative process had been
completed, the final values were printed out and the entire
calculation process was repeated for the left hand heater.
The left hand heater calculations were similar to those used
for the right hand with the exception of variable names and
thermocouple numbers. Because of a limitation on the total
number of thermocouples which could be controlled by the
HP 3497A, there were no thermocouples available to measure
the inside and outside surface temperature of the plexiglas
sidewall section adjacent to the bottom edge of the left
hand heater. This prevented the calculation of a loss
estimate based on a direct measurement. To compensate for
this, it was assumed that the losses from the sidewall
sections adjacent to the top and bottom edges of the heater

were identical to one another. Once the left hand heater
computations were completed and the results displayed, cal-
culations were begun on an energy balance. The objective
was to determine the total amount of energy entering the bed
and then compare that with the amount calculated to be leaving
in order to validate the data and the calculations used. The
first parameter to be determined was the density of the air
within the bed ρ_a.

$$\rho_a = \frac{1.325 \times P_a}{(T_a + 459.69)} \tag{5.19}$$

$$P_a = 29.92 \text{ in. Hg}$$

$$T_a = T(55)$$

Since the air entering a fluidized bed is known to assume
the bed temperature within a very short distance of entry,
the air outlet temperature was used as the bed air temperature.

Using this value of density, the amount of energy carried
out of the bed by the fluidizing air stream (q_{ao}) was
calculated.

$$q_{ao} = \dot{m} \, C_p \, (T_{ao} - T_{ai}) \tag{3.20}$$

$$q_{ao} = \dot{V} \times \rho_{ab} \times 60 \text{ Min/Hr} \times 0.241 \times (T_{ao} - T_{ai}) \tag{3.21}$$

$$T_{ai} = \{T(47) + T(48) + T(49)\}/3$$

$$T_{ao} = T(55)$$

The heat loss through the front and rear walls (q_{fra}) was then estimated. Only the rear wall was instrumented, however, because of symmetry, it was assumed that the loss through the front wall would be identical.

$$q_{fra} = \frac{k_{fr} \times A_{fr} \times \{T(75) - T(74)\}}{L_{fr}} \qquad (3.22)$$

k_{fr} = 0.112 Btu/Hr-Ft-$^\circ$F

A_{fr} = 12 in. x W x ($\frac{1\ Ft}{12\ in.}$) x 2 (to account for both front and rear walls)

W = Bed Width

L_{fr} = 0.5 in.

The total heat flux leaving the bed q_o was then calculated. It was assumed that the only flux paths out of the bed were via the front and rear walls and via the outgoing air stream. The side walls were considered to be at a sufficiently elevated temperature as to block the flow of heat outward from the bed. The floor of the bed was considered to be free of losses since any heat passing through it would be returned to the bed by the fluidizing air stream as it passed through the distributor.

$$q_o = q_{oa} + q_{fra} \qquad (3.23)$$

The total energy into the bed from all right hand sources was then calculated (q_{br}). This included both the flux

through the plate and the flux through the sidewalls
adjacent to the heater.

$$q_{br} = q_{ei} - q_a \qquad (3.24)$$

A similar calculation was performed for the left hand
sources (q_{bl}) and then the total energy into the bed from
all sources was calculated (q_b).

$$q_b = q_{br} + q_{bl} \qquad (3.25)$$

The superficial gas velocity (U) (in Ft/Sec) was calculated
using the following equation:

$$U = \frac{\dot{V} \times (\frac{1\ Min}{60\ Sec})}{A_d} \qquad (3.26)$$

A_d = Distributor Area = 6 in. x W x $(\frac{1\ Ft^2}{144\ in^2})$

The superficial gas mass velocity (G) was then calculated.

$$G = \frac{Lbm}{Hr\text{-}Ft^2} = \frac{\dot{m}}{A_d} = U\ (\frac{Ft}{Sec}) \times \rho_a\ (\frac{Lbm}{Ft^3}) \times (\frac{3600\ Sec}{Hr})$$

$$G = U \times \rho_a \times 3600 \qquad (3.27)$$

66

The final calculation of the program was the determination of the particle Reynolds Number (Re).

$$Re = \frac{\rho V D_p}{\mu g_c} = \frac{G \times D_p}{3600 \times \mu \times g_c} \qquad (3.28)$$

$$\mu = 3.96 \times 10^{-7} \ Lbf\text{-}Sec/Ft^2$$

$$g_c = 32.174 \ Lbm\text{-}Ft/Lbf\text{-}Sec^2$$

$$D_p = 0.012 \ in. \times \left(\frac{1 \ Ft}{12 \ in.}\right)$$

Following the completion of this calculation the energy balance section of page six was printed out and the program was terminated.

IV. PRESENTATION AND DISCUSSION OF RESULTS

A. FLOW PATTERNS

The particle flow patterns observed in the course of this study were in general agreement with those described in the literature for a bubbling bed. The particles moved upward near the centerline of the bed as did most of the bubbles. Once the particles reached the surface of the bed they were thrown outward from the center and then proceeded to travel downward along the bed walls as shown in Figure 25. The area of greatest activity was roughly cylindrical in shape with the corner areas exhibiting considerably less particle motion. Observed particle stagnation regions are shown in Figure 26. No indications of channeling were observed visually at any time. At high fluidization flow rates in the narrow bed configuration, slugging was occasionally observed. This was characterized by the appearance of large bubbles and the sudden lifting of the bed surface to a level two to three inches above its previous position. Once the bubble reached the top of the bed, the surface would suddenly collapse and resume its former level until the next bubble appeared.

The particles within the bed were observed to behave in a manner much like a viscous fluid. The layer of particles directly adjacent to the walls showed little, if any, movement. Because of their transparent composition it was possible

68
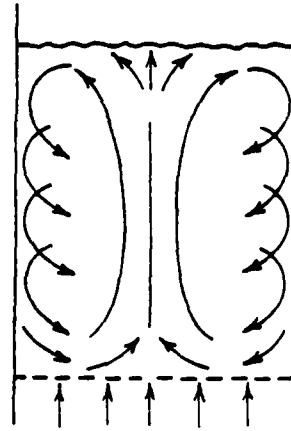
Figure 25. Observed Particle Circulation Flow Paths
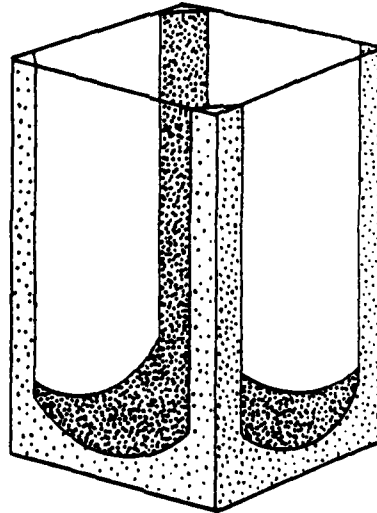
Figure 26. Observed Particle Stagnation Regions

69

to observe that the next layer of particles was moving at a slightly higher velocity and that the third layer inboard was moving even faster. This movement was not steady but tended to occur in surges. It is possible that a static charge contributed to the "No slip" condition observed at the boundary. After the fluidizing air flow was secured upon completion of a test run it was noted that numerous particles were clinging to the container walls in the upper portion of the bed. In an attempt to eliminate this condition, an anti-static film was sprayed on the upper portions of the bed walls. For a short period of time, the walls remained free of cling-ing particles, however, the effect did not last for more than two or three data runs. Following this, no further attempts were made to alter this phenomenon. Research by Miller and Logwinuk [Ref. 2] suggested that the presence of such a static charge could contribute to erratic heat transfer results, how-ever for the purpose of this study, any affect was considered to be negligible.

Closer examination of the bubble flow path showed that many bubbles tended to originate from the left side of the bed near the bottom of the movable side wall. As a result, there was a shift in overall particle activity to the left of center and a corresponding alteration of the quiescent zone near the bottom of the bed such that the majority of stagnant particles were located in the right hand corner.
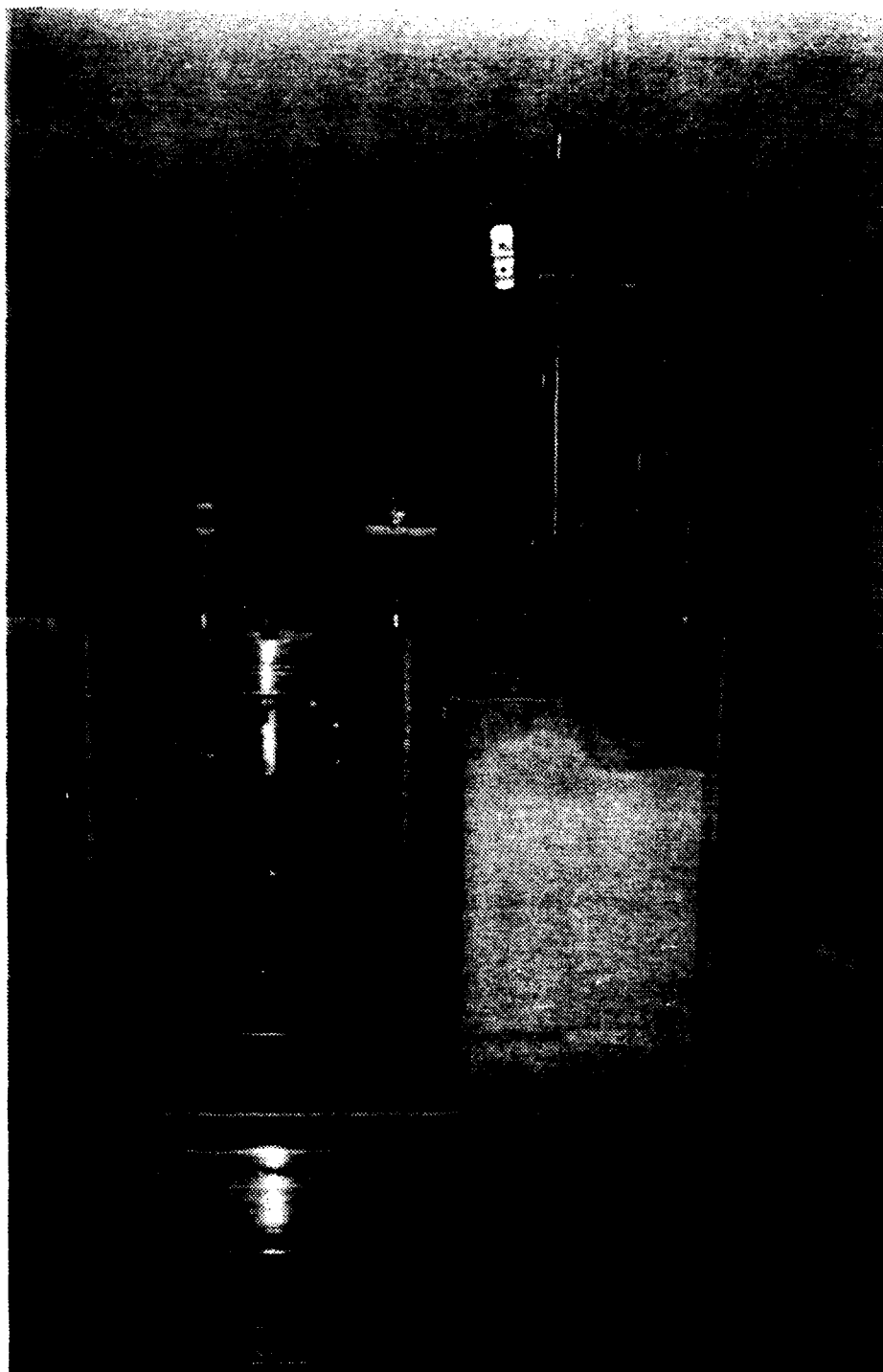
Figure 27. Photograph of Off-Center Bubble

71

This phenomenon was particularly noticeable in the wide bed configurations. An example of this off-center activity is shown in Figure 27.

Examination of the apparatus revealed that a stream of air was being injected into the bed from the area between the baffle plate and the distributor. Air from the inlet plenum was passing through the unused portion of the distributor to the left of the movable wall. Once the air was through the distributor, further upward progress was blocked by the baffle plate and the sealed joints. There was however, a very thin horizontal passage between the baffle and the top of the distributor as shown in Figure 28. The air flowed along this path until it emptied into the bed itself. Because of this "peripheral injection" there was an uneven distribution of fluidizing air and a resulting shift in the center of activity toward the left hand side. In order to determine the effect of this phenomenon an entire set of data was taken with the unused portion of the distributor masked-off from the underside so that no air could enter. During these masked data runs it was observed that the bubble path was very well centered as was the quiescent zone near the bottom of the bed. All other data runs were taken with the distributor unmasked in order to study the difference in heat transfer performance between the two sides. A detailed study of particle cell flow patterns for this apparatus was presented by Morgan [Ref. 2] in 1981.
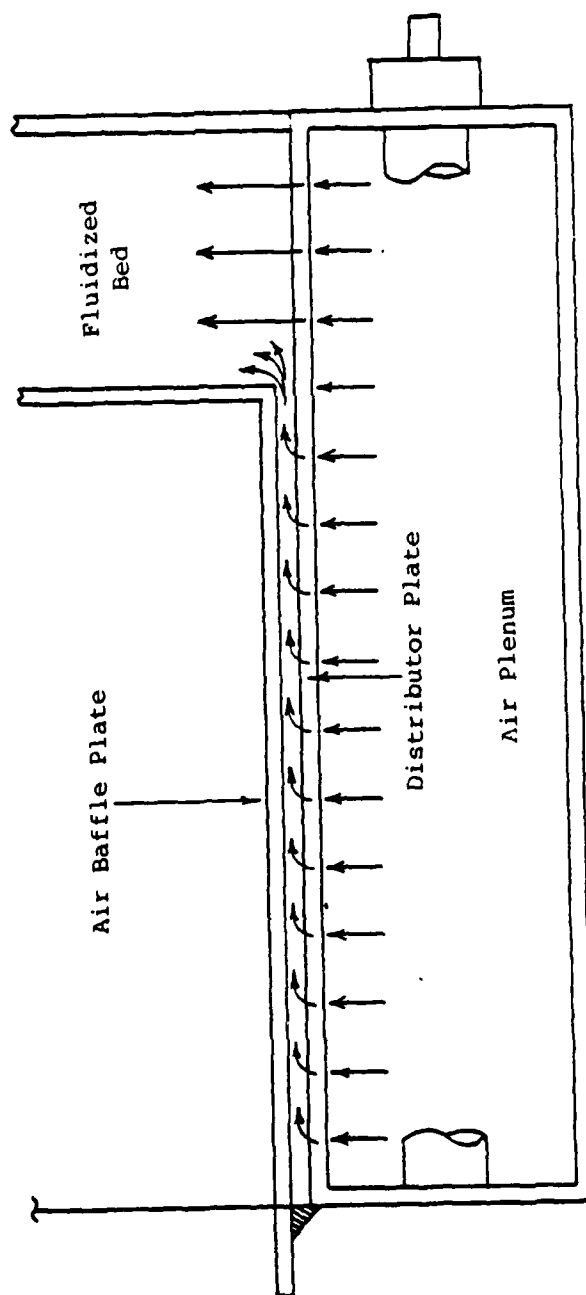
Figure 28. Air Baffle Leakage Flow Path

73

B. PRESSURE DROP DATA

Measurements were taken of the pressure drop across the bed for all flow rates and bed configurations. This data can be found in Appendix A. Plots were constructed of LOG ΔP vs. LOG G for each bed configuration in order to study the variation in pressure drop with changes in the superficial mass velocity. These plots are shown in Figures 29 through 32. An ideal pressure drop curve is shown in Figure 33. Each of the plots display the same basic characteristics of the ideal curve in that the pressure drop increases steadily until the point of minimum fluidization (G_{mf}) is reached. From that point onward, the pressure tends to remain relatively constant despite further increases in air flow rate. This is because of the fact that once the bed is fluidized, any further increase in the flow rate imparts an increased lift to the particles because of the viscous drag force exerted on them by the moving air stream. As the lift increases, expansion of the bed occurs and voidage (ε) increases. As the voidage increases, the interstitial spacing between the particles also increases. This results in a reduction of the interstitial gas velocity, which in turn, lowers the drag exerted on the particles until the gravitational force and the lift are once again in balance. As a result of the increased voidage, the pressure drop across the bed remains constant or may even decrease.

74

Examination of the pressure drop curve for the 6.25 inch configuration (Fig. 29) shows a deviation from ideal behavior in that the pressure drops sharply after reaching the point of minimum fluidization. A pressure drop of this sort is normally associated with channeling. As indicated previously, no visual indications of channeling were detected, however it is possible that "intermittent channeling" was taking place. This type of channeling would be difficult to differentiate from rapid bubbling because the channel does not extend through the entire depth of the bed as it does in "through channeling." An alternate explanation for the drop in pressure is the effect of particle interlocking which sometimes manifests itself during the initial fluidization of a bed. It is noted that subsequent data runs did not demonstrate such behavior.

Based on the curve shown in Figure 29 the point of minimum fluidization for the 6.25 inch configuration occurred at $G = 159.6$ Lbm/Hr-Ft^2 (26% flow). It was was noted the visual observation of fluidization onset occurred at the same air flow rate as was predicted by this curve.

The pressure drop curve for the 8 inch configuration (Fig. 30) is in very close agreement with the ideal curve with no indications of channeling or slugging. Based on this curve the point of minimum fluidization occurred at $G = 132.6$ Lbm/Hr-Ft^2 (28% flow). Fluidization was visually observed to commence at 137 Lbm/Hr-Ft^2 (29% flow).
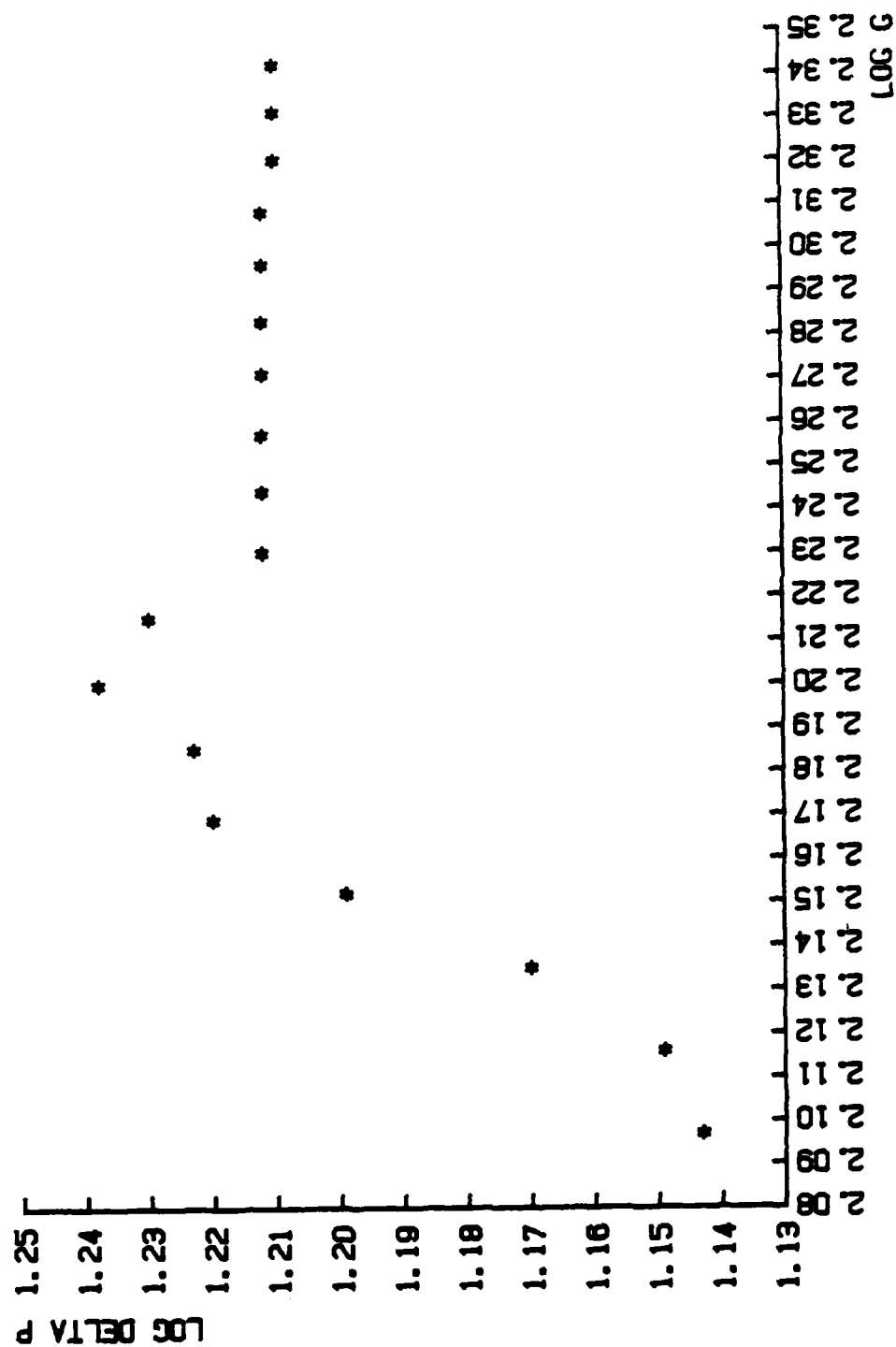
Figure 29. Pressure Drop vs Superficial Mass Velocity;
6.25 in. Bed
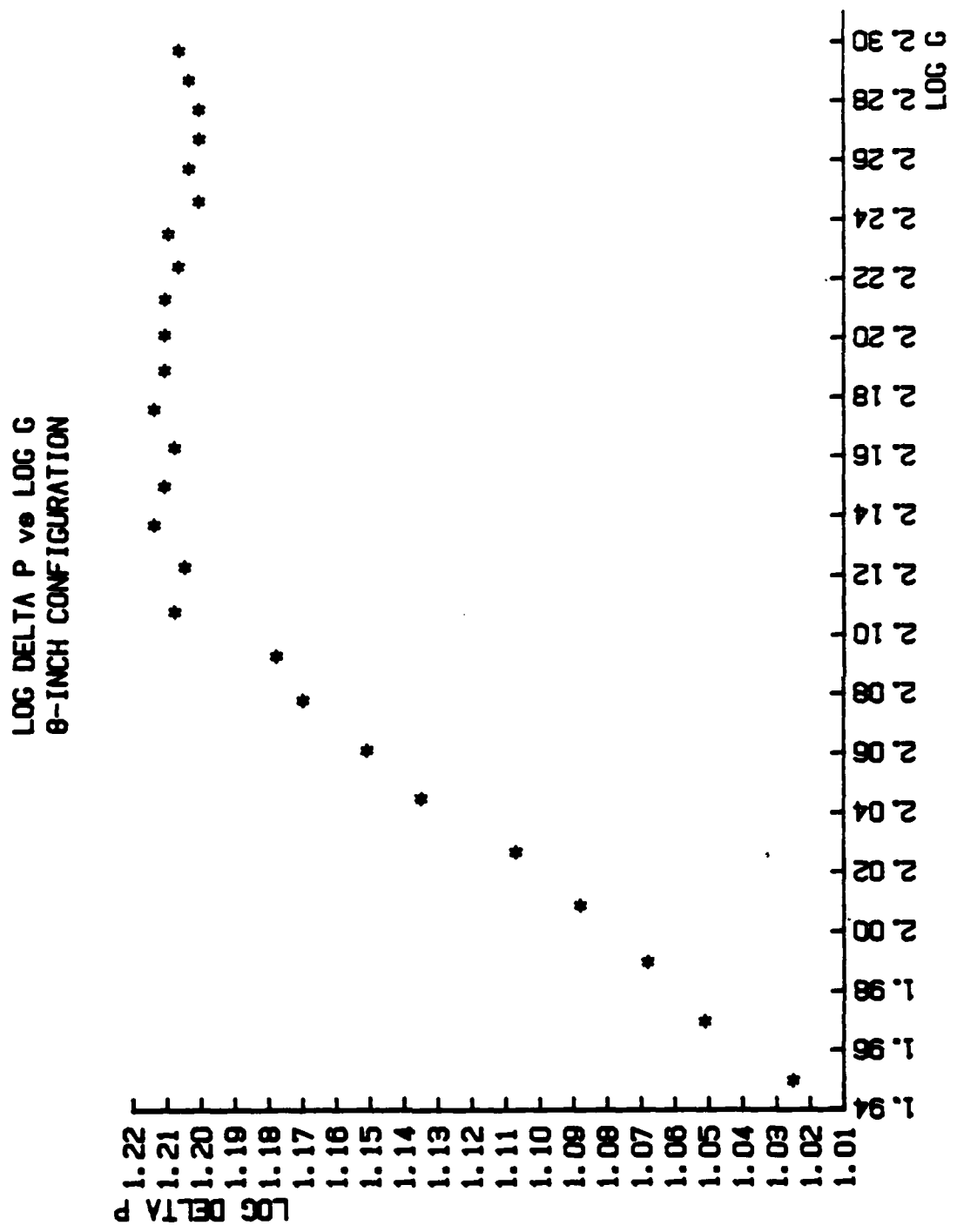
Figure 30. Pressure Drop vs Superficial Mass Velocity; 8.0 in. Bed
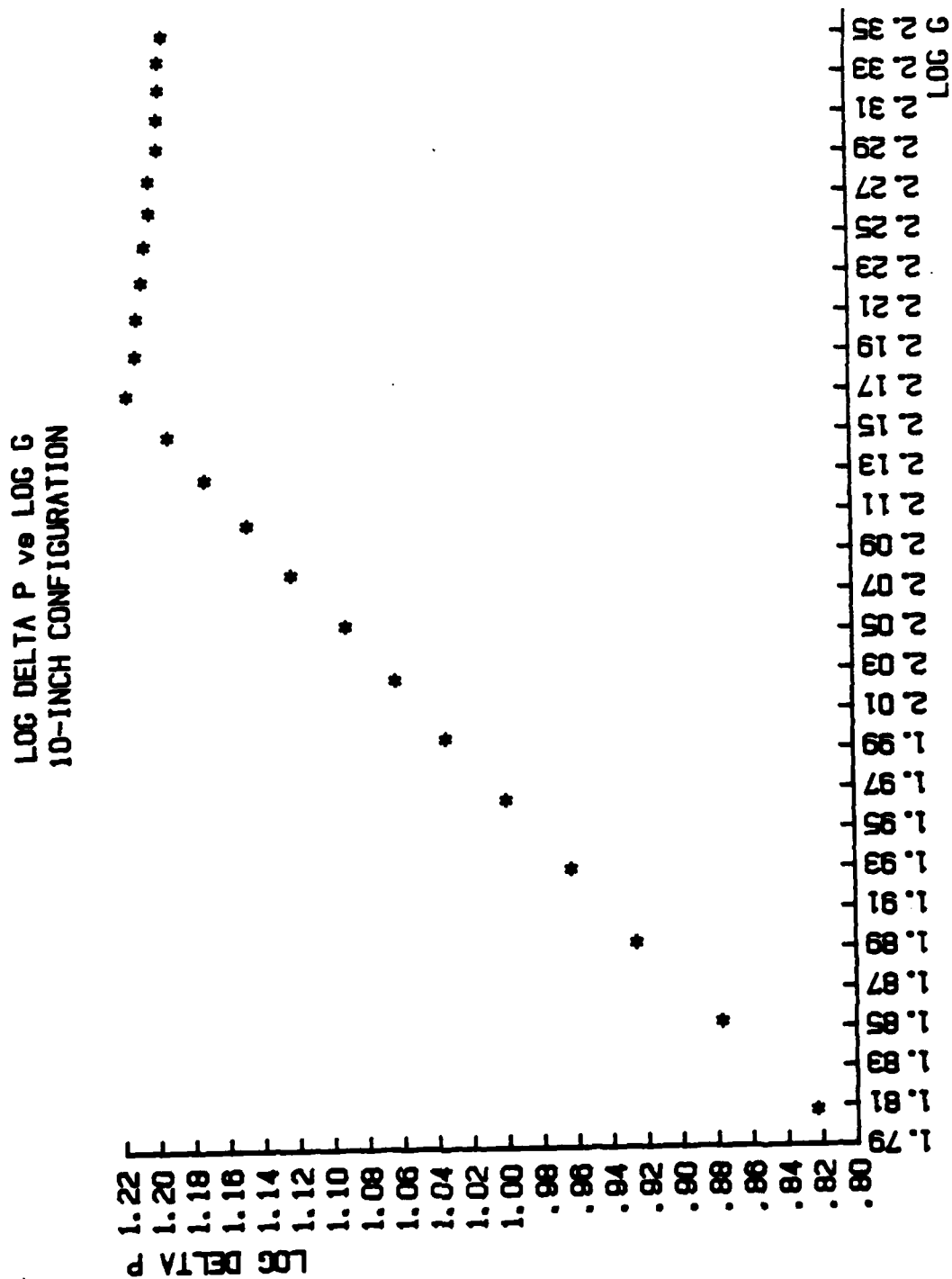
Figure 31. Pressure Drop vs Superficial Mass Velocity; 10.0 in. Bed
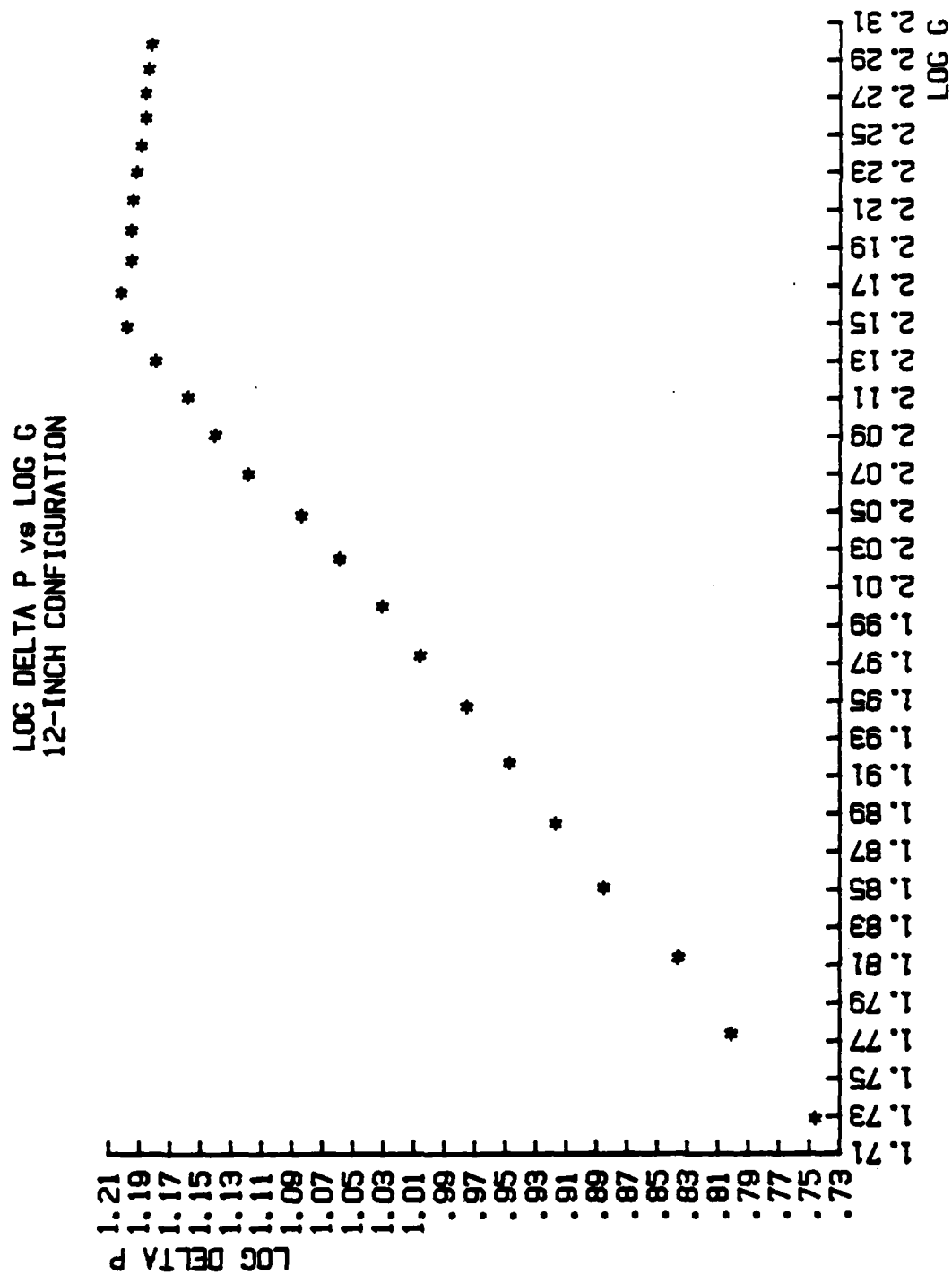
Figure 32.   Pressure Drop vs Superficial Mass Velocity;
            12.0 in. Bed

79
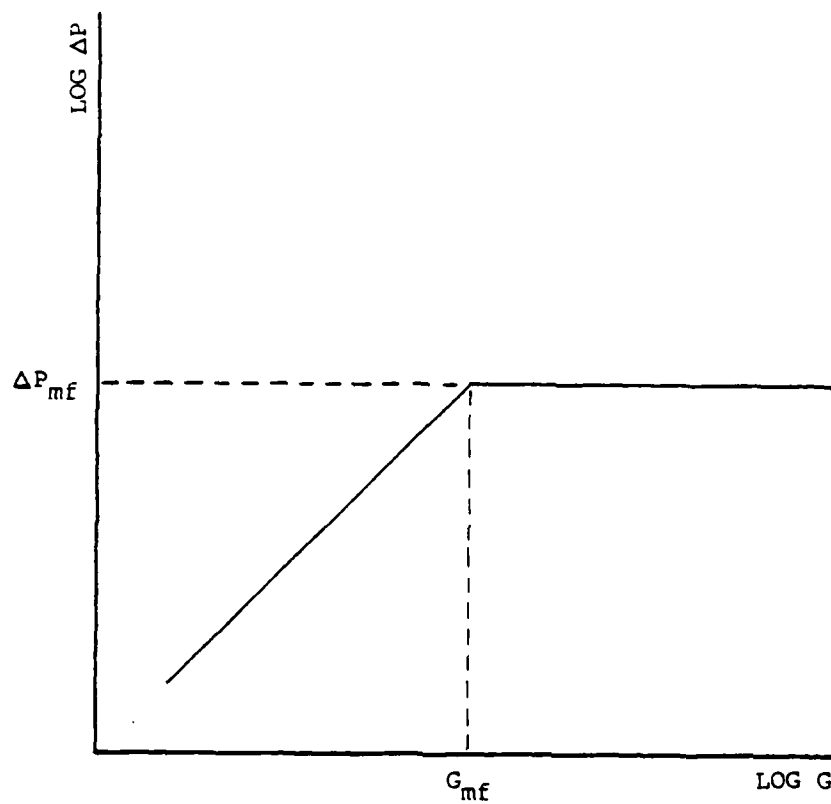
Figure 33. Pressure Drop vs Superficial Mass Velocity; Ideal

The curve for the 10 inch configuration (Fig. 31) was smoother than the previous configurations and matched the ideal curve closely except for a gradual decrease in pressure following fluidization onset. The reason for this decrease was not readily apparent. The curve shows that fluidization commenced at $G=148$ Lbm/Hr-Ft^2 (40% flow). The observed starting point of fluidization was also at 40% flow.

The 12 inch configuration curve (Fig. 32) was also very smooth and similar to the ideal. Like the 10 inch curve, a slight decrease in differential pressure was noted. The starting point of fluidization (G_{mf}) indicated by the curve was $G=146.5$ Lbm/Hr-Ft^2 (48% flow). Fluidization was visually observed to commence at the same point.

A combined graph showing the pressure drop curves for all four configurations is shown in Figure 34. With the exception of the 8 inch configuration, they show a slight gradual decrease in the minimum fluidization superficial mass velocity (G_{mf}) as the bed width is increased. A similar trend was observed by Morgan [Ref. 2] who attributed this to a reduction in the effect of the wall frictional drag as a fraction of the overall drag experienced by the bed.

The average bed pressure drop at minimum fluidization (P_{mf}) for all configurations was approximately 16.0 in. H_2O or 0.577 psi. Research by Trivedi et al [Ref. 6] indicated that the pressure drop across a fluidized bed should equal
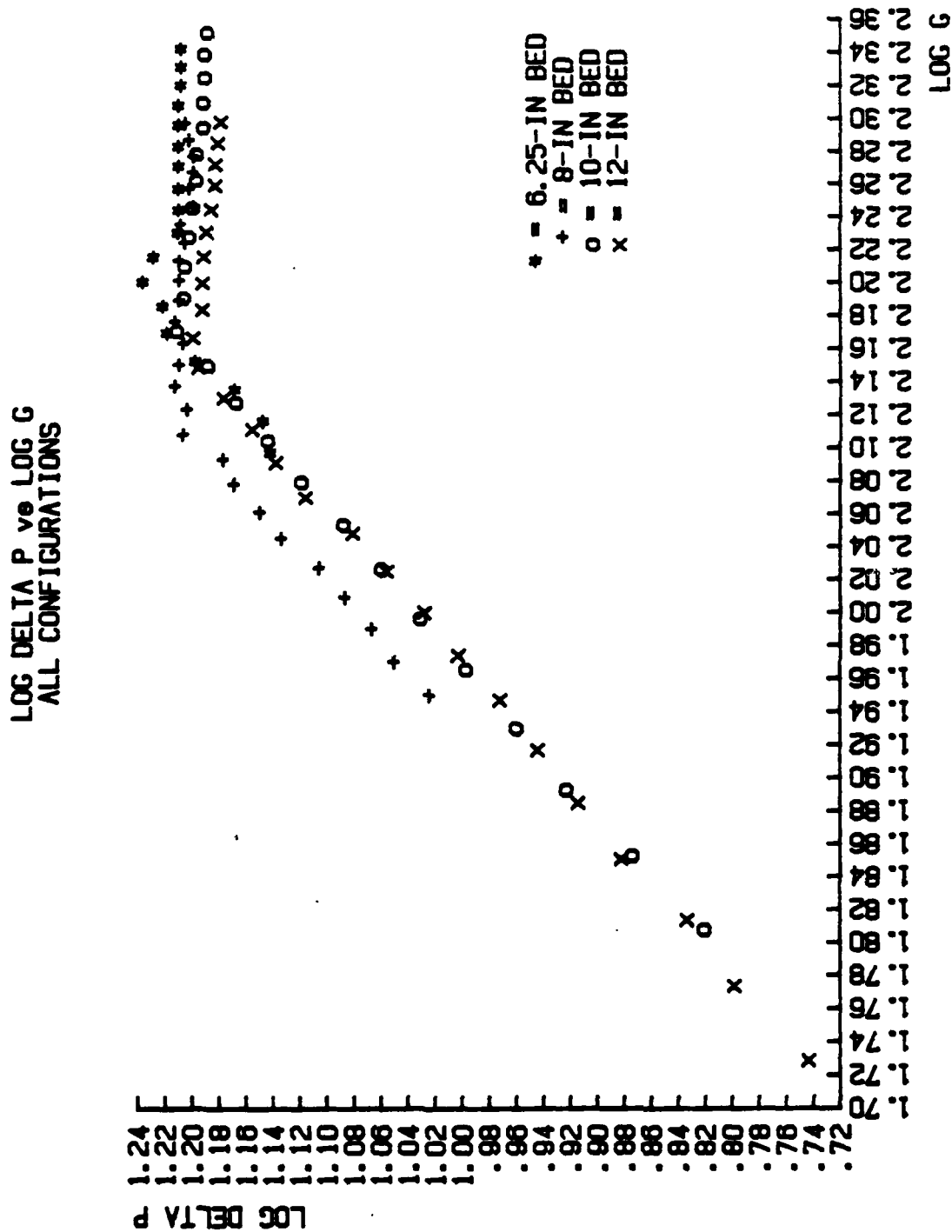
Figure 34. Pressure Drop vs Superficial Mass Velocity;
           All Configurations

82

the weight of the bed material per unit cross sectional area.
The settled bed density for the glass beads used in this ex-
periment was 96 Lbm/Ft^3 which resulted in a weight-to-area
ratio of 0.681 Lbm/In^2. Thus, the pressure drop observed
was slightly less than the theoretical value. Recalculation
of the weight-to-area ratio based on the expanded bed density
yielded essentially the same results.

C. TEMPERATURE DISTRIBUTION

The temperature distribution across each of the heater
surfaces was examined for all data runs and two distinct
trends were found to be evident. First; the four thermo-
couple readings in any horizontal row were found to be in
very close agreement with one another in all cases as shown
in Appendix E. This even distribution of temperature hori-
zontally across the plate suggested that the local rate of
heat transfer from the plate was the same for any given point
along the plate surface at a given bed depth. This conclusion
was based on the assumption that the heat flux into the plate
was also horizontally uniform. The second trend observed was
that there was a variation in heater temperature from the top
of the plate to the bottom and that this "temperature profile"
displayed a distinct and predictable change in shape as the
air fluidization flow rate was increased. Figures 35 through
44 illustrate these trends. At low air flow rates the point
of greatest temperature was always at the top of the plate.
Moving downward, the temperature then gradually dropped in

a non-linear but smooth fashion to a level approximately three to five degrees less than that observed at the top of the plate. Examination of the plots of temperature vs bed depth for the low flow rate runs showed all of the curves to have the same shape with each curve displaying a positive slope. It was noted that as the flow rates increased, the slope of these curves became more positive until they assumed a vertical orientation and then reversed their slope to become negative. It was further noted that this slope reversal occurred at or near the point of fluidization onset. The change in slope of these curves meant that the peak temperature within the plate was moving downward from the top of the plate toward the bottom as the fluidization air flow rate was increased. A possible explanation of such behavior lies in the fact that prior to fluidization onset, when the particles were not in motion, the heater was primarily cooled by an upward flow of air from the distributor. Because of this upward flow path, the temperature of the heater tended to increase with an upward movement along the plate. Once the bed was fluidized, however, a significant amount of cooling was then provided by the moving particles sweeping along the plate surface. Since the particles were moving downward along the wall a thermal gradient was introduced which was opposite to that caused by the upward flow of air. The peak temperature within the plate would consequently be observed at the point where these two gradients met. If the

84

cooling due to the particles was greater than that provided by the upward air flow, the peak temperature would be found toward the bottom of the plate. Conversely, if the air flow cooling predominated, the peak temperature would be seen in the upper section of the plate. An increase in the fluidization air flow rate would provide more upward flowing cooling air while simultaneously increasing the downward moving particle activity.

Experimental results showed that an increase in air flow rate caused the peak temperature to move downward. This suggested that, as the flow rate was increased, the increase in particle cooling predominated over the increase in air cooling. The reason for this predominance may have been that the particles had a much higher specific heat capacity than the air and a lower mean velocity. Consequently, they were able to remove a larger quantity of heat. Another possible cause for the particle cooling predominance as flow rates were increased was that the motion of the cooling air may have been altered once fluidization commenced so that more of the upward moving gas was concentrated in the center of the bed. Although there was no objective evidence that this was occurring, it may have been that any increase in flow rate was merely diverted to the center of the bed and consequently did not increase the amount of cooling air available near the wall.

Another trend which was observed while studying the heater temperature distributions was that as the bed width increased,

the shift in the orientation of the temperature curve became less pronounced. In the 6 inch configuration the peak temperature point moved from the top of the bed downward to the very bottom as fluidization activity increased. The maximum temperature differential observed between the top and the bottom of the plate was approximately 17 degrees. In the 8 inch configuration, the peak temperature point also transited down the entire length of the plate, however it did so at a slower rate than in the 6 inch configuration. The maximum top-to-bottom differential was essentially the same as that seen for the 6 inch bed. With the bed configured to the 10 inch width, the peak temperature did not move down the entire length of the plate, but instead stopped at a level approximately 3 inches above the bottom edge. The shift in temperature orientation was even more gradual than in the 8 inch configuration. The maximum observed temperature differential was approximately 11 degrees. While in the 12 inch configuration, very little change was observed in the temperature distribution as the flow rate was increased. The peak temperature shifted from the top of the plate to just above center, however the maximum temperature differential of 6 degrees was significantly less than that observed in the other configurations.

In general, the right hand heater temperature distribution proved to be more sensitive to changes in flow rate than did the left hand heater.

A characteristic unique to the left hand heater was that immediately prior to commencement of the downward transit of the peak temperature point, the temperature differential between the top and the bottom of the plate suddenly increased to approximately three times its previous value. As the flow rate was further increased, this differential abruptly dropped back down to its former level. This trend is shown in Figures 40 through 43. It is believed that this fluctuation could be related to a possible reorientation of air flow patterns as fluidization commences. This phenomenon was not evident in the right hand heater temperatures.

Examination of the data in Appendix C shows that for each flow rate and bed configuration, the average temperature of the left hand heater was lower than for the right hand heater.

In many cases, the difference in cooling of the plates was quite significant. During the data runs with the distributor masked-off, it was observed that the left and right hand heaters were being cooled to approximately the same degree, since the average heater temperatures were in close agreement with one another.

The temperature profile of the bed itself, as measured by the immersed probes, showed a non-uniform distribution prior to the commencement of fluidization for all configurations. The temperatures were highest near the heater surfaces where particle heating was taking place by conduction. Because of the relatively low rate of heat transfer the
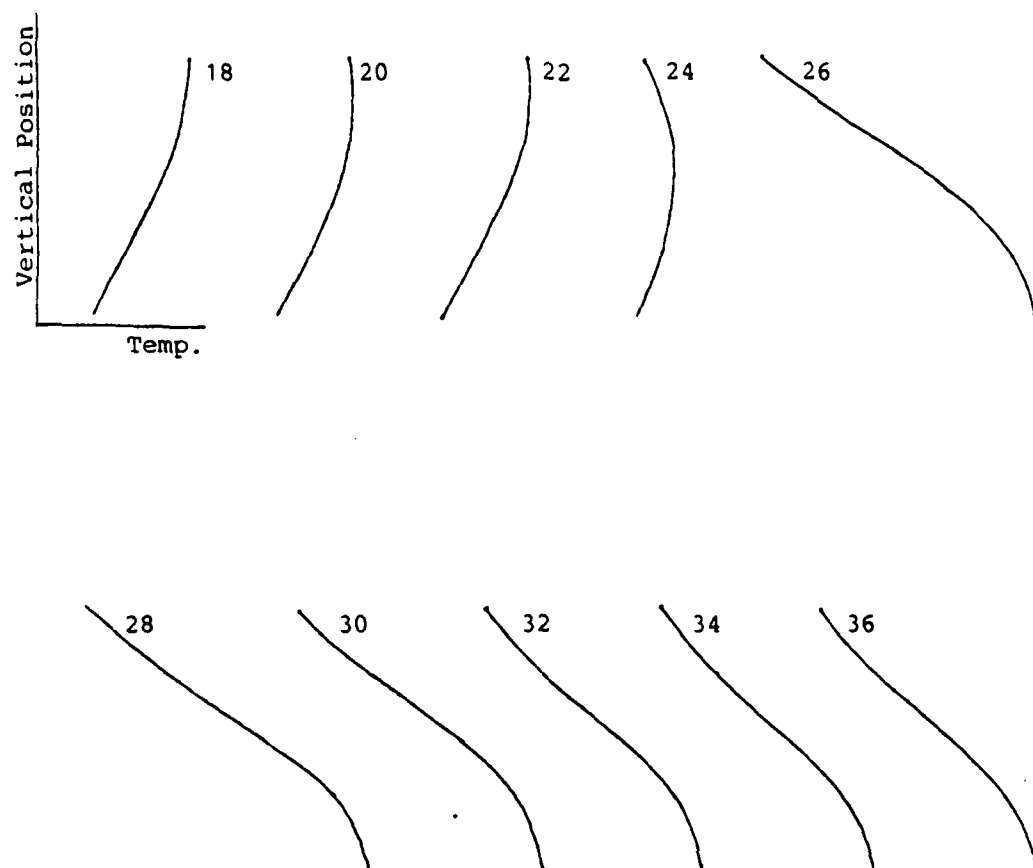
NOTE: Numerical values represent flowmeter readings as a
percentage of maximum rotometer capacity.

Figure 35. Right Hand Heater Temperature Profiles; 6.25 in.
Configuration
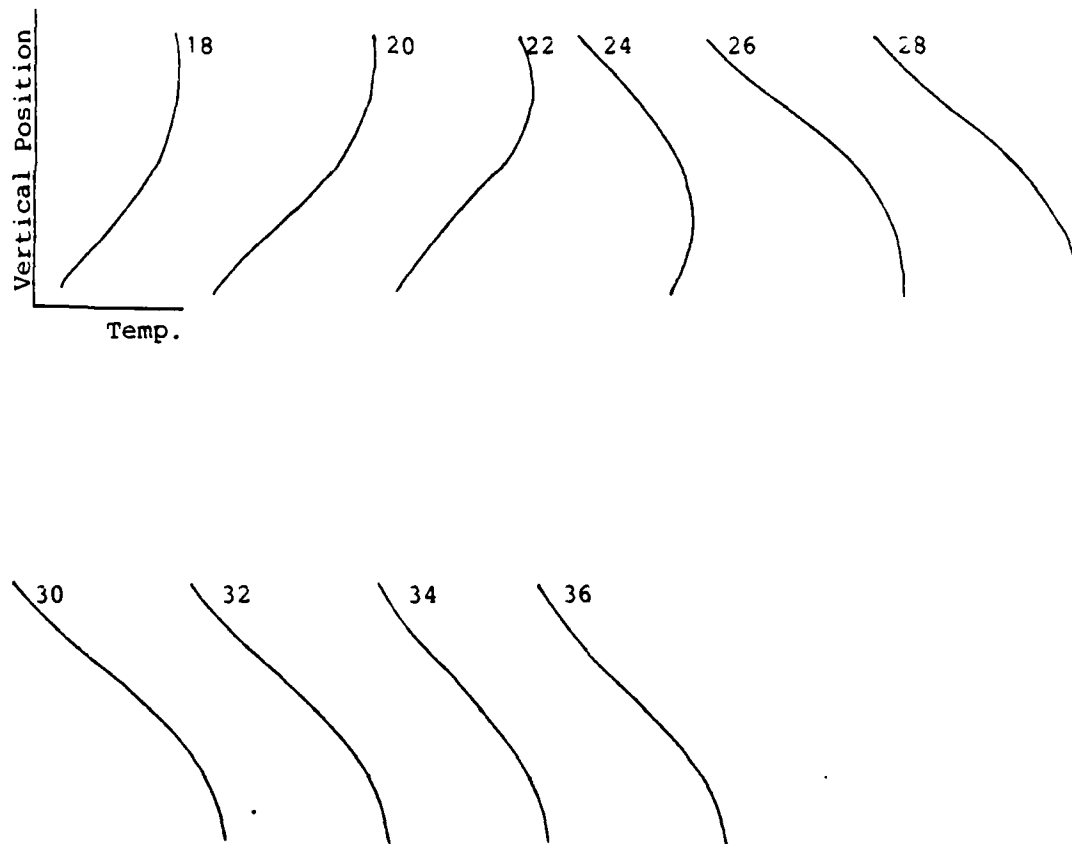
NOTE: Numerical values represent flowmeter readings as a percentage of maximum rotometer capacity.

Figure 36.   Right Hand Heater Temperature Profiles; 6.25 in. Masked Configuration
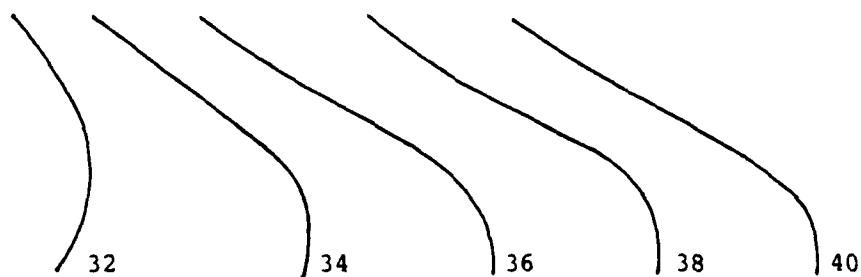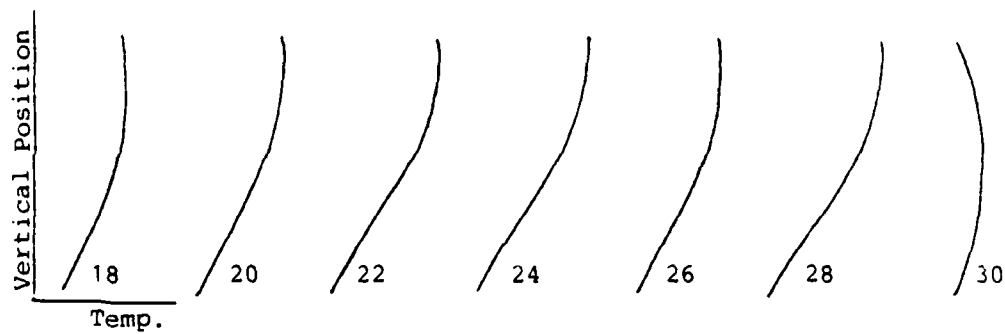
89

NOTE: Numerical values represent flowmeter readings as a percentage of maximum rotometer capacity.

Figure 37. Right Hand Heater Temperature Profiles; 8.0 in. Configuration
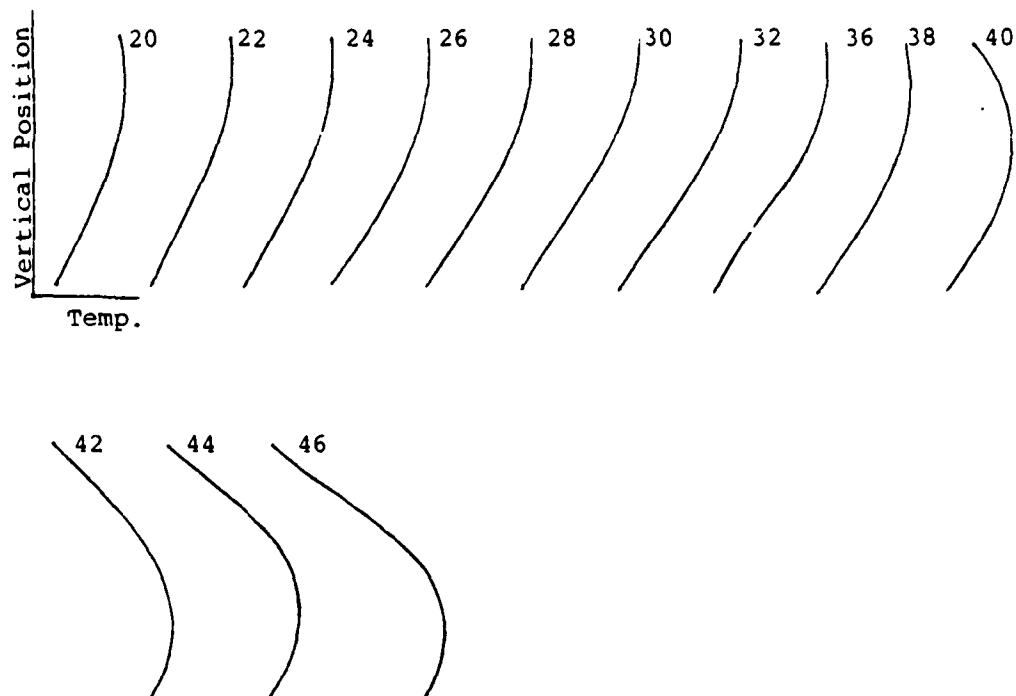
NOTE: Numerical values represent flowmeter readings as a
      percentage of maximum rotometer capacity.

Figure 38.   Right Hand Heater Temperature Profiles; 10.0 in.
             Configuration
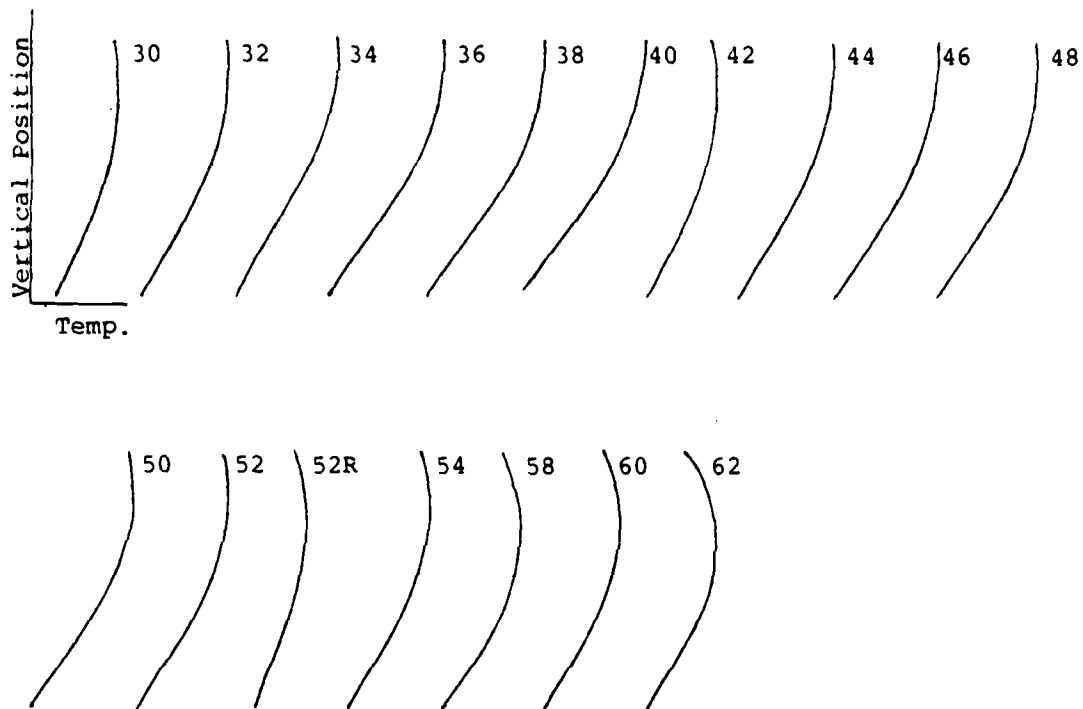
Vertical Position

30 32 34 36 38 40 42 44 46 48

Temp.

50 52 52R 54 58 60 62

NOTE: Numerical values represent flowmeter readings as a
percentage of maximum rotometer capacity.

Figure 39. Right Hand Heater Temperature Profiles; 12.0 in.
            Configuration
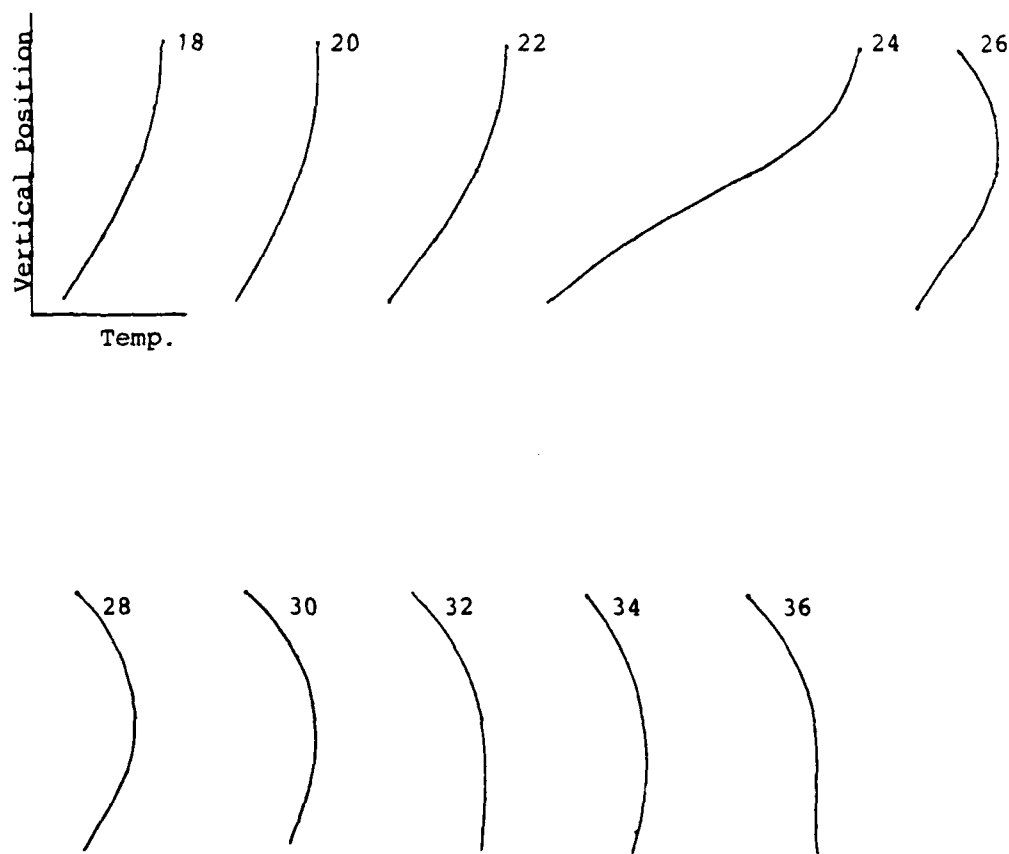
NOTE: Numerical values represent flowmeter readings as a
percentage of maximum rotometer capacity.

Figure 40.   Left Hand Heater Temperature Profiles; 6.25 in.
             Configuration
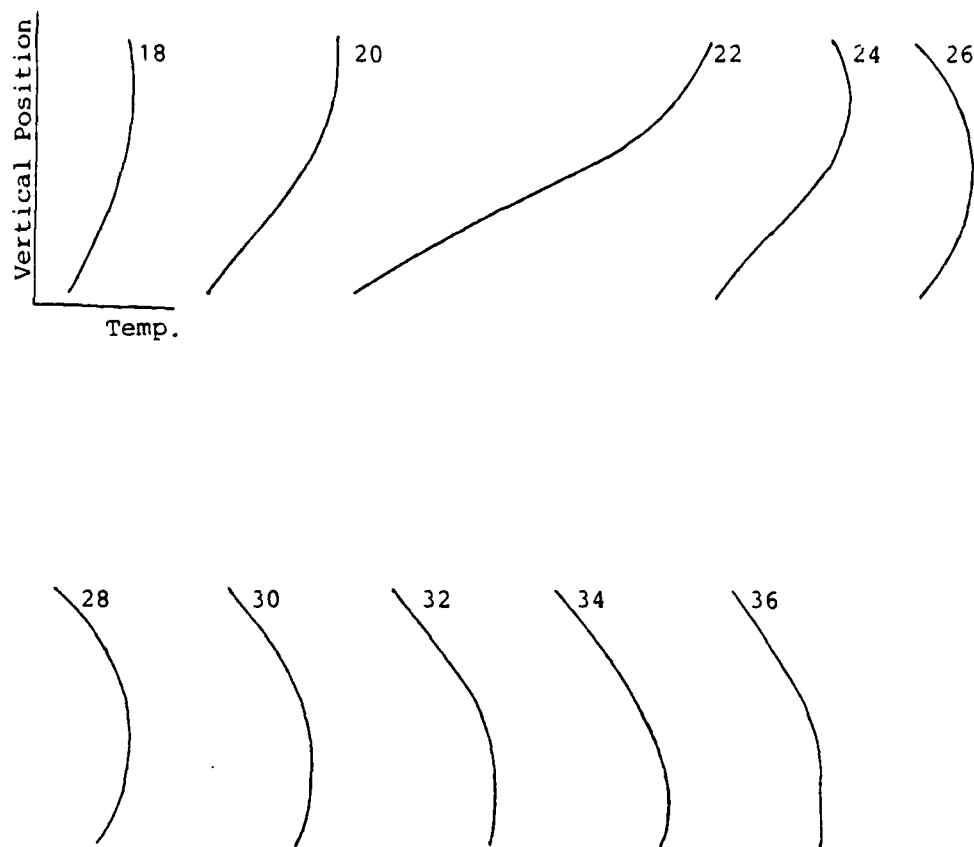
NOTE: Numerical values represent flowmeter readings as a percentage of maximum rotometer capacity.

Figure 41. Left Hand Heater Temperature Profiles; 6.25 in. Masked Configuration
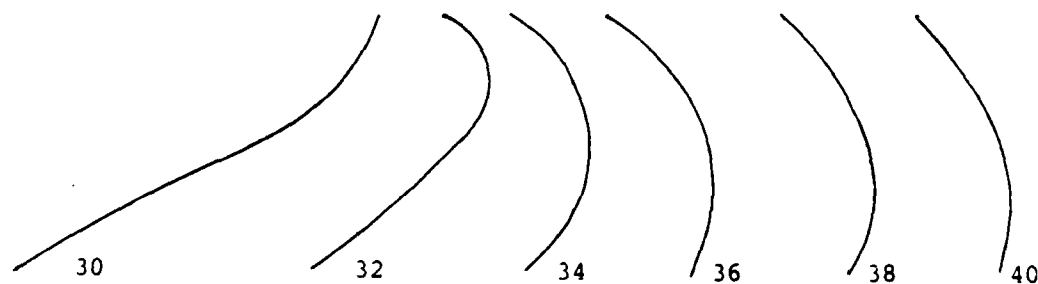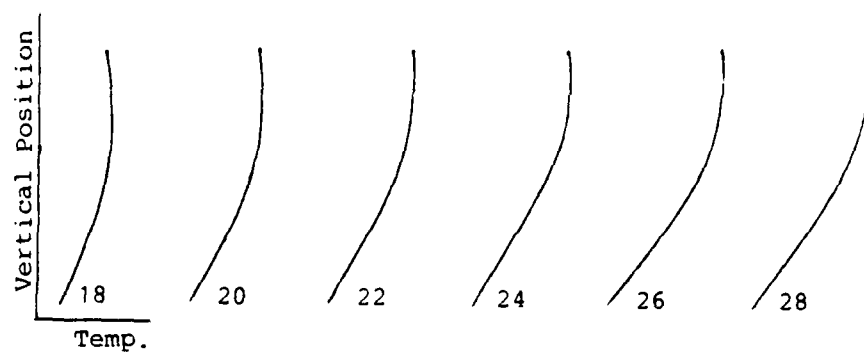
NOTE: Numerical values represent flowmeter readings as a
percentage of maximum rotometer capacity.

Figure 42. Left Hand Heater Temperature Profiles; 8.0 in.
Configuration

95
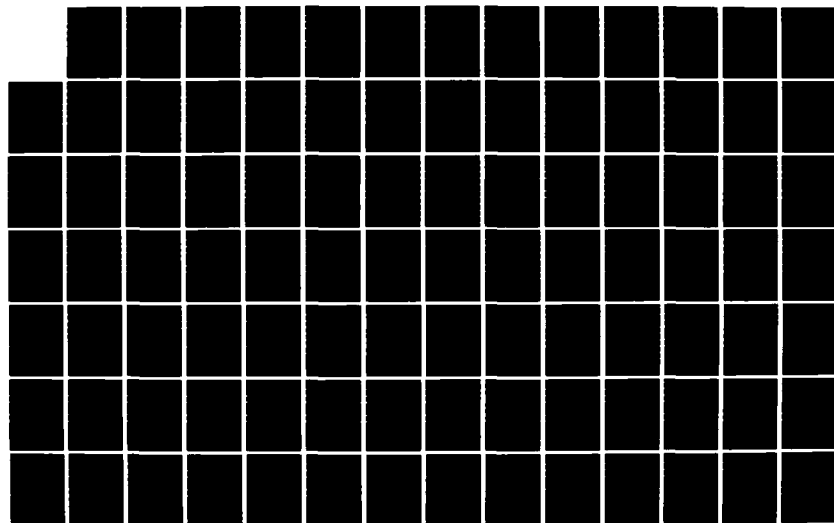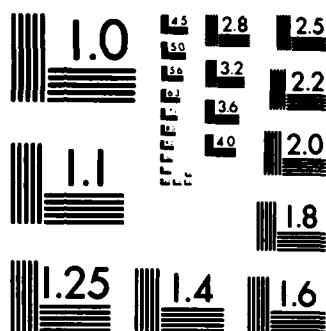
MICROCOPY RESOLUTION TEST CHART

NATIONAL BUREAU OF STANDARDS-1963-A
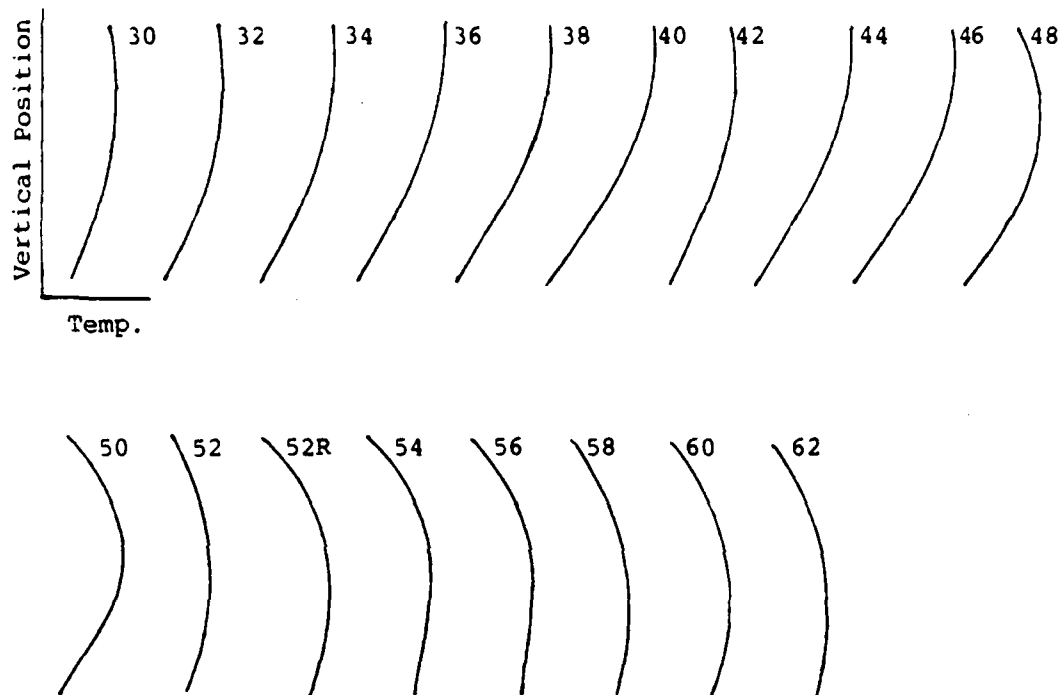
NOTE: Numerical values represent flowmeter readings as a percentage of maximum rotometer capacity.

Figure 44.   Left Hand Heater Temperature Profiles; 12.0 in. Configuration
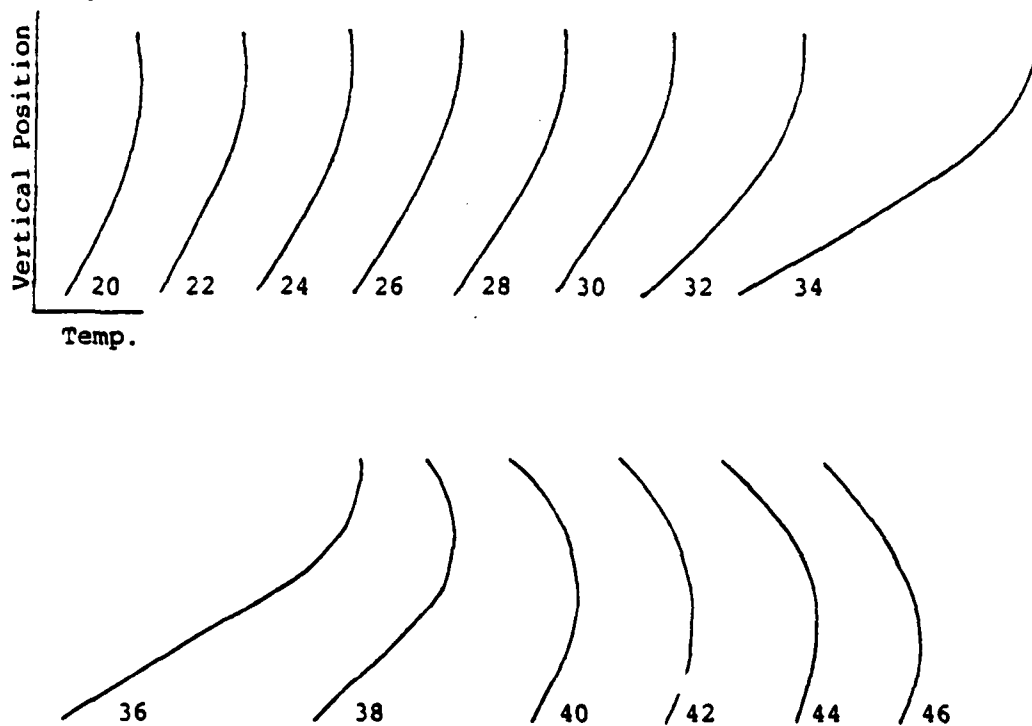
NOTE: Numerical values represent flowmeter readings as a percentage of maximum rotometer capacity.

Figure 43. Left Hand Heater Temperature Profiles; 10.0 in. Configuration

temperature tended to decrease toward the center. Immediately upon commencement of fluidization, however, the temperature distribution within the bed became extremely uniform and remained so as fluidization flow rates increased. This was directly attributable to the thorough mixing induced by the fluidized particle motion. In most cases, the temperature of the outgoing airstream was within two or three of the temperature of the bed itself.

D. HEAT TRANSFER COEFFICIENTS

In order to establish a performance baseline, data was collected for a bed from which all of the particles had been removed and an average heat transfer coefficient of 3.8 Btu/Hr-Ft^2-^{o}F was calculated. All remaining runs were accomplished with the apparatus filled to a settled bed depth of approximately 12 inches. The resulting heat transfer data for all runs is tabulated in Appendix C and plots of heat transfer coefficient vs. superficial mass velocity are shown in Figures 45 through 53. Each of these plots demonstrates the same basic trend in that initially, during low gas flow rate conditions, the heat transfer coefficient was correspondingly low (approximately 4.5 Btu/Hr-Ft^2-^{o}F) and remained low until a flow rate approaching the minimum fluidization superficial mass velocity (G_{mf}) was attained. From this point onward, the heat transfer coefficient increased in a roughly linear fashion as the gas flow rate was increased.

98
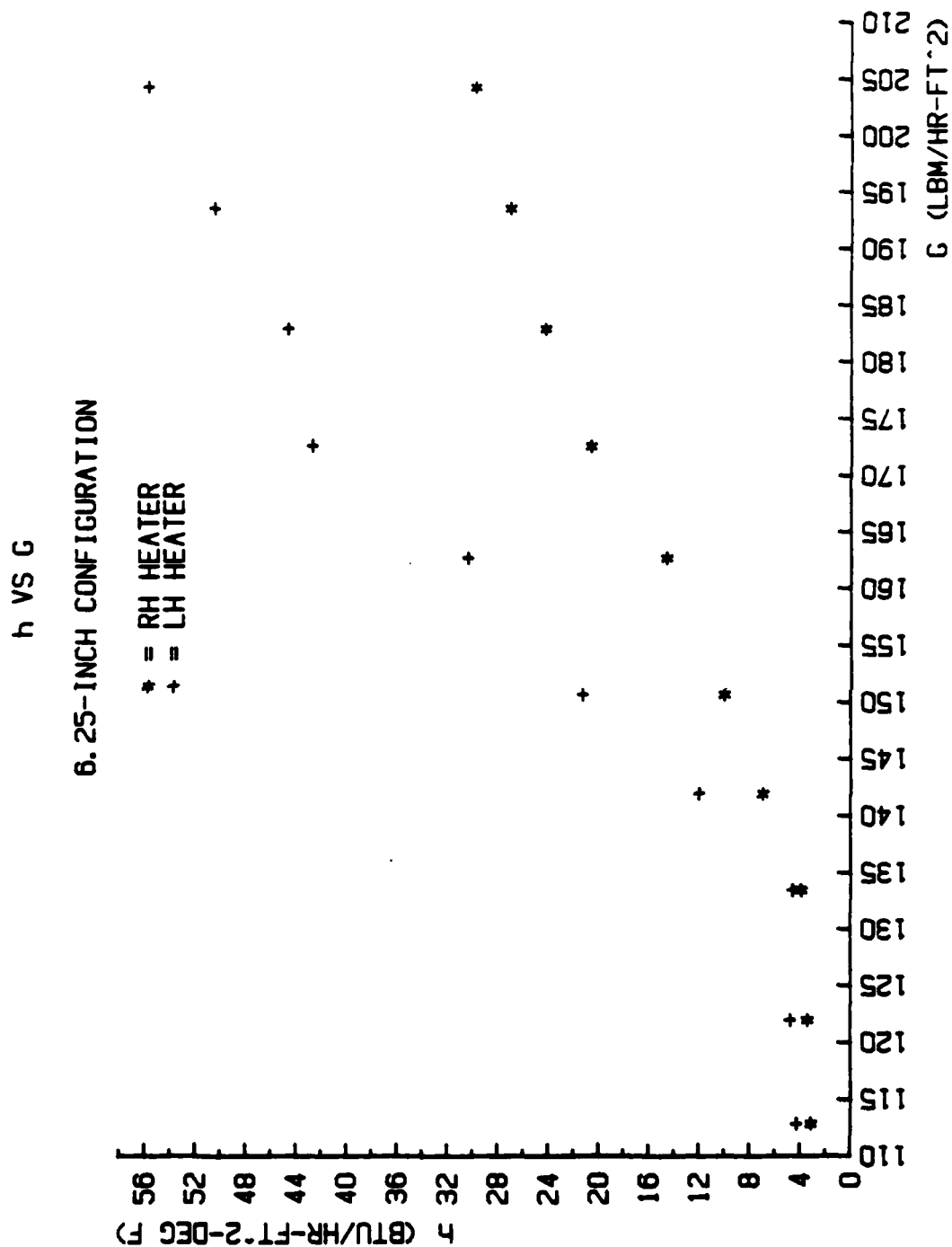
Figure 45. Heat Transfer Coefficient vs Superficial Mass
Velocity; 6.25 in. Configuration

99

h VS G

6.25-INCH CONFIGURATION-MASKED DISTRIBUTOR

* = RH HEATER
+ = LH HEATER

G (LBM/HR-FT^2)

h (BTU/HR-FT.2-DEG F)
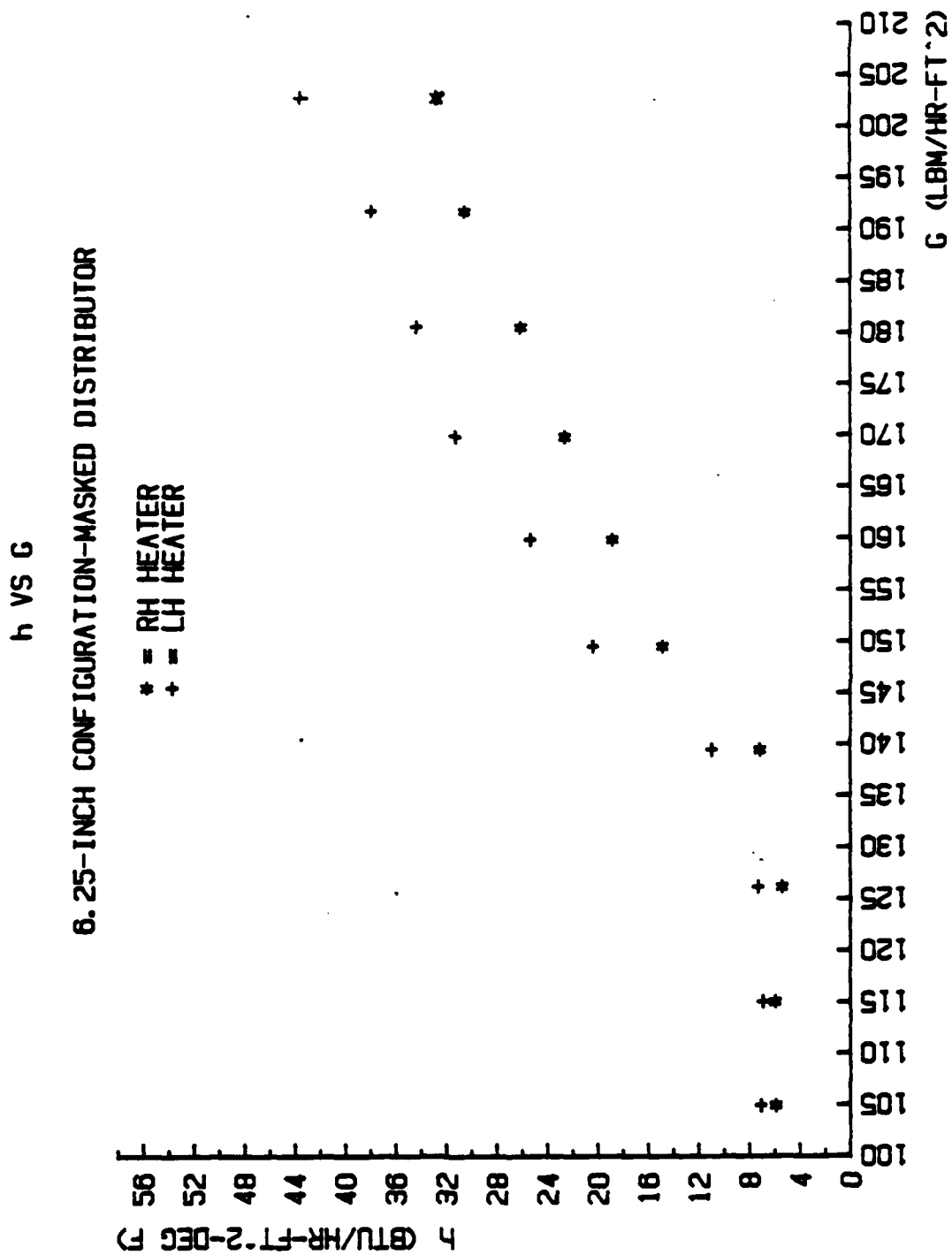
Figure 46. Heat Transfer Coefficient vs Superficial Mass
Velocity; 6.25 in. Masked Configuration

100
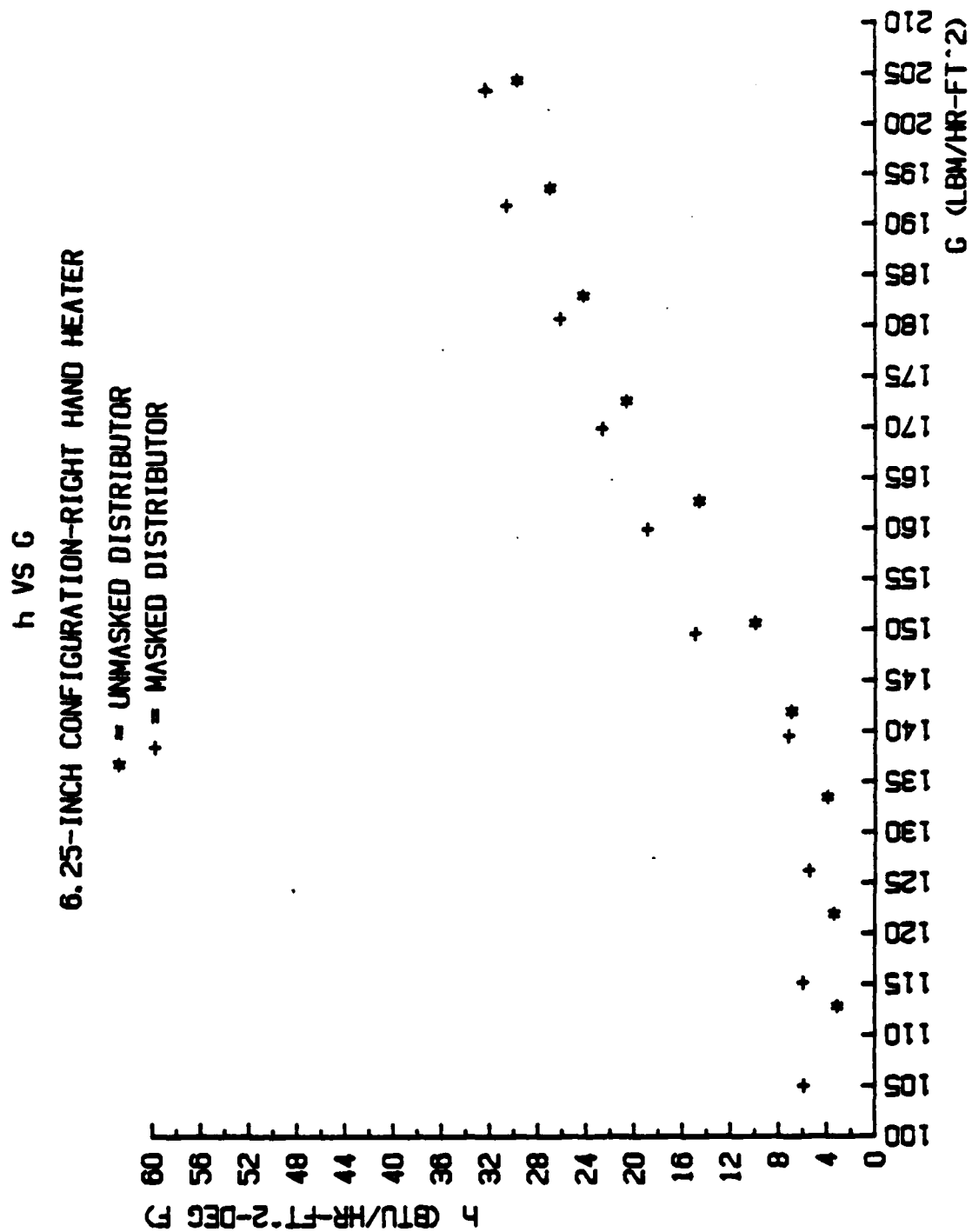
Figure 47. Heat Transfer Coefficient vs Superficial Mass Velocity; Right Hand Heater, 6.25 in. Configuration

101
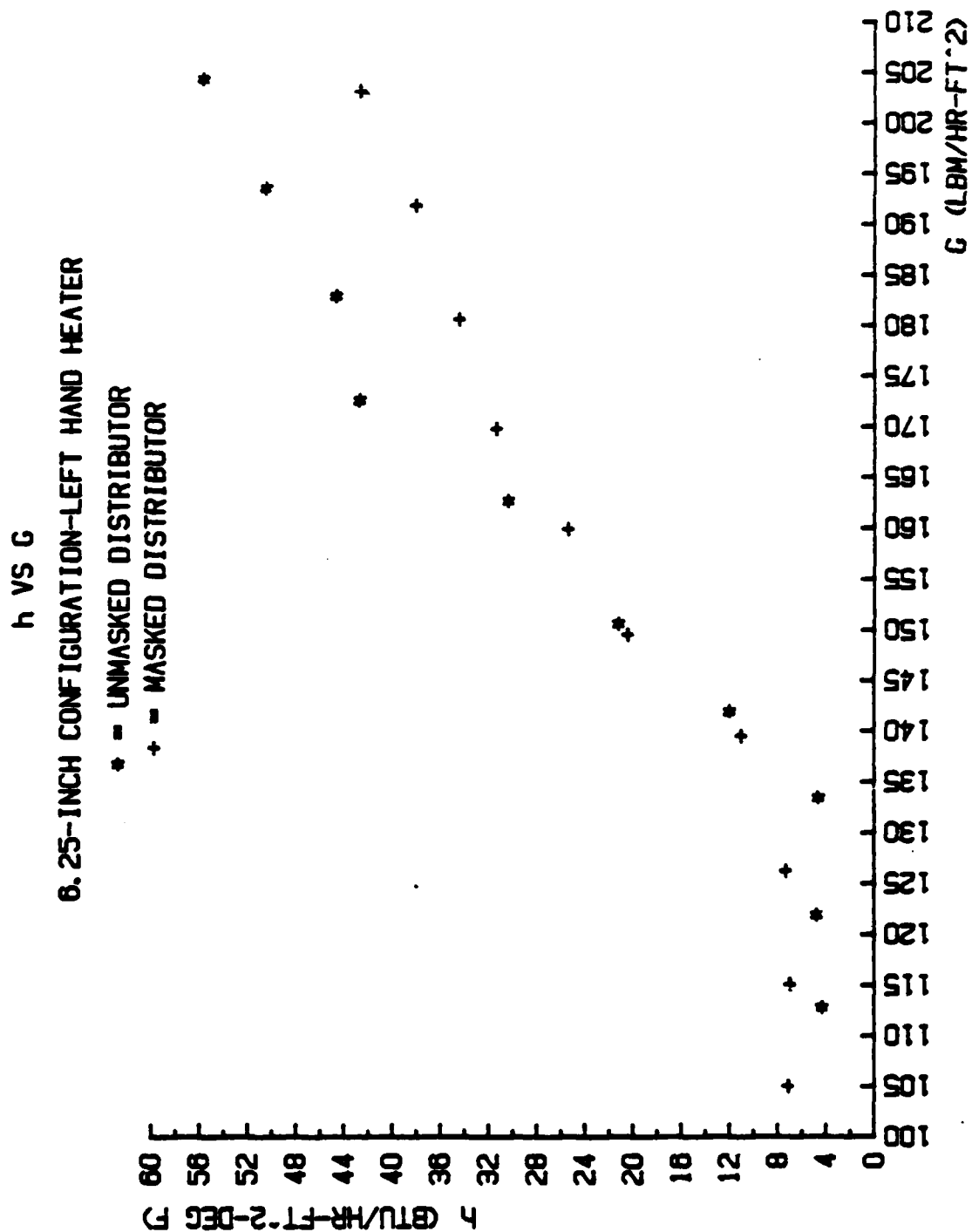
Figure 48. Heat Transfer Coefficient vs Superficial Mass Velocity; Left Hand Heater, 6.25 in. Configuration

102
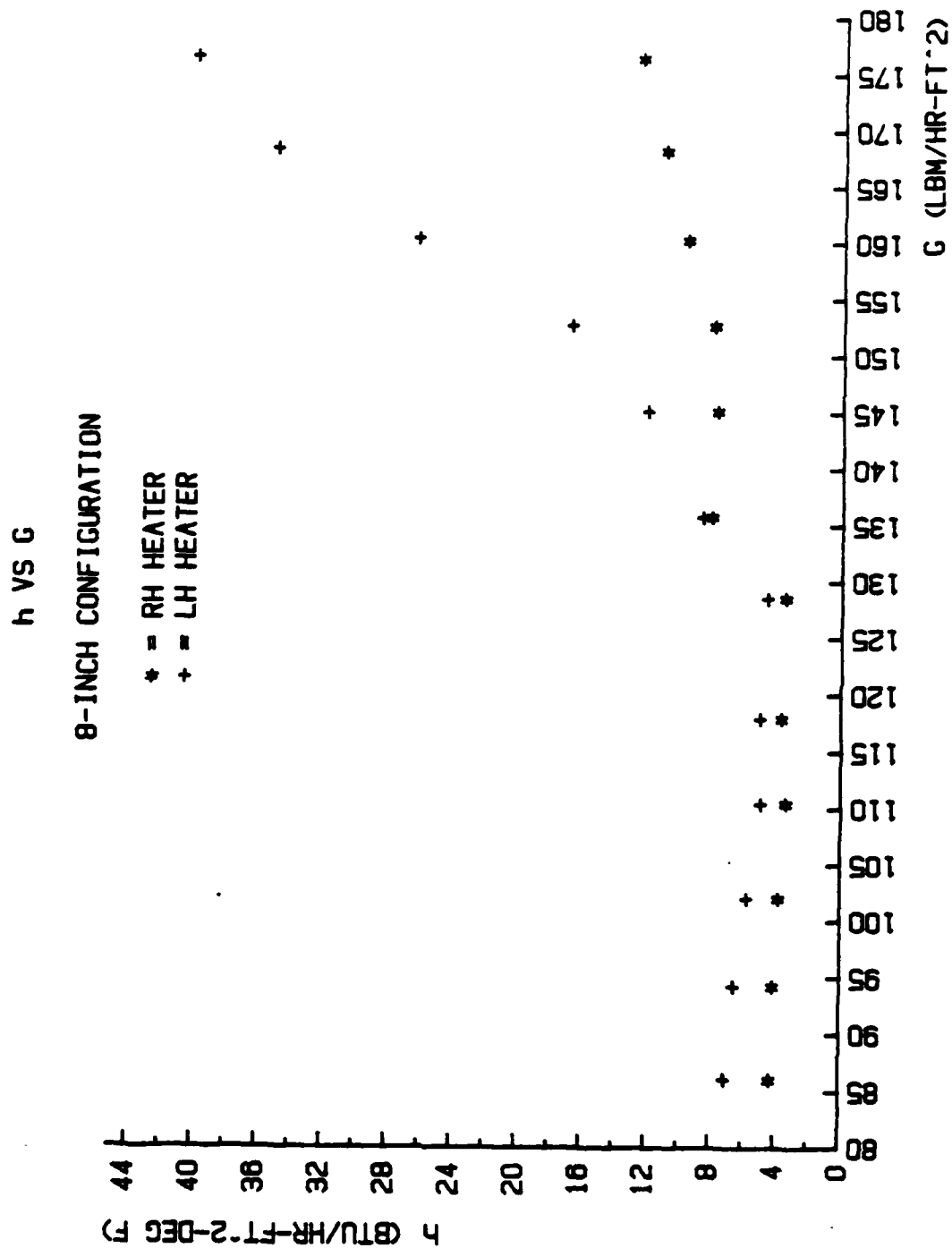
Figure 49.   Heat Transfer Coefficient vs Superficial Mass
Velocity; 8.0 in. Configuration

103
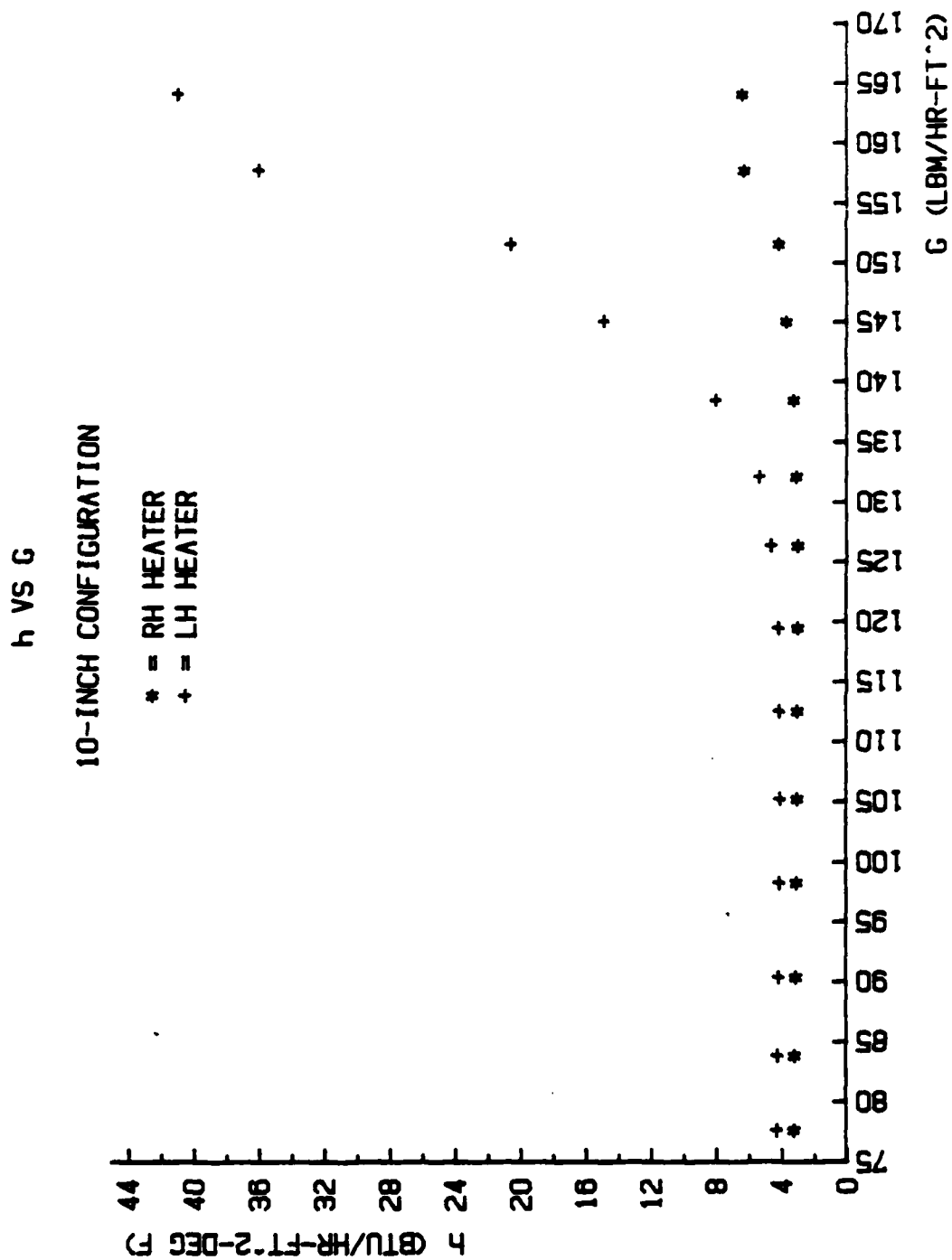
Figure 50. Heat Transfer Coefficient vs Superficial Mass Velocity; 10.0 in. Configuration

104
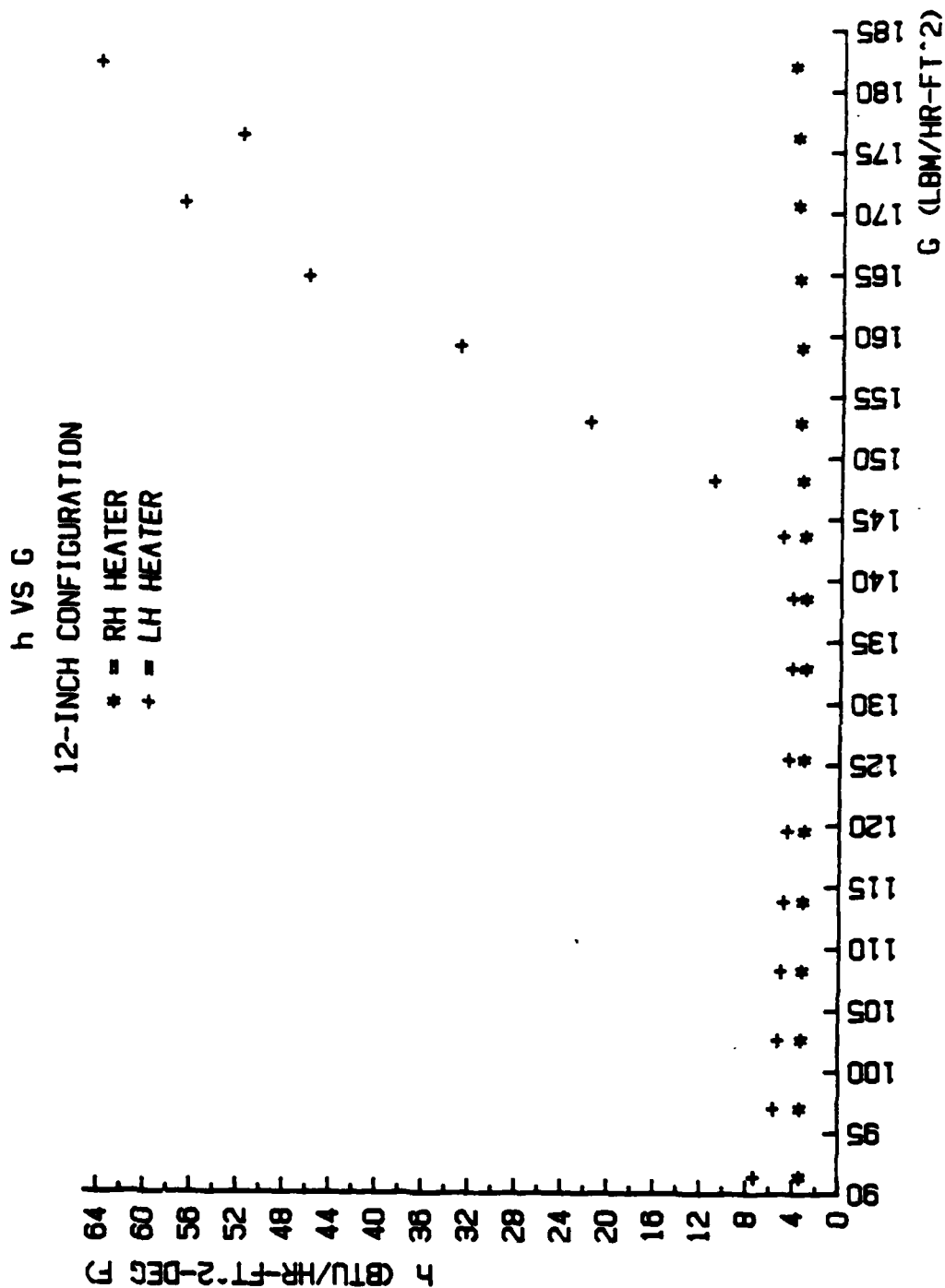
Figure 51. Heat Transfer Coefficient vs Superficial Mass
Velocity; 12.0 in. Configuration

105
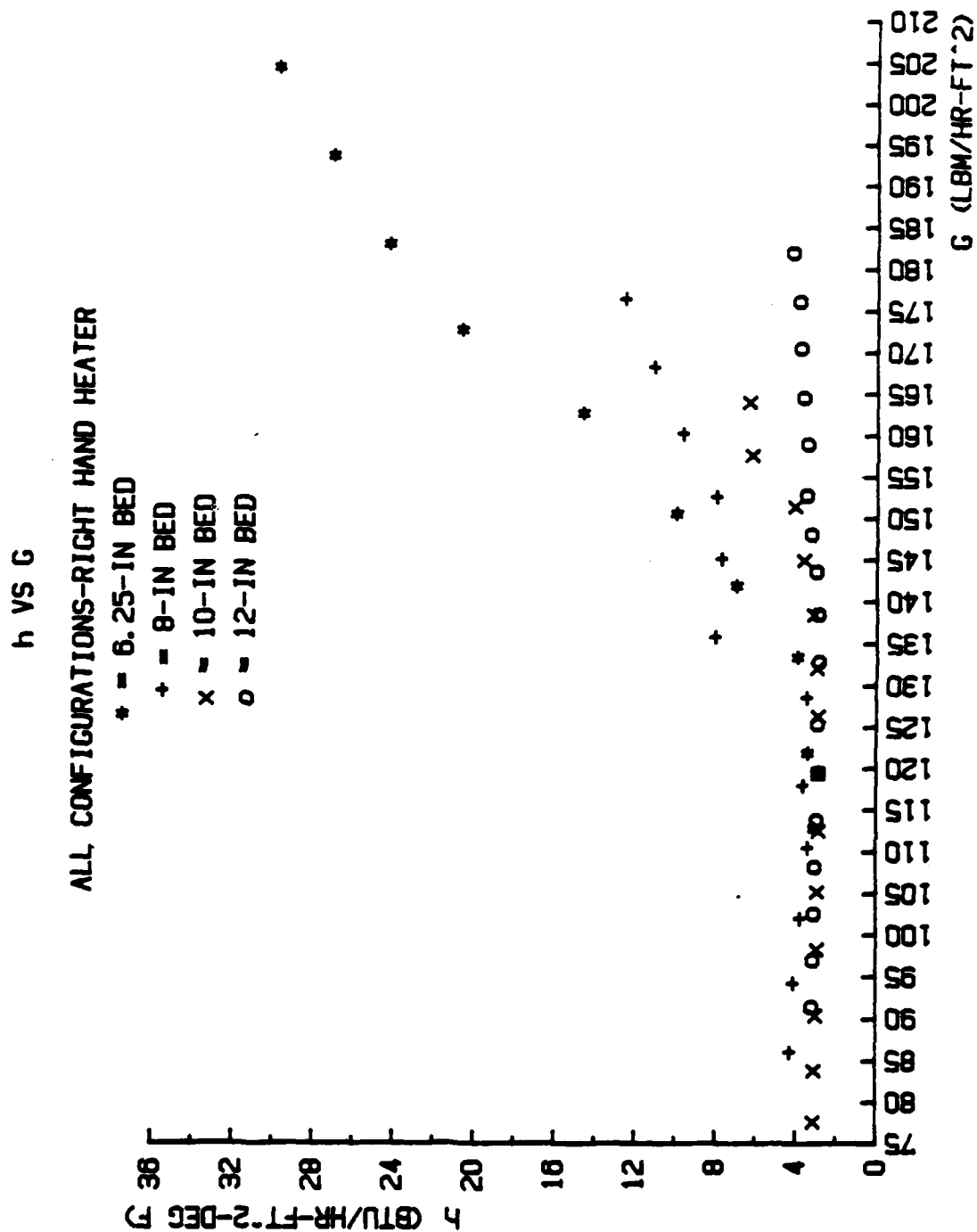
Figure 52. Heat Transfer Coefficient vs Superficial Mass
Velocity; Right Hand Heater, All Configurations

106
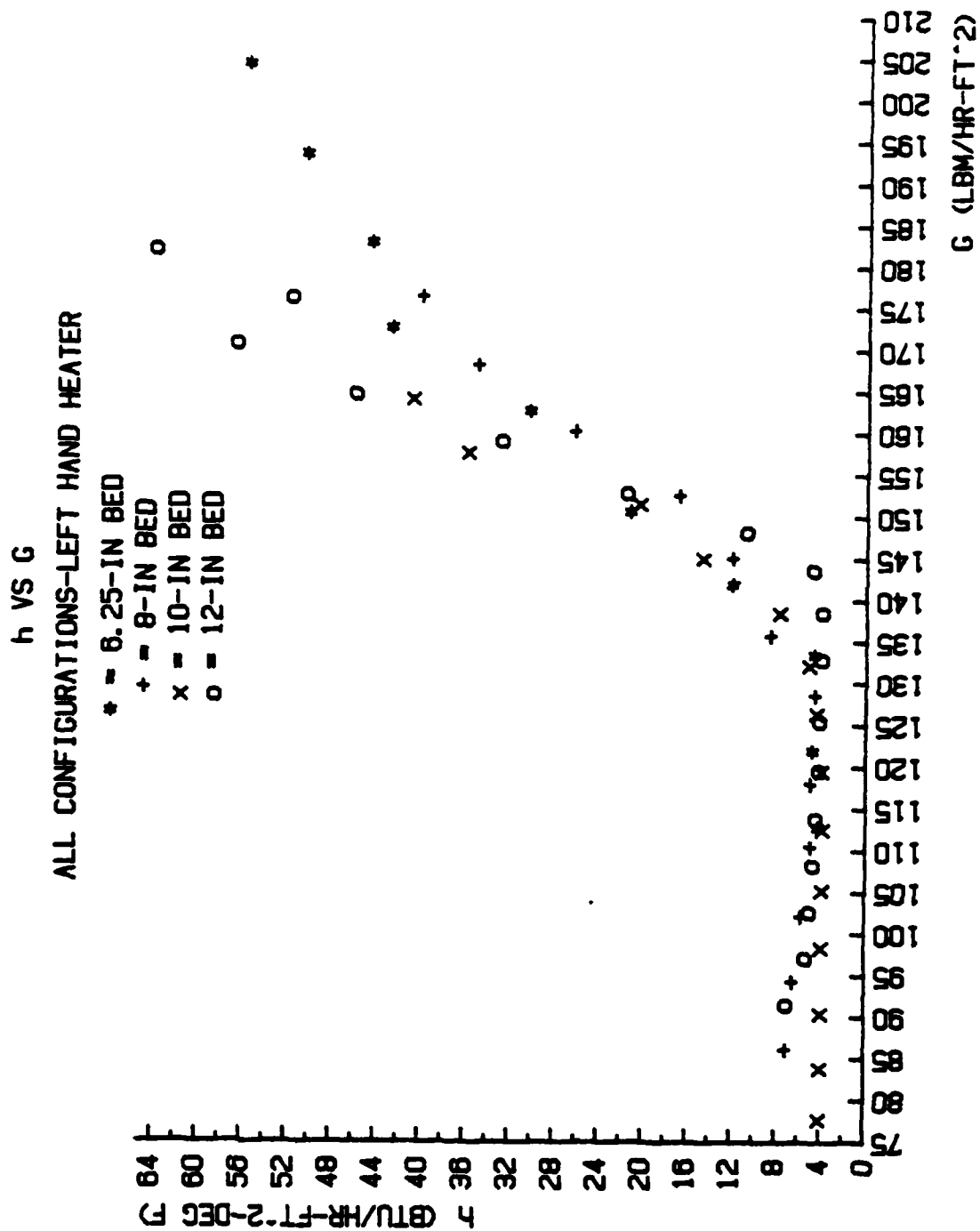
Figure 53. Heat Transfer Coefficient vs Superficial Mass
Velocity; Left Hand Heater, All Configurations

107

A second significant trend which was observed was the fact that the heat transfer coefficient for the left hand heater was significantly higher than for the right hand heater, particularly as the bed width was increased. In the wide bed configurations the heat transfer coefficient for the right hand heater showed very little improvement in response to an increase in flow rate. With a high height-to-width ratio (narrow bed), the heat transfer coefficient for the left hand heater was roughly twice the value for the right hand heater at high gas flow rates. With a low height-to-width ratio (wide bed), the left hand heat transfer coefficient exceeded that for the right by a factor of 15 to 1.

The exception to this trend occurred during the data runs accomplished with the distributor masked-off. Under this condition, the heat transfer coefficents for the left hand and right hand heaters were in much closer agreement with one another than in all other cases. The effect of masking the distributor was to increase the heat transfer coefficient for the right hand heater by approximately 10% while simultaneously reducing the heat transfer coefficient for the left hand heater by approximately 25%. It would be expected that, with the distributor masked-off, the heat transfer coefficients would be the same for both the left hand and right hand heaters. Although there is a much closer match than in the unmasked configuration, it is

observed that the left hand heater still achieved higher rates

of heat transfer. There are several possible explanations

for this difference. The first of these is that the unused

portion of the distributor may not have been completely sealed

by the masking and as a result, some peripheral injection

could have still have been taking place. Secondly, it was

noted that there was a small amount of gas leakage past the

movable side wall gaskets which may have altered the gas and

particle flow patterns along the left wall. This, in turn,

may have altered the heat transfer coefficients. Thirdly,

it is possible that the movable side wall may not have been

perfectly vertical. Although care was taken to accurately

position and secure the side wall, deviations from a true

vertical orientation of as much as 1° are considered possible.

Research conducted in the Soviet Union by Filippovskii and

Baskakov [Ref. 7] has indicated that plate angle has a con-

siderable influence on heat transfer coefficients. Because

of the small angle involved in this case, the contribution

of this effect is not considered to be the principle cause

of the difference in performance between the two plates.

A final effect which may have made a minor contribution to

this difference is the fact that the losses from the heater

backing to the atmosphere were lower for the left hand heater

than for the right. As a result, more of the electrical

energy going into the heater was directed through the copper

plate and on to the bed, thus resulting in a minor improvement

109

in the heat transfer coefficient. Because of the configuration of the apparatus, the left hand heater mounting block was enclosed within the unused portions of the apparatus walls. Because of this, there was a stagnation of the air in the vicinity of the mounting block as well as an elevation of the local ambient temperature. These effects combined to reduce the amount of heat lost through the mounting block. Because of the specialized conditions which were found to exist near the left hand wall, the performance of the right hand heater shall be considered as being representative of a typical flat plate.

The magnitude of the heat transfer coefficients calculated as a result of this study were within the range of values found in the literature, however it should be noted that there is a wide variation in the coefficients found by other researchers due to the effect of differing bed sizes and geometries, particle size and composition, fluidizing gas properties, superficial mass velocities, and bed operating temperatures.

There is also a wide variety of empirical correlations available for the prediction of heat transfer coefficients, however each of these serves, for the most part, only to describe the particular test apparatus and conditions from which they were derived. For this reason, no attempt was made to fit the data to the correlations currently available

nor was an attempt made to develop a new correlation to describe the performance of the apparatus used in this experiment.

A review of the literature shows that numerous researchers have observed heat transfer curves similar to that shown in Figure 54. This typical curve displays a peak heat transfer coefficient (h_{max}) at some optimum superficial mass velocity (G_{opt}). Flow rates above this optimum value resulted in a reduction in the heat transfer coefficient. This has been attributed to the fact that as the voidage is increased, there is a point at which the beneficial contribution of increased particle activity is offset by the negative effect of reducing the solids concentration within the emulsion. In this study such an optimum flow rate was not achieved. It is believed that, due to the design of the fluidization apparatus, the range of gas flow rates was restricted by the relatively shallow "freeboard" region above the level of the settled bed. When the bed was undergoing active fluidization, particles within the "splash zone" reached the top of the container and blocked the air exit ports. This was believed to be taking place at gas flow rates below the optimum level. It is possible that a reduction in the settled bed depth and a consequent increase in the height of the freeboard region would permit higher superficial mass velocities and result in higher levels of heat transfer.
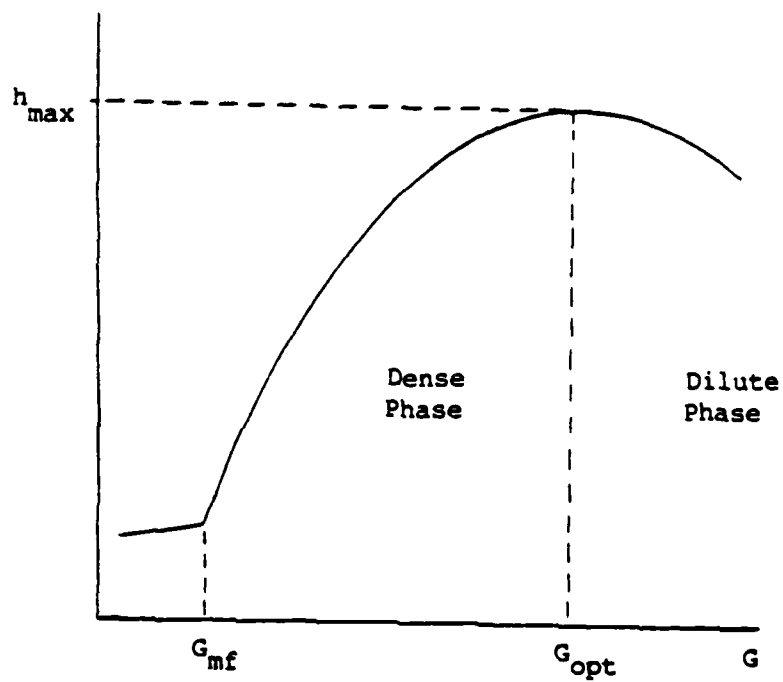
Figure 54. Heat Transfer Coefficient vs Superficial Mass
Velocity; Typical

The difference in the level of heat transfer between the left and right hand walls is clearly related to the high level of cooling observed at the left hand wall. This, in turn, is related to the large amount of particle activity observed to the left of center. The exact mechanism of heat transfer which takes place at the wall cannot be stated with certainty. Although there are many theories as to the mechanism of heat transfer within a fluidized bed, the bulk of the models postulated to date fall into one of two broad categories. The first of these models proposes that the heat transfer is primarily through a gas film adjacent to the heat transfer surface. The heat is transferred by steady state conduction through the film to the downward moving particles. This film is kept thin by the scrubbing action of the solid particles which come in contact with the surface. This reduction in the boundary layer thickness is thought to be the key to achieving high rates of heat transfer. The second model theorizes that heat transfer is primarily by unsteady conduction to "packets" which are made up of several solid particles grouped together for a short period of time. These packets are thought to be in contact with the heat transfer surface for only brief periods of time before they move away from the surface and are replaced or "replenished" by fresh packets. As a result, there is always a high temperature differential between the surface and the packets and this, in turn, yields high levels

113

of heat transfer. A significant factor shared by both the packet model and the film conduction model is that they both rely on the free motion of particles to effect high rates of heat transfer. It is believed that in this apparatus a high level of particle activity near the wall promotes the frequent exchange of particles from within the bed core where it is comparatively cool. As the frequency of particle or packet replenishment increases, the temperature differential between the wall and the particles also increases. This, in turn, increases the overall heat transfer. Conversely, when there is comparatively little particle activity near the wall, the replenishment rate is low and the same particles remain in contact with the hot wall for longer periods of time as they move downward. Because of the long residence time, the temperature differential is diminished and the heat transfer coefficient is reduced. In this study, the level of particle activity near the right hand wall was comparatively low and so was the heat transfer coefficient. A study of the temperature profiles for the right hand plate shows a steady increase in plate temperature with a downward change in vertical position. This profile is consistent with that expected for long particle residence times since the downward moving particles would experience a steady increase in temperature as they approached the bottom of the plate. It is noted that when the configuration of the bed is tall and narrow, the bubble flow path is very close to

the bed walls. This causes a high degree of particle activity
near the wall and a corresponding increase in the particle
replenishment rate. As the bed height-to-width ratio is
decreased by increasing the bed width, the bubble flow path
moves further away from the wall. This causes a reduction
in the amount of activity near the wall and a corresponding
decrease in the replenishment rate. This scenario is con-
sistent with the observed reduction in heat transfer coef-
ficient as the bed width was increased. Conversely, the
amount of activity seen by the left hand plate was consis-
tently high as a result of the peripheral injection effect
described previously. The degree of activity and consequently
the heat transfer coefficient, remained unaffected by an in-
crease in bed width. In addition, the heater temperature
profile showed no sharp transition from top to bottom, thus
indicating that the particle residence time was short.
Based on the findings of this study, it may be concluded
that peripheral injection is an effective means of promoting
particle activity or turbulence along the wall of the con-
tainer. The idea of turbulence promoters in fluidized beds
is not a new one. Early research by the Babcock and Wilcox
Company [Ref. 8] included the use of spirally shaped strips
to create a rotational motion which forced the solids toward
the walls by centrifugal force. The result was a significant
increase in heat transfer. Recently Sokolov et al [Ref. 9]
in the Soviet Union studied the use of angled louvers

positioned within the bed in order to redirect the motion of the particles outward toward the walls, thus destroying the stagnant layer which was insulating the surface. The result was a marked improvement in heat transfer performance. Although more study is obviously warranted, the use of peripheral injection would appear to offer benefits similar to other enhancement techniques while eliminating the need for in-bed structures which occupy valuable space and which require periodic replacement as a consequence of particle errosion. In addition, the amount of turbulence created at the wall by the injection technique could easily be adjusted to optimum levels by controlling the flow rate of the injection gas. Such a system could be used to offset the low rates of heat transfer at the walls of wide fluidized beds.

As discussed previously, an energy balance was conducted in order to confirm the validity of the numerical results. The results of this energy balance were disappointingly poor. In most cases, the measured heat flux leaving the bed with the outgoing airstream was found to be only half of that calculated to be entering the bed via the electrical heaters. It is believed that the disagreement was primarily due to incorrect measurement of the fluidizing gas flow rate. Despite the poor energy balance, the conclusions reached as a result of this study are considered to be valid since they were based on observed trends rather than on the magnitude of specific numerical results.

V. CONCLUSIONS AND RECOMMENDATIONS

A. CONCLUSIONS

Based on the experimental results of this study the following conclusions may be drawn:

1. The plate-to-bed heat transfer coefficient for a flat vertical plate serving as a containing wall decreases with a decrease in the bed height-to-width ratio.

2. The plate-to-bed heat transfer coefficient increases with an increase in superficial mass velocity above the minimum required to initiate fluidization.

3. The plate-to-bed heat transfer coefficient remains small and relatively constant at superficial mass velocities below the minimum required to initiate fluidization.

4. The plate-to-bed heat transfer coefficient increases with an increase in the particle activity or turbulence in the vicinity of the wall.

5. The particle turbulence near the vertical plate, and consequently the heat transfer coefficient, may be enhanced by the injection of air from beneath the plate in a direction perpendicular to the primary fluidizing air flow path.

6. The temperature profile of a vertical flat plate may be used to provide insights as to the nature of particle activity in the vicinity of the plate.

7. The particle flow pattern within a rectangular fluidized
bed is in very close agreement with that described in the
literature for cylindrical fluidized beds with upward motion
of the particles taking place along the centerline of the
container and downward return flow of the particles taking
place along the periphery.

8. Slugging or heaving of the bed was more prevalent in the
narrow bed configuration as opposed to the wide bed configura-
tion where this phenomenon was not observed.

9. Fluidized bed particle motion along a non-moving boundary
matches the behavior of a viscous fluid in that a "no-slip"
condition is observed.

10. The bed pressure drop characteristics for a rectangular
fluidized bed match those found in the literature for a cy-
lindrical fluidized bed in that the pressure drop across the
bed increases linearly with an increase in air flow rate
until the point of fluidization onset. Once fluidization
has commenced, the pressure drop remains constant.

11. The temperature of the heater surface at a given depth
remains constant for any point in a horizontal direction.

12. The bed temperature will assume a uniform temperature
distribution once fluidized.

B. RECOMMENDATIONS FOR FURTHER STUDIES

In order to better pursue the ojbectives of this study at
sometime in the future, the following recommendations and/or
suggestions are made:

1. Replace the three circular air exhaust tubes on the top
of the fluidization apparatus with a rectangular exhaust
port which runs the entire twenty-four inch length of the
bed. This would provide a non-restrictive exit path for
the fluidizing air which would minimize the amount of swirl-
ing and mixing in the region above the bed.

2. Repair severed wire on thermocouple #15.

3. Replace malfunctioning thermocouples #4 and #40.

4. Install a minimum of four new thermocouples to monitor
air exit temperature. At present only one thermocouple can
be used for this purpose (T(55)) for bed configurations of
12 inches or less.

5. Provide a more positive means of securing the baffle
plate to the distributor plate so as to prevent leak-by into
the bed.

6. Install a bypass valve around the existing air inlet con-
trol valve to permit fine adjustment of fluidization flow rates.

7. Install two additional thermocouples in the left hand
movable wall 1/4 inch below the bottom of the heater in
order to obtain a more accurate estimate of wall losses.

8. Install two additional thermocouples in the front wall
of the bed so as to obtain a more accurate estimate of wall
losses.

9. Substitute the existing power supplies with units, which
are capable of providing additional current and which are
equipped with controls to vary power as well as voltage.

119

This would permit equalization of input power to the two heaters and allow the desired temperature differential between the plate and the bed to be maintained.

10. Install a movable wall in the air plenum beneath the distributor plate so that the flow path followed by the incoming air is identical for the left and right sides.

11. Prior to the commencement of future data runs, apply caulking material to the movable side wall so as to prevent leakage of fluidizing air past the gaskets.

12. Modify the fluidization apparatus so that a controlled amount of injection air may be applied to each of the heater plates. Such a modification would permit additional study of the effects of the peripheral injection phenomenon.

C. CLOSING REMARKS

Gas fluidization is a fascinating process which promises to provide a multitude of beneficial applications. Full enjoyment of the potential which exists depends on a more complete understanding of the many complex phenomenon associated with fluidization. It is hoped that this thesis has, in some small way, contributed to that understanding or helped to stimulate additional thought and research in this exciting field of study.

120

EXPERIMENTAL PRESSURE DROP DATA

Table I. Bed Pressure/Gas Mass Flow Data (6.25 in. Bed)

Rotometer Reading (%)	Air Flow (SCFM)	G Gas Mass Velocity (Lbm/Hr-Ft^2)	LOG G	Pressure Above Distributor (in. H$_2$O)	Pressure Above Bed (in. H$_2$O)	ΔP (in. H$_2$O)	LOG ΔP
20	7.29	125.17	2.097	13.9	0.0	13.9	1.143
21	7.61	130.73	2.116	14.1	0.0	14.1	1.149
22	7.94	136.32	2.135	14.8	0.0	14.8	1.170
23	8.26	141.90	2.152	15.8	0.0	15.8	1.199
24	8.58	147.47	2.169	16.6	0.0	16.6	1.220
25	8.91	153.05	2.185	16.7	0.0	16.7	1.223
26	9.23	158.62	2.200	17.3	0.0	17.3	1.238
27	9.56	164.20	2.215	17.0	0.0	17.0	1.230
28	9.88	169.76	2.230	16.3	0.0	16.3	1.212
29	10.21	175.35	2.244	16.3	0.0	16.3	1.212
30	10.53	180.91	2.257	16.3	0.0	16.3	1.212
31	10.86	186.50	2.271	16.3	0.0	16.3	1.212
32	11.18	192.06	2.283	16.3	0.0	16.3	1.212
33	11.51	197.65	2.296	16.3	0.0	16.3	1.212
34	11.83	203.23	2.308	16.3	0.0	16.3	1.212
35	12.15	208.80	2.320	16.2	0.0	16.2	1.210
36	12.48	214.38	2.331	16.2	0.0	16.2	1.210
37	12.80	219.95	2.342	16.2	0.0	16.2	1.210

Table II. Bed Pressure/Gas Mass Flow Data (8.0 in. Bed)

Rotometer Reading (%)	Air Flow (SCFM)	G Gas Mass Velocity (Lbm/Hr-Ft^2)	LOG G	Pressure Above Distributor (in. H$_2$O)	Pressure Above Bed (in. H$_2$O)	ΔP (in. H$_2$O)	LOG ΔP
18	6.64	89.08	1.950	10.6	0.0	10.6	1.025
19	6.96	93.43	1.970	11.25	0.0	11.25	1.051
20	7.29	97.79	1.990	11.7	0.0	11.7	1.068
21	7.61	102.14	2.009	12.25	0.0	12.25	1.088
22	7.94	106.50	2.027	12.8	0.0	12.8	1.107
23	8.26	110.86	2.045	13.65	0.0	13.65	1.135
24	8.58	115.21	2.061	14.15	0.0	14.15	1.151
25	8.91	119.57	2.078	14.8	0.0	14.8	1.170
26	9.23	123.92	2.093	15.1	0.05	15.05	1.178
27	9.56	128.28	2.108	16.2	0.05	16.15	1.208
28	9.88	132.63	2.123	16.1	0.05	16.05	1.205
29	10.21	136.99	2.137	16.4	0.05	16.35	1.214
30	10.53	141.34	2.150	16.3	0.05	16.25	1.211
31	10.86	145.70	2.163	16.2	0.05	16.15	1.208
32	11.18	150.05	2.176	16.4	0.05	16.35	1.214
33	11.51	154.41	2.189	16.3	0.05	16.25	1.211
34	11.83	158.77	2.201	16.3	0.05	16.25	1.211
35	12.15	163.12	2.213	16.3	0.05	16.25	1.211
36	12.48	167.48	2.224	16.2	0.1	16.1	1.207
37	12.80	171.83	2.235	16.3	0.1	16.2	1.210
38	13.13	176.19	2.248	16.0	0.1	15.9	1.201
39	13.45	180.54	2.257	16.1	0.1	16.0	1.204
40	13.78	184.90	2.267	16.0	0.1	15.9	1.201
41	14.10	189.25	2.277	16.0	0.1	15.9	1.201
42	14.43	193.61	2.287	16.1	0.1	16.0	1.204
43	14.75	197.96	2.297	16.2	0.1	16.1	1.207

Table III. Bed Pressure/Gas Mass Flow Data (10.0 in. Bed)

Rotometer Reading (%)	Air Flow (SCFM)	G Gas Mass Velocity (Lbm/Hr-Ft²)	LOG G	Pressure Above Distributor (in. H₂O)	Pressure Above Bed (in. H₂O)	ΔP (in. H₂O)	LOG ΔP
16	5.99	64.29	1.808	6.68	0.02	6.66	0.823
18	6.64	71.26	1.853	7.56	0.03	7.53	0.877
20	7.29	78.23	1.893	8.48	0.05	8.43	0.926
22	7.94	85.20	1.930	9.25	0.06	9.19	0.963
24	8.58	92.17	1.965	10.08	0.07	10.01	1.000
26	9.23	99.13	1.996	10.90	0.08	10.82	1.034
28	9.88	106.10	2.026	11.65	0.09	11.56	1.063
30	10.53	113.07	2.053	12.43	0.10	12.33	1.091
32	11.18	120.04	2.079	13.35	0.10	13.25	1.122
34	11.83	127.02	2.104	14.13	0.10	14.03	1.147
36	12.48	133.99	2.127	14.90	0.11	14.81	1.171
38	13.13	140.96	2.149	15.68	0.12	15.56	1.192
40	13.78	147.92	2.170	16.55	0.13	16.42	1.215
42	14.43	154.89	2.190	16.35	0.15	16.20	1.210
44	15.08	161.86	2.209	16.35	0.16	16.19	1.209
46	15.72	168.83	2.227	16.25	0.18	16.07	1.206
48	16.37	175.80	2.245	16.20	0.19	16.01	1.204
50	17.02	182.77	2.262	16.10	0.20	15.90	1.201
52	17.67	189.73	2.278	16.00	0.22	15.88	1.201
54	18.32	196.70	2.294	15.95	0.23	15.72	1.196
56	18.97	203.68	2.309	15.95	0.25	15.70	1.196
58	19.62	210.64	2.324	15.95	0.28	15.67	1.195
60	20.27	217.62	2.338	15.95	0.30	15.65	1.195
62	20.92	224.59	2.351	15.90	0.30	15.60	1.193

Table IV. Bed Pressure/Gas Mass Flow Data (12.0 in. Bed)

Rotometer Reading (%)	Air Flow (SCFM)	G Gas Mass Velocity (Lbm/Hr-Ft^2)	LOG G	Pressure Above Distributor (in. H$_2$O)	Pressure Above Bed (in. H$_2$O)	ΔP (in. H$_2$O)	LOG ΔP
16	5.99	53.58	1.729	5.60	0.03	5.57	0.746
18	6.64	59.38	1.774	6.35	0.03	6.32	0.801
20	7.29	65.19	1.814	6.90	0.04	6.86	0.836
22	7.94	71.00	1.851	7.70	0.03	7.67	0.885
24	8.58	76.81	1.885	8.30	0.04	8.26	0.917
26	9.23	82.61	1.917	8.90	0.04	8.86	0.947
28	9.88	88.42	1.947	9.50	0.05	9.45	0.975
30	10.53	94.23	1.974	10.20	0.05	10.15	1.006
32	11.18	100.03	2.000	10.80	0.05	10.75	1.031
34	11.83	105.85	2.025	11.50	0.05	11.45	1.059
36	12.48	111.66	2.048	12.20	0.06	12.14	1.084
38	13.13	117.46	2.070	13.20	0.06	13.14	1.119
40	13.78	123.27	2.091	13.90	0.07	13.83	1.141
42	14.43	129.08	2.111	14.50	0.07	14.43	1.159
44	15.08	134.88	2.130	15.20	0.08	15.12	1.180
46	15.72	140.69	2.148	15.90	0.09	15.81	1.199
48	16.37	146.50	2.166	16.05	0.09	15.96	1.203
50	17.02	152.30	2.183	15.80	0.10	15.70	1.196
52	17.67	158.11	2.199	15.80	0.10	15.70	1.196
54	18.32	163.92	2.215	15.75	0.10	15.65	1.195
56	18.97	169.73	2.230	15.70	0.11	15.59	1.193
58	19.62	175.53	2.244	15.60	0.11	15.49	1.190
60	20.27	181.35	2.259	15.50	0.12	15.38	1.187
62	20.92	187.15	2.272	15.50	0.13	15.37	1.187
64	21.57	192.96	2.285	15.45	0.15	15.30	1.185
66	22.22	198.77	2.298	15.40	0.15	15.25	1.183

EXPERIMENTAL ROTOMETER CALIBRATION DATA

ROTOMETER CALIBRATION
ASME HERSCHEL-TYPE VENTURI
4.26/2.13 IN DIA

20 PERCENT READING
————————————————

EXPERIMENTAL DATA

ATMOSPHERIC PRESSURE =   29.76910 IN Hg
VENTURI INLET TEMPERATURE =   72.0 DEG F
VENTURI INLET STATIC GAGE PRESSURE =   10.70 IN H2O
VENTURI DIFFERENTIAL PRESSURE =   .010 IN RED OIL
SPECIFIC GRAVITY OF RED OIL =   .834

CALCULATED VALUES

ATMOSPHERIC PRESSURE =   14.6259 PSI
VENTURI INLET GAGE PRESSURE =   .38654 PSI
VENTURI INLET ABSOLUTE PRESSURE =   14.23932 PSI
VENTURI DIFFERENTIAL PRESSURE =   .00030 PSI
VENTURI INLET AIR DENSITY =   .07230 LBM/FT3
VENTURI PRESSURE DROP RATIO (X) =   .00002
EXPANSION FACTOR (Y) =   1.00
ASSUMED REYNOLDS NUMBER =   3000
DISCHARGE COEFFICIENT (C) =   .889
VELOCITY OF APPROACH FACTOR (E) =   1.03280
FLOW COEFFICIENT (K) =   .91816
AIR MASS FLOW RATE =   .01021 LBM/SEC
AIR VOLUMETRIC FLOW RATE =   8.469 CFM
VENTURI INLET REYNOLDS NUMBER =   3002

ROTOMETER CALIBRATION
ASME HERSCHEL-TYPE VENTURI
4.26/2.13 IN DIA

25 PERCENT READING

EXPERIMENTAL DATA

ATMOSPHERIC PRESSURE =	29.76910 IN Hg
VENTURI INLET TEMPERATURE =	72.0 DEG F
VENTURI INLET STATIC GAGE PRESSURE =	12.35 IN H2O
VENTURI DIFFERENTIAL PRESSURE =	.011 IN RED OIL
SPECIFIC GRAVITY OF RED OIL =	.834

CALCULATED VALUES

ATMOSPHERIC PRESSURE =	14.6259 PSI
VENTURI INLET GAGE PRESSURE =	.44614 PSI
VENTURI INLET ABSOLUTE PRESSURE =	14.17972 PSI
VENTURI DIFFERENTIAL PRESSURE =	.00033 PSI
VENTURI INLET AIR DENSITY =	.07200 LBM/FT3
VENTURI PRESSURE DROP RATIO (X) =	.00002
EXPANSION FACTOR (Y) =	1.00
ASSUMED REYNOLDS NUMBER =	3150
DISCHARGE COEFFICIENT (C) =	.891
VELOCITY OF APPROACH FACTOR (E) =	1.03280
FLOW COEFFICIENT (K) =	.91970
AIR MASS FLOW RATE =	.01070 LBM/SEC
AIR VOLUMETRIC FLOW RATE =	8.916 CFM
VENTURI INLET REYNOLDS NUMBER =	3147

126

****ROTOMETER CALIBRATION****
ASME HERSCHEL-TYPE VENTURI
4.26/2.13 IN DIA

30 PERCENT READING

****EXPERIMENTAL DATA****

```
ATMOSPHERIC PRESSURE =                      29.76910 IN Hg
VENTURI INLET TEMPERATURE =                     72.0 DEG F
VENTURI INLET STATIC GAGE PRESSURE =   14.75 IN H2O
VENTURI DIFFERENTIAL PRESSURE =     .015 IN RED OIL
SPECIFIC GRAVITY OF RED OIL =                    .834
```

****CALCULATED VALUES****

```
ATMOSPHERIC PRESSURE =                      14.6259 PSI
VENTURI INLET GAGE PRESSURE =                .53284 PSI
VENTURI INLET ABSOLUTE PRESSURE =       14.09302 PSI
VENTURI DIFFERENTIAL PRESSURE =             .00045 PSI
VENTURI INLET AIR DENSITY =             .07156 LBM/FT3
VENTURI PRESSURE DROP RATIO (X) =               .00003
EXPANSION FACTOR (Y) =                            1.00
ASSUMED REYNOLDS NUMBER =                        3700
DISCHARGE COEFFICIENT (C) =                       .895
VELOCITY OF APPROACH FACTOR (E) =             1.03280
FLOW COEFFICIENT (K) =                         .92435
AIR MASS FLOW RATE =                     .01252 LBM/SEC
AIR VOLUMETRIC FLOW RATE =               10.497 CFM
VENTURI INLET REYNOLDS NUMBER =                 3682
```

ROTOMETER CALIBRATION
ASME HERSCHEL-TYPE VENTURI
4.26/2.13 IN DIA

35 PERCENT READING

EXPERIMENTAL DATA

ATMOSPHERIC PRESSURE =   29.76910 IN Hg
VENTURI INLET TEMPERATURE =   72.0 DEG F
VENTURI INLET STATIC GAGE PRESSURE =   17.50 IN H2O
VENTURI DIFFERENTIAL PRESSURE =   .020 IN RED OIL
SPECIFIC GRAVITY OF RED OIL =   .834

CALCULATED VALUES

ATMOSPHERIC PRESSURE =   14.6259 PSI
VENTURI INLET GAGE PRESSURE =   .63219 PSI
VENTURI INLET ABSOLUTE PRESSURE =   13.99367 PSI
VENTURI DIFFERENTIAL PRESSURE =   .00060 PSI
VENTURI INLET AIR DENSITY =   .07105 LBM/FT3
VENTURI PRESSURE DROP RATIO (X) =   .00004
EXPANSION FACTOR (Y) =   1.00
ASSUMED REYNOLDS NUMBER =   4250
DISCHARGE COEFFICIENT (C) =   .899
VELOCITY OF APPROACH FACTOR (E) =   1.03280
FLOW COEFFICIENT (K) =   .92797
AIR MASS FLOW RATE =   .01446 LBM/SEC
AIR VOLUMETRIC FLOW RATE =   12.211 CFM
VENTURI INLET REYNOLDS NUMBER =   4253

```
                    **ROTOMETER CALIBRATION**
                    ASME HERSCHEL-TYPE VENTURI
                         4.26/2.13 IN DIA

                       40 PERCENT READING
                    ------------------------


                      **EXPERIMENTAL DATA**


ATMOSPHERIC PRESSURE =                   29.76910 IN Hg
VENTURI INLET TEMPERATURE =                 72.0 DEG F
VENTURI INLET STATIC GAGE PRESSURE =     20.30 IN H2O
VENTURI DIFFERENTIAL PRESSURE =        .025 IN RED OIL
SPECIFIC GRAVITY OF RED OIL =                    .834


                      **CALCULATED VALUES**


ATMOSPHERIC PRESSURE =                    14.6259 PSI
VENTURI INLET GAGE PRESSURE =              .73334 PSI
VENTURI INLET ABSOLUTE PRESSURE =        13.89252 PSI
VENTURI DIFFERENTIAL PRESSURE =            .00075 PSI
VENTURI INLET AIR DENSITY =            .07054 LBM/FT3
VENTURI PRESSURE DROP RATIO (X) =            .00005
EXPANSION FACTOR (Y) =                         1.00
ASSUMED REYNOLDS NUMBER =                      4750
DISCHARGE COEFFICIENT (C) =                    .901
VELOCITY OF APPROACH FACTOR (E) =           1.03280
FLOW COEFFICIENT (K) =                       .93086
AIR MASS FLOW RATE =                  .01616 LBM/SEC
AIR VOLUMETRIC FLOW RATE =               13.744 CFM
VENTURI INLET REYNOLDS NUMBER =                4753
```

```
            **ROTOMETER CALIBRATION**
            ASME HERSCHEL-TYPE VENTURI
               4.26/2.13 IN DIA

            45 PERCENT READING
            _____


            **EXPERIMENTAL DATA**


ATMOSPHERIC PRESSURE =                    29.76910 IN Hg
VENTURI INLET TEMPERATURE =                   72.0 DEG F
VENTURI INLET STATIC GAGE PRESSURE =     24.30 IN H2O
VENTURI DIFFERENTIAL PRESSURE =         .031 IN RED OIL
SPECIFIC GRAVITY OF RED OIL =                      .834


            **CALCULATED VALUES**


ATMOSPHERIC PRESSURE =                     14.6259 PSI
VENTURI INLET GAGE PRESSURE =                .87784 PSI
VENTURI INLET ABSOLUTE PRESSURE =         13.74802 PSI
VENTURI DIFFERENTIAL PRESSURE =             .00093 PSI
VENTURI INLET AIR DENSITY =               .06981 LBM/FT3
VENTURI PRESSURE DROP RATIO (X) =            .00007
EXPANSION FACTOR (Y) =                         1.00
ASSUMED REYNOLDS NUMBER =                      5300
DISCHARGE COEFFICIENT (C) =                    .904
VELOCITY OF APPROACH FACTOR (E) =           1.03280
FLOW COEFFICIENT (K) =                       .93365
AIR MASS FLOW RATE =                      .01795 LBM/SEC
AIR VOLUMETRIC FLOW RATE =                 15.431 CFM
VENTURI INLET REYNOLDS NUMBER =               5281
```

130

ROTOMETER CALIBRATION
ASME HERSCHEL-TYPE VENTURI
4.26/2.13 IN DIA

50 PERCENT READING

EXPERIMENTAL DATA

```
ATMOSPHERIC PRESSURE =                     29.76910 IN Hg
VENTURI INLET TEMPERATURE =                  72.0 DEG F
VENTURI INLET STATIC GAGE PRESSURE =    27.30 IN H2O
VENTURI DIFFERENTIAL PRESSURE =         .037 IN RED OIL
SPECIFIC GRAVITY OF RED OIL =                     .834
```

CALCULATED VALUES

```
ATMOSPHERIC PRESSURE =                      14.6259 PSI
VENTURI INLET GAGE PRESSURE =                .98621 PSI
VENTURI INLET ABSOLUTE PRESSURE =         13.63965 PSI
VENTURI DIFFERENTIAL PRESSURE =              .00111 PSI
VENTURI INLET AIR DENSITY =               .06926 LBM/FT3
VENTURI PRESSURE DROP RATIO (X) =             .00008
EXPANSION FACTOR (Y) =                          1.00
ASSUMED REYNOLDS NUMBER =                       5750
DISCHARGE COEFFICIENT (C) =                     .906
VELOCITY OF APPROACH FACTOR (E) =            1.03280
FLOW COEFFICIENT (K) =                        .93592
AIR MASS FLOW RATE =                      .01958 LBM/SEC
AIR VOLUMETRIC FLOW RATE =                 16.967 CFM
VENTURI INLET REYNOLDS NUMBER =                 5760
```

131

ROTOMETER CALIBRATION
ASME HERSCHEL-TYPE VENTURI
4.26/2.13 IN DIA

55 PERCENT READING

EXPERIMENTAL DATA

```
ATMOSPHERIC PRESSURE =                          29.76910 IN Hg
VENTURI INLET TEMPERATURE =                         72.0 DEG F
VENTURI INLET STATIC GAGE PRESSURE =    31.85 IN H2O
VENTURI DIFFERENTIAL PRESSURE =         .044 IN RED OIL
SPECIFIC GRAVITY OF RED OIL =                          .834
```

CALCULATED VALUES

```
ATMOSPHERIC PRESSURE =                          14.6259 PSI
VENTURI INLET GAGE PRESSURE =                   1.15058 PSI
VENTURI INLET ABSOLUTE PRESSURE =       13.47528 PSI
VENTURI DIFFERENTIAL PRESSURE =                 .00133 PSI
VENTURI INLET AIR DENSITY =             .06842 LBM/FT3
VENTURI PRESSURE DROP RATIO (X) =                 .00010
EXPANSION FACTOR (Y) =                              1.00
ASSUMED REYNOLDS NUMBER =                          6250
DISCHARGE COEFFICIENT (C) =                        .909
VELOCITY OF APPROACH FACTOR (E) =               1.03280
FLOW COEFFICIENT (K) =                            .93830
AIR MASS FLOW RATE =                    .02128 LBM/SEC
AIR VOLUMETRIC FLOW RATE =              18.662 CFM
VENTURI INLET REYNOLDS NUMBER =                   6259
```

132

ROTOMETER CALIBRATION
ASME HERSCHEL-TYPE VENTURI
4.26/2.13 IN DIA

60 PERCENT READING

EXPERIMENTAL DATA

```
ATMOSPHERIC PRESSURE =                      29.76910 IN Hg
VENTURI INLET TEMPERATURE =                     72.0 DEG F
VENTURI INLET STATIC GAGE PRESSURE =   37.00 IN H2O
VENTURI DIFFERENTIAL PRESSURE =        .051 IN RED OIL
SPECIFIC GRAVITY OF RED OIL =                     .834
```

CALCULATED VALUES

```
ATMOSPHERIC PRESSURE =                      14.6259 PSI
VENTURI INLET GAGE PRESSURE =               1.33663 PSI
VENTURI INLET ABSOLUTE PRESSURE =          13.28923 PSI
VENTURI DIFFERENTIAL PRESSURE =              .00154 PSI
VENTURI INLET AIR DENSITY =                 .06748 LBM/FT3
VENTURI PRESSURE DROP RATIO (X) =            .00012
EXPANSION FACTOR (Y) =                         1.00
ASSUMED REYNOLDS NUMBER =                      6700
DISCHARGE COEFFICIENT (C) =                    .911
VELOCITY OF APPROACH FACTOR (E) =           1.03280
FLOW COEFFICIENT (K) =                        .94036
AIR MASS FLOW RATE =                        .02280 LBM/SEC
AIR VOLUMETRIC FLOW RATE =                  20.277 CFM
VENTURI INLET REYNOLDS NUMBER =                6707
```

133

Table V.   Experimental Heat Transfer Data (6.25 in. Bed)

Rotometer Reading (%)	Air Flow (SCFM)	G Gas Mass Velocity (Lbm/Hr-Ft^2)	$\overline{T}_{RH}$ Avg. Temp. RH Heater (^oF)	$\overline{T}_{LH}$ Avg. Temp. LH Heater (^oF)	$\overline{T}_B$ Avg. Temp. Bed (^oF)	h_{RH} Ht. Coeff. RH Heater (Btu/ Hr-Ft^2-^oF)	h_{LH} Ht. Coeff. LH Heater (Btu/ Hr-Ft^2-^oF)
18	6.64	112.82	172.65	161.32	79.04	3.11	4.27
20	7.29	121.92	173.30	164.87	89.68	3.39	4.77
22	7.94	133.45	169.03	167.25	85.70	3.95	4.64
24	8.58	141.93	174.83	145.22	93.53	6.96	12.01
26	9.23	150.65	159.84	132.60	101.79	9.97	21.26
28	9.88	162.71	139.94	123.07	98.93	14.61	30.40
30	10.53	172.57	131.15	118.39	100.91	20.66	42.76
32	11.18	182.88	127.65	118.22	101.49	24.28	44.69
34	11.83	193.50	124.45	115.73	100.89	27.05	50.55
36	12.48	204.27	121.77	114.02	100.54	29.79	55.80

Table VI. Experimental Heat Transfer Data (6.25 in. Masked Bed)

Rotometer Reading (%)	Air Flow (SCFM)	G Gas Mass Velocity (Lbm/Hr-Ft^2)	$\bar{T}_{RH}$ Avg. Temp. RH Heater (°F)	$\bar{T}_{LH}$ Avg. Temp. LH Heater (°F)	$\bar{T}_B$ Avg. Temp. Bed (°F)	h_{RH} Ht. Coeff. RH Heater (Btu/Hr-Ft^2-°F)	h_{LH} Ht. Coeff. LH Heater (Btu/Hr-Ft^2-°F)
18	6.64	104.99	180.50	180.70	121.00	5.91	7.10
20	7.29	115.10	180.79	183.30	118.27	5.99	6.97
22	7.94	126.20	175.72	161.60	100.06	5.45	7.34
24	8.58	139.49	166.40	148.46	102.35	7.20	11.01
26	9.23	149.57	146.53	139.02	106.17	14.94	20.48
28	9.88	159.89	139.44	134.01	107.10	18.94	25.45
30	10.53	169.83	136.51	131.56	109.34	22.71	31.37
32	11.18	180.57	132.28	128.64	108.26	26.23	34.48
34	11.83	191.76	126.29	124.42	105.92	30.68	38.06
36	12.48	202.78	123.77	121.36	108.07	40.18	56.11

Table VII. Experimental Heat Transfer Data (8.0 in. Bed)

Rotometer Reading (%)	Air Flow (SCFM)	G Gas Mass Velocity (Lbm/Hr-Ft²)	$\bar{T}_{RH}$ Avg. Temp. RH Heater (°F)	$\bar{T}_{LH}$ Avg. Temp. LH Heater (°F)	$\bar{T}_B$ Avg. Temp. Bed (°F)	h_{RH} Ht. Coeff. RH Heater (Btu/Hr-Ft²-°F)	h_{LH} Ht. Coeff. LH Heater (Btu/Hr-Ft²-°F)
18	6.64	86.02	175.50	156.66	94.36	4.25	7.04
20	7.29	94.24	178.50	161.09	94.87	4.11	6.53
22	7.94	102.02	180.54	164.21	90.63	3.79	5.75
24	8.58	110.44	181.63	166.28	82.51	3.39	4.94
26	9.23	117.92	179.12	169.98	86.74	3.65	4.97
28	9.88	128.54	179.17	171.56	81.97	3.45	4.56
30	10.53	135.74	159.35	162.84	90.60	8.04	8.63
32	11.18	145.09	167.76	147.18	94.44	7.72	12.04
34	11.83	152.60	165.06	132.03	94.11	7.98	16.82
36	12.48	160.23	156.89	122.22	97.65	9.67	26.29
38	13.13	168.17	151.11	117.65	99.01	11.08	35.09
40	13.78	176.34	145.52	115.99	99.42	12.56	40.08

Table VIII. Experimental Heat Transfer Data (10.0 in. Bed)

Rotometer Reading (%)	Air Flow (SCFM)	G Gas Mass Velocity (Lbm/Hr-Ft^2)	$\overline{T}_{RH}$ Avg. Temp. RH Heater (°F)	$\overline{T}_{LH}$ Avg. Temp. LH Heater (°F)	$\overline{T}_{B}$ Avg. Temp. Bed (°F)	h_{RH} Ht. Coeff. RH Heater (Btu/Hr-Ft^2-°F)	h_{LH} Ht. Coeff. LH Heater (Btu/Hr-Ft^2-°F)
20	7.29	77.64	175.08	169.21	74.46	3.28	4.32
22	7.94	83.84	177.20	170.31	74.56	3.22	4.27
24	8.58	90.37	178.99	171.05	74.46	3.16	4.23
26	9.23	98.28	180.05	171.38	74.22	3.12	4.19
28	9.88	105.20	180.89	171.49	73.94	3.09	4.17
30	10.53	112.48	181.53	170.85	73.66	3.06	4.18
32	11.18	119.42	181.93	169.14	73.40	3.05	4.24
34	11.83	126.32	182.19	160.13	73.89	3.06	4.72
36	12.48	132.08	181.54	151.07	75.31	3.14	5.42
38	13.13	138.42	180.26	130.26	78.54	3.31	8.08
40	13.78	144.97	177.90	114.88	86.72	3.80	14.99
42	14.43	151.45	171.44	104.17	83.52	4.27	20.71
44	15.07	157.61	174.74	104.72	87.11	6.41	36.19
46	15.72	163.97	174.72	104.39	88.59	6.53	41.16

137

Table IX. Experimental Heat Transfer Data (12.0 in. Bed)

Rotometer Reading (%)	Air Flow (SCFM)	G Gas Mass Velocity (Lbm/Hr-Ft^2)	$\bar{T}_{RH}$ Avg. Temp. RH Heater (°F)	$\bar{T}_{LH}$ Avg. Temp. LH Heater (°F)	$\bar{T}_B$ Avg. Temp. Bed (°F)	h_{RH} Ht. Coeff. RH Heater (Btu/Hr-Ft^2-°F)	h_{LH} Ht. Coeff. LH Heater (Btu/Hr-Ft^2-°F)
30	10.53	91.38	182.26	156.03	90.62	3.33	7.29
32	11.18	96.98	182.98	159.32	90.99	3.31	5.61
34	11.83	102.56	183.10	161.68	89.65	3.26	5.26
36	12.48	108.17	182.92	162.79	88.29	3.22	5.05
38	13.13	113.76	182.48	163.60	85.95	3.15	4.81
40	13.78	119.49	181.82	164.08	82.28	3.05	4.53
42	14.43	125.38	178.36	163.99	80.66	3.11	4.46
44	15.07	132.81	179.50	166.37	80.10	3.05	4.28
46	15.72	138.47	179.16	166.88	80.19	3.08	4.26
48	16.37	143.54	178.29	154.29	81.46	3.17	5.10
50	17.02	148.07	177.72	117.84	84.26	3.44	11.11
52	17.67	152.79	181.27	107.46	89.04	3.69	21.84
54	18.32	158.94	181.76	100.15	88.29	3.65	33.14
56	18.97	164.53	181.77	97.46	88.51	3.86	46.29
58	19.62	170.49	181.17	96.54	89.15	3.98	57.01
60	20.27	176.06	180.41	96.20	87.62	4.06	52.07
62	20.92	181.89	180.11	95.89	88.63	4.39	64.38

APPENDIX D.

SAMPLE THERMOCOUPLE CALIBRATION DATA

THERMOCOUPLE # 14
****

TEMP SET ****	PLAT RESIST ******	TC OUTPUT ******	BATH TEMP ****
1	27.4555	.733	18.59
2	27.5595	.774	19.61
3	28.1879	1.024	25.82
4	28.6638	1.221	30.53
5	29.4569	1.549	38.39
6	29.9557	1.759	43.35
7	30.7738	2.107	51.49
8	31.3107	2.340	56.85
9	32.1887	2.727	65.63
10	32.7447	2.974	71.20
11	33.6864	3.401	80.65
12	33.9723	3.531	83.53
13	33.3729	3.257	77.50
14	32.4592	2.844	68.33
15	31.9182	2.605	62.92
16	31.0491	2.225	54.24
17	30.5287	2.002	49.05
18	29.7070	1.652	40.88
19	29.2117	1.444	35.96
20	28.4275	1.121	28.19

139
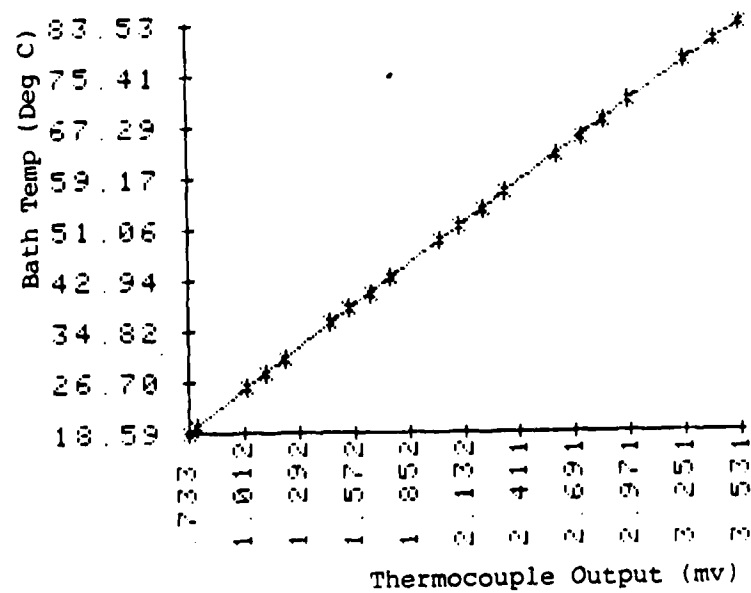
```
-----------------------------------
    ***POLYNOMIAL FUNCTION***
          (ORDER =4)

Y=-.3632175541 + 26.8755193719
*X-1.5852579638 *X^ 2 +
 .30623489 *X^ 3 -.03048987888
*X^ 4

      X        Y (ACT)      Y (CALC)
     ***       *******      *******
     .733       18.59        18.5966
     .774       19.61        19.6198
    1.024       25.82        25.7903
    1.221       30.53        30.5781
    1.549       38.39        38.4259
    1.759       43.35        43.3807
    2.107       51.49        51.4894
    2.340       56.85        56.8549
    2.727       65.63        65.6616
    2.974       71.20        71.2135
    3.401       80.65        80.6717
    3.531       83.53        83.5115
    3.257       77.50        77.5034
    2.844       68.33        68.2984
    2.605       62.92        62.8993
    2.225       54.24        54.2127
    2.002       49.05        49.0553
    1.652       40.88        40.8624
    1.444       35.96        35.9290
    1.121       28.19        28.1554

SUM OF SQUARE ERRORS=
 .012263527709
```

APPENDIX E.

SAMPLE HEAT TRANSFER DATA REDUCTION COMPUTER PRINTOUTS

1. Non-fluidized 6.25 in. configuration.

EXPERIMENTAL DATA
RUN # 06B20
06/08/82 - 0425

RUN NUMBER =   06B20

BED WIDTH =   6.25 INCHES

STATIC BED HEIGHT =   12.5   INCHES

AIR FLOW RATE =   7.29 CFM

AMBIENT TEMPERATURE =   74.50 DEG F

RIGHT HEATER VOLTAGE =   44.0 VOLTS

RIGHT HEATER CURRENT =   .82 AMPS

LEFT HEATER VOLTAGE =   45.0 VOLTS

LEFT HEATER CURRENT =   1.00 AMPS

BED EXPANSION =   0.0   INCHES

COMMENTS: NON-FLUIDIZED/NON-EXPANDED
BED WITH SMALL LOCAL SPOUT AT 10-10

141

EXPERIMENTAL DATA
RUN # 06B20
06/08/82 - 0425

THERMOCOUPLE READINGS

TC#	OUTPUT (mV)	TEMP (DEG F)		TC#	OUTPUT (mV)	TEMP (DEG F)
1	3.332	174.65		41	2.110	124.98
2	3.331	174.55		42	2.076	123.54
3	3.336	174.76		43	1.958	118.62
4	.977	79.23		44	2.087	123.87
5	3.330	174.55		45	2.112	124.92
6	3.337	174.81		46	2.002	120.34
7	3.343	175.05		47	.911	73.51
8	3.335	174.71		48	.911	73.49
9	3.312	173.78		49	.910	73.46
10	3.322	174.17		50	1.430	96.22
11	3.319	174.07		51	1.408	95.30
12	3.316	173.94		52	1.385	94.33
13	3.278	172.36		53	.953	75.34
14	3.282	172.50		54	.948	75.11
15	3.287	172.72		55	1.202	86.16
16	3.286	172.60		56	1.422	95.85
17	3.230	170.36		57	1.417	95.62
18	3.235	170.55		68	2.035	121.70
19	3.238	170.72		69	2.483	140.40
20	3.232	170.58		70	1.952	118.20
21	3.129	166.36		71	2.111	124.90
22	3.132	166.51		72	1.890	115.58
23	3.127	166.26		73	2.072	123.26
24	3.129	166.35		74	.936	74.29
25	3.130	166.41		75	.940	74.47
26	3.131	166.47		76	2.119	125.24
27	3.128	166.34		77	2.381	136.19
28	3.128	166.31		78	1.872	114.81
29	3.110	165.59		79	2.028	121.41
30	3.113	165.70				
31	3.111	165.63				
32	3.108	165.43				
33	3.077	164.22				
34	3.075	164.14				
35	3.075	164.11				
36	3.072	163.96				
37	3.016	161.74				
38	3.021	161.93				
39	3.019	161.83				
40	3.020	162.13				

RIGHT-HAND HEATER
TEMPERATURE PROFILE

	COL 1	COL 2	COL 3	COL 4	AVE
ROW 1	174.65	174.55	174.76	******	174.66
ROW 2	174.55	174.81	175.05	174.71	174.78
ROW 3	173.78	174.17	174.07	173.94	173.99
ROW 4	172.36	172.50	172.72	172.60	172.54
ROW 5	170.36	170.55	170.72	170.58	170.55

NOTE: TEMPERATURES SHOWN ARE IN DEGREES FAHRENHEIT
AND ARE ARRANGED AS SEEN FROM WITHIN THE BED

RIGHT-HAND HEATER
TEMP vs DEPTH

NOTE: PLOTTED TEMPERATURES ARE AVERAGES OF EACH
HORIZONTAL ROW

143
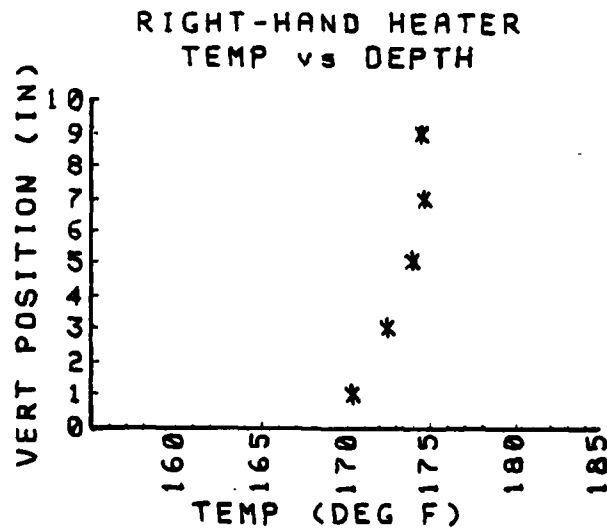
LEFT-HAND HEATER
TEMPERATURE PROFILE

	COL 1	COL 2	COL 3	COL 4	AVE
ROW 1	166.36	166.51	166.26	166.35	166.37
ROW 2	166.41	166.47	166.34	166.31	166.38
ROW 3	165.59	165.70	165.63	165.43	165.59
ROW 4	164.22	164.14	164.11	163.96	164.10
ROW 5	161.74	161.93	161.83	162.13	161.91

NOTE: TEMPERATURES SHOWN ARE IN DEGREES FAHRENHEIT
AND ARE ARRANGED AS SEEN FROM WITHIN THE BED

LEFT-HAND HEATER
TEMP vs DEPTH

NOTE: PLOTTED TEMPERATURES ARE AVERAGES OF EACH
HORIZONTAL ROW

144
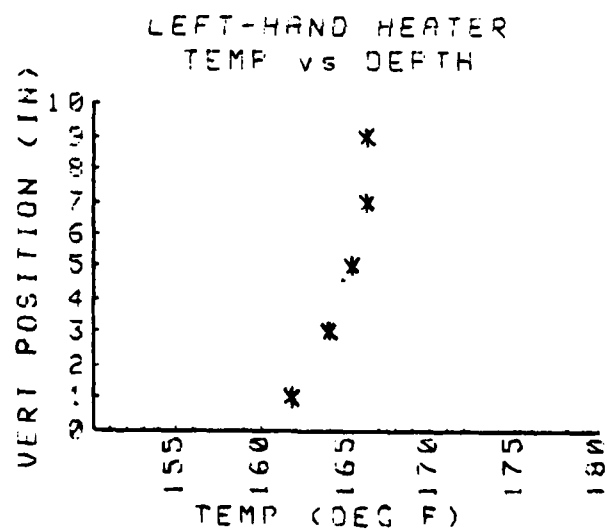
FLUIDIZED BED
TEMPERATURE PROFILE

```
----------------------------
:
:
:   95.85    75.34    96.22  :
:
:                    95.30  :
:
:   95.62    75.11    94.33  :
:  ,
:
----------------------------
```

NOTE: TEMPERATURES SHOWN ARE IN DEGREES FAHRENHEIT
AND ARE ARRANGED AS SEEN FROM ABOVE THE BED

CALCULATED RESULTS
RUN # 06B20
06/08/82 - 0425

RIGHT-HAND HEATER

AVERAGE HEATER TEMPERATURE =   173.30 DEG F
AVERAGE PLATE SURFACE TEMPERATURE =   173.28 DEG F
AVERAGE BED TEMPERATURE =   89.68 DEG F
ELECTRICAL ENERGY INTO HEATER =   123.11 BTU/HR
LOSS FROM HTR BACKING TO ATM =   11.22 BTU/HR
h(HTR BACKING-ATM) =   .52 BTU/HR-FT^2-DEG F
LOSS FROM HTR PERIMETER TO BED =   13.50 BTU/HR
HEAT FLUX THRU PLATE =   98.39 BTU/HR
h(PLATE-BED) =   3.39 BTU/HR-FT^2-DEG F

LEFT-HAND HEATER

AVERAGE HEATER TEMPERATURE =   164.87 DEG F
AVERAGE PLATE SURFACE TEMPERATURE =   164.84 DEG F
AVERAGE BED TEMPERATURE =   89.68 DEG G
ELECTRICAL ENERGY INTO HEATER =   153.54 BTU/HR
LOSS FROM HTR BACKING TO ATM =   9.20 BTU/HR
h(HTR BACKING-ATM) =   .42 BTU/HR-FT^2-DEG F
LOSS FROM HTR PERIMETER TO BED =   19.77 BTU/HR
HEAT FLUX THRU PLATE =   124.58 BTU/HR
h(PLATE-BED) =   4.77 BTU/HR-FT^2-DEG F

ENERGY BALANCE

AVERAGE AIR INLET TEMPERATURE =   73.49 DEG F
AIR OUTLET TEMPERATURE =   86.16 DEG F
AVERAGE BED TEMPERATURE =   89.68 DEG F
q(AIR OUT) =   96.97 BTU/HR
q(LOSS F/R WALL) =   .50 BTU/HR
q(TOTAL OUT OF BED) =   97.47 BTU/HR
q(TOTAL INTO BED) =   256.23 BTU/HR
SUPERFICIAL VELOCITY =   .47 FT/SEC
SUPERFICIAL MASS VELOCITY =   121.92 LBM/HR-FT^2
PARTICLE REYNOLDS NUMBER =   2.44

146

2. Fluidized 6.24 in. configuration.

EXPERIMENTAL DATA
RUN # 06B26
06/08/82 - 0510

RUN NUMBER =   06B26

BED WIDTH =   6.25 INCHES

STATIC BED HEIGHT =   12.5   INCHES

AIR FLOW RATE =   9.23 CFM

AMBIENT TEMPERATURE =   74.50 DEG F

RIGHT HEATER VOLTAGE =   60.0 VOLTS

RIGHT HEATER CURRENT =   1.12 AMPS

LEFT HEATER VOLTAGE =   60.0 VOLTS

LEFT HEATER CURRENT =   1.28 AMPS

BED EXPANSION =   .1   INCHES

COMMENTS: FLUIDIZATION WITH 2-3 INCH
DIA BUBBLES ERUPTING AT LOCATION 5-5
AND VICINITY/ACTIVE BOT LEFT

****EXPERIMENTAL DATA****
RUN # 06B26
06/08/82 - 0510

THERMOCOUPLE READINGS

TC#	OUTPUT (mV)	TEMP (DEG F)	TC#	OUTPUT (mV)	TEMP (DEG F)
1	2.729	150.44	41	2.146	126.48
2	2.728	150.36	42	2.116	125.21
3	2.724	150.18	43	1.996	120.22
4	.961	78.19	44	2.160	126.91
5	2.855	155.53	45	2.154	126.67
6	2.859	155.67	46	2.041	121.97
7	2.858	155.63	47	.922	74.00
8	2.848	155.21	48	.922	73.98
9	2.991	160.95	49	.922	73.99
10	3.000	161.31	50	1.564	101.98
11	2.996	161.15	51	1.555	101.63
12	2.988	160.85	52	1.551	101.49
13	3.107	165.53	53	1.556	101.66
14	3.106	165.48	54	1.588	103.00
15	3.106	165.49	55	1.526	100.12
16	3.106	165.43	56	1.551	101.40
17	3.141	166.80	57	1.550	101.35
18	3.144	166.92	68	1.927	117.14
19	3.140	166.81	69	1.958	118.46
20	3.137	166.79	70	1.930	117.27
21	2.259	130.99	71	2.368	135.64
22	2.290	132.28	72	1.916	116.68
23	2.291	132.28	73	2.039	121.87
24	2.297	132.51	74	1.045	79.10
25	2.340	134.30	75	1.260	88.51
26	2.336	134.16	76	1.839	113.41
27	2.335	134.10	77	1.856	114.14
28	2.348	134.63	78	1.673	106.34
29	2.346	134.56	79	1.925	117.06
30	2.335	134.06			
31	2.339	134.26			
32	2.354	134.79			
33	2.298	132.51			
34	2.285	131.94			
35	2.291	132.18			
36	2.310	132.97			
37	2.233	129.78			
38	2.218	129.16			
39	2.225	129.44			
40	2.259	131.11			

RIGHT-HAND HEATER
TEMPERATURE PROFILE

	COL 1	COL 2	COL 3	COL 4	AVE
ROW 1	150.44	150.36	150.18	******	150.33
ROW 2	155.53	155.67	155.63	155.21	155.51
ROW 3	160.95	161.31	161.15	160.85	161.07
ROW 4	165.53	165.48	165.49	165.43	165.48
ROW 5	166.80	166.92	166.81	166.79	166.83

NOTE: TEMPERATURES SHOWN ARE IN DEGREES FAHRENHEIT
AND ARE ARRANGED AS SEEN FROM WITHIN THE BED

RIGHT-HAND HEATER
TEMP vs DEPTH

NOTE: PLOTTED TEMPERATURES ARE AVERAGES OF EACH
HORIZONTAL ROW

149
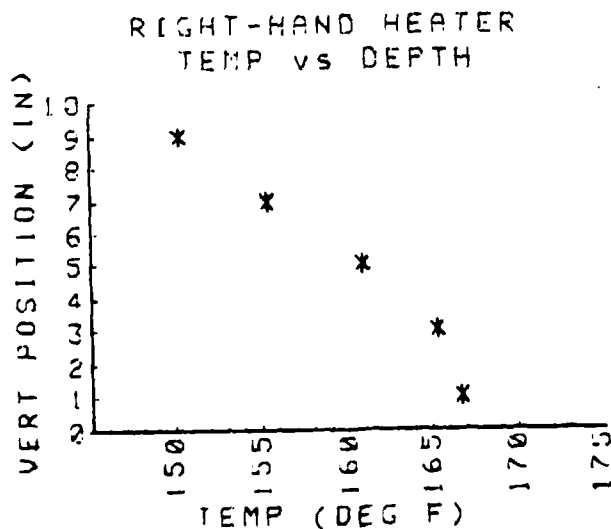
LEFT-HAND HEATER
TEMPERATURE PROFILE

	COL 1	COL 2	COL 3	COL 4	AVE
ROW 1	130.99	132.28	132.28	132.51	132.02
ROW 2	134.30	134.16	134.10	134.63	134.30
ROW 3	134.56	134.06	134.26	134.79	134.42
ROW 4	132.51	131.94	132.18	132.97	132.40
ROW 5	129.78	129.16	129.44	131.11	129.87

NOTE: TEMPERATURES SHOWN ARE IN DEGREES FAHRENHEIT
AND ARE ARRANGED AS SEEN FROM WITHIN THE BED

LEFT-HAND HEATER
TEMP vs DEPTH

NOTE: PLOTTED TEMPERATURES ARE AVERAGES OF EACH
HORIZONTAL ROW

150
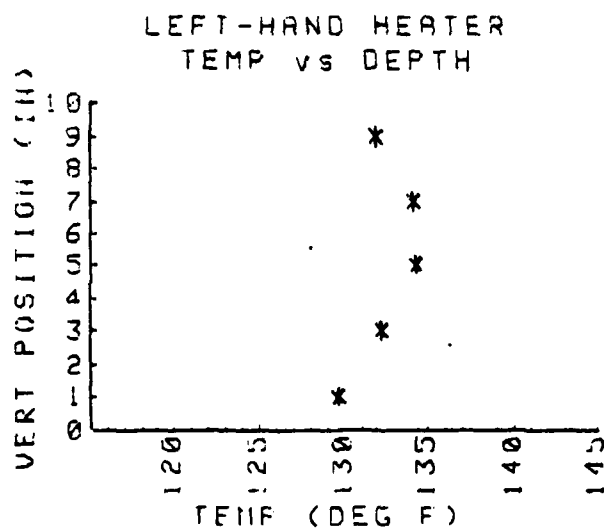
```
**EXPERIMENTAL DATA**
       RUN# 06B26
    06/08/82 - 0510


       FLUIDIZED BED
    TEMPERATURE PROFILE


  ---------------------------
 |                           |
 |                           |
 |  101.40   101.66   101.98 |
 |                           |
 |                           |
 |                    101.63 |
 |                           |
 |  101.35   103.00   101.49 |
 |                           |
  ---------------------------
```

NOTE: TEMPERATURES SHOWN ARE IN DEGREES FAHRENHEIT
AND ARE ARRANGED AS SEEN FROM ABOVE THE BED

151

CALCULATED RESULTS
RUN # 06B26
06/08/82 - 0510

RIGHT-HAND HEATER

```
AVERAGE HEATER TEMPERATURE =                159.84 DEG F
AVERAGE PLATE SURFACE TEMPERATURE =         159.79 DEG F
AVERAGE BED TEMPERATURE =                   101.79 DEG F
ELECTRICAL ENERGY INTO HEATER =            229.29 BTU/HR
LOSS FROM HTR BACKING TO ATM =               7.92 BTU/HR
h(HTR BACKING-ATM) =                 .36 BTU/HR-FT^2-DEG F
LOSS FROM HTR PERIMETER TO BED =            20.58 BTU/HR
HEAT FLUX THRU PLATE =                     200.79 BTU/HR
h(PLATE-BED) =                      9.97 BTU/HR-FT^2-DEG F
```


LEFT-HAND HEATER

```
AVERAGE HEATER TEMPERATURE =                132.60 DEG F
AVERAGE PLATE SURFACE TEMPERATURE =         132.54 DEG F
AVERAGE BED TEMPERATURE =                   101.79 DEG G
ELECTRICAL ENERGY INTO HEATER =            262.05 BTU/HR
LOSS FROM HTR BACKING TO ATM =               1.54 BTU/HR
h(HTR BACKING-ATM) =                 .07 BTU/HR-FT^2-DEG F
LOSS FROM HTR PERIMETER TO BED =            33.49 BTU/HR
HEAT FLUX THRU PLATE =                     227.02 BTU/HR
h(PLATE-BED) =                     21.26 BTU/HR-FT^2-DEG F
```


ENERGY BALANCE

```
AVERAGE AIR INLET TEMPERATURE =             73.99 DEG F
AIR OUTLET TEMPERATURE =                   100.12 DEG F
AVERAGE BED TEMPERATURE =                   101.79 DEG F
q(AIR OUT) =                               247.04 BTU/HR
q(LOSS F/R WALL) =                          26.35 BTU/HR
q(TOTAL OUT OF BED) =                      273.39 BTU/HR
q(TOTAL INTO BED) =                        481.88 BTU/HR
SUPERFICIAL VELOCITY =                        .59 FT/SEC
SUPERFICIAL MASS VELOCITY =           150.65 LBM/HR-FT^2
PARTICLE REYNOLDS NUMBER =                     3.01
```


152

3. Non-fluidized 12.0 in. configuration.

EXPERIMENTAL DATA
RUN # 12B30E
06/17/82 - 0055

RUN NUMBER =   12B30E

BED WIDTH =   12.00 INCHES

STATIC BED HEIGHT =   12.5   INCHES

AIR FLOW RATE =   10.53 CFM

AMBIENT TEMPERATURE =   78.60 DEG F

RIGHT HEATER VOLTAGE =   46.0 VOLTS

RIGHT HEATER CURRENT =   .85 AMPS

LEFT HEATER VOLTAGE =   56.0 VOLTS

LEFT HEATER CURRENT =   1.02 AMPS

BED EXPANSION =   0.0   INCHES

COMMENTS: NON-FLUIDIZED/NON-EXPANDED
BED/NO BUBBLES BOTTOM LEFT

EXPERIMENTAL DATA
RUN # 12B30E
06/17/82 - 0055

THERMOCOUPLE READINGS

TC#	OUTPUT (mV)	TEMP (DEG F)	TC#	OUTPUT (mV)	TEMP (DEG F)
1	3.556	183.47	41	2.123	125.52
2	3.550	183.20	42	2.145	126.42
3	3.553	183.34	43	2.041	122.10
4	1.140	89.84	44	1.785	111.20
5	3.554	183.39	45	1.862	114.45
6	3.559	183.55	46	1.795	111.65
7	3.565	183.83	47	.967	75.99
8	3.556	183.41	48	.966	75.92
9	3.541	182.84	49	.966	75.94
10	3.551	183.22	50	1.438	96.56
11	3.545	183.03	51	1.429	96.21
12	3.541	182.80	52	1.403	95.11
13	3.512	181.62	53	1.273	89.41
14	3.515	181.69	54	1.277	89.56
15	3.516	181.78	55	1.257	88.55
16	3.514	181.61	56	1.261	88.86
17	3.468	179.84	57	1.260	88.80
18	3.471	179.90	58	1.265	89.01
19	3.468	179.81	59	1.274	89.40
20	3.458	179.52	60	1.255	88.87
21	2.886	156.60	61	1.257	88.95
22	2.886	156.63	62	1.262	89.15
23	2.883	156.46	63	1.239	88.13
24	2.886	156.58	68	1.954	118.29
25	2.893	156.89	69	2.477	140.15
26	2.894	156.94	70	2.173	127.50
27	2.891	156.82	71	2.527	142.22
28	2.890	156.75	72	1.974	119.13
29	2.886	156.59	73	2.200	128.63
30	2.888	156.65	74	1.095	81.29
31	2.887	156.62	75	1.165	84.36
32	2.886	156.51	76	1.977	119.26
33	2.869	155.85	77	2.092	124.10
34	2.867	155.76	78	1.773	110.61
35	2.869	155.81	79	1.740	109.20
36	2.866	155.67			
37	2.828	154.16			
38	2.836	154.47			
39	2.832	154.30			
40	2.831	154.51			

RIGHT-HAND HEATER
TEMPERATURE PROFILE

	COL 1	COL 2	COL 3	COL 4	AVE
ROW 1	183.47	183.20	183.34	*****	183.34
ROW 2	183.39	183.55	183.83	183.41	183.55
ROW 3	182.84	183.22	183.03	182.80	182.97
ROW 4	181.62	181.69	181.78	181.61	181.68
ROW 5	179.84	179.90	179.81	179.52	179.77

NOTE: TEMPERATURES SHOWN ARE IN DEGREES FAHRENHEIT
AND ARE ARRANGED AS SEEN FROM WITHIN THE BED
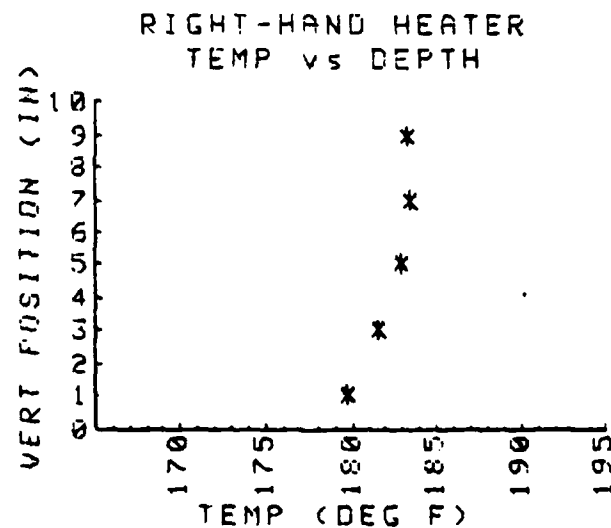
RIGHT-HAND HEATER
TEMP vs DEPTH

NOTE: PLOTTED TEMPERATURES ARE AVERAGES OF EACH
HORIZONTAL ROW

155

LEFT-HAND HEATER
TEMPERATURE PROFILE

	COL 1	COL 2	COL 3	COL 4	AVE
ROW 1	156.60	156.63	156.46	156.58	156.57
ROW 2	156.89	156.94	156.82	156.75	156.85
ROW 3	156.59	156.65	156.62	156.51	156.59
ROW 4	155.85	155.76	155.81	155.67	155.77
ROW 5	154.16	154.47	154.30	154.51	154.36

NOTE: TEMPERATURES SHOWN ARE IN DEGREES FAHRENHEIT
AND ARE ARRANGED AS SEEN FROM WITHIN THE BED

LEFT-HAND HEATER
TEMP vs DEPTH

NOTE: PLOTTED TEMPERATURES ARE AVERAGES OF EACH
HORIZONTAL ROW

156
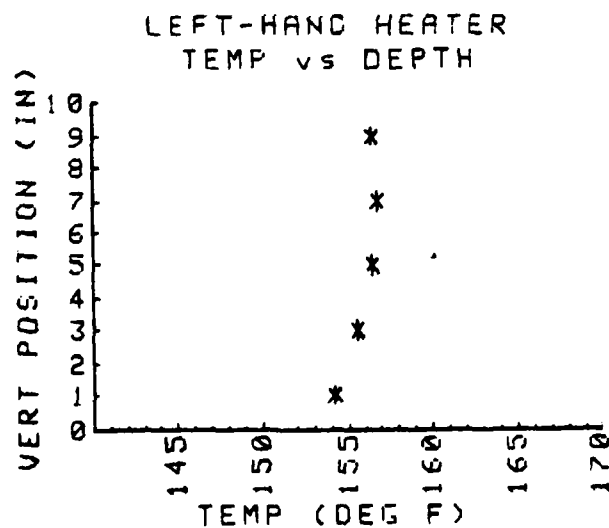
EXPERIMENTAL DATA
RUN# 12B30E
06/17/82 - 0055

FLUIDIZED BED
TEMPERATURE PROFILE

88.95	89.01	88.86	89.41	96.56
89.15	89.40			96.21
88.13	88.87	88.80	89.56	95.11

NOTE: TEMPERATURES SHOWN ARE IN DEGREES FAHRENHEIT
AND ARE ARRANGED AS SEEN FROM ABOVE THE BED

CALCULATED RESULTS
RUN # 12B30E
06/17/82 - 0055

RIGHT-HAND HEATER

```
AVERAGE HEATER TEMPERATURE =              182.26 DEG F
AVERAGE PLATE SURFACE TEMPERATURE =       182.23 DEG F
AVERAGE BED TEMPERATURE =                  90.62 DEG F
ELECTRICAL ENERGY INTO HEATER =           133.41 BTU/HR
LOSS FROM HTR BACKING TO ATM =             12.85 BTU/HR
h(HTR BACKING-ATM) =              .61 BTU/HR-FT^2-DEG F
LOSS FROM HTR PERIMETER TO BED =           14.77 BTU/HR
HEAT FLUX THRU PLATE =                    105.80 BTU/HR
h(PLATE-BED) =                   3.33 BTU/HR-FT^2-DEG F
```

LEFT-HAND HEATER

```
AVERAGE HEATER TEMPERATURE =              156.03 DEG F
AVERAGE PLATE SURFACE TEMPERATURE =       155.98 DEG F
AVERAGE BED TEMPERATURE =                  90.62 DEG G
ELECTRICAL ENERGY INTO HEATER =           194.90 BTU/HR
LOSS FROM HTR BACKING TO ATM =              9.90 BTU/HR
h(HTR BACKING-ATM) =              .63 BTU/HR-FT^2-DEG F
LOSS FROM HTR PERIMETER TO BED =           19.57 BTU/HR
HEAT FLUX THRU PLATE =                    165.43 BTU/HR
h(PLATE-BED) =                   7.29 BTU/HR-FT^2-DEG F
```

ENERGY BALANCE

```
AVERAGE AIR INLET TEMPERATURE =            75.95 DEG F
AIR OUTLET TEMPERATURE =                   88.55 DEG F
AVERAGE BED TEMPERATURE =                  90.62 DEG F
q(AIR OUT) =                              138.71 BTU/HR
q(LOSS F/R WALL) =                         16.49 BTU/HR
q(TOTAL OUT OF BED) =                     155.20 BTU/HR
q(TOTAL INTO BED) =                       305.56 BTU/HR
SUPERFICIAL VELOCITY =                       .35 FT/SEC
SUPERFICIAL MASS VELOCITY =        91.38 LBM/HR-FT^2
PARTICLE REYNOLDS NUMBER =                   1.83
```

158

4. Fluidized 12.0 in. configuration.

EXPERIMENTAL DATA
RUN # 12B48E
06/17/82 - 0155

RUN NUMBER =   12B48E

BED WIDTH =   12.00 INCHES

STATIC BED HEIGHT =   12.5 INCHES

AIR FLOW RATE =   16.37 CFM

AMBIENT TEMPERATURE =   81.50 DEG F

RIGHT HEATER VOLTAGE =   46.0 VOLTS

RIGHT HEATER CURRENT =   .85 AMPS

LEFT HEATER VOLTAGE =   46.0 VOLTS

LEFT HEATER CURRENT =   1.02 AMPS

BED EXPANSION =   0.1 INCHES

COMMENTS: FLUIDIZATION WITH 2-3 INCH
BUBBLES ERUPTING AT LOCATION 4-4

EXPERIMENTAL DATA
RUN # 12B48E
06/17/82 - 0155

THERMOCOUPLE READINGS

TC#	OUTPUT (mV)	TEMP (DEG F)	TC#	OUTPUT (mV)	TEMP (DEG F)
1	3.471	180.14	41	2.279	132.01
2	3.474	180.21	42	2.244	130.53
3	3.478	180.39	43	2.097	124.44
4	1.083	86.14	44	2.121	125.29
5	3.472	180.16	45	2.136	125.92
6	3.479	180.41	46	2.024	121.26
7	3.484	180.63	47	.959	75.64
8	3.476	180.27	48	.959	75.62
9	3.445	179.05	49	.960	75.67
10	3.455	179.43	50	1.073	80.65
11	3.450	179.27	51	1.122	82.84
12	3.445	179.04	52	1.044	79.41
13	3.394	176.96	53	.989	76.94
14	3.399	177.13	54	1.089	81.33
15	3.398	177.12	55	1.128	82.94
16	3.393	176.84	56	1.097	81.67
17	3.338	174.67	57	1.100	81.79
18	3.343	174.84	58	1.100	81.79
19	3.339	174.72	59	1.105	82.01
20	3.327	174.35	60	1.096	81.90
21	2.831	154.38	61	1.167	85.01
22	2.833	154.49	62	1.096	81.87
23	2.833	154.44	63	1.095	81.82
24	2.839	154.68	68	2.133	125.82
25	2.866	155.80	69	2.600	145.23
26	2.866	155.81	70	2.088	123.93
27	2.864	155.73	71	2.571	144.03
28	2.864	155.70	72	1.946	117.95
29	2.869	155.90	73	2.063	122.88
30	2.867	155.80	74	1.031	78.48
31	2.863	155.65	75	1.021	78.04
32	2.863	155.58	76	2.024	121.24
33	2.833	154.39	77	2.246	130.55
34	2.827	154.14	78	1.806	112.01
35	2.821	153.87	79	2.033	121.62
36	2.817	153.69			
37	2.766	151.65			
38	2.764	151.55			
39	2.756	151.22			
40	2.755	151.43			

160

RIGHT-HAND HEATER
TEMPERATURE PROFILE

	COL 1	COL 2	COL 3	COL 4	AVE
ROW 1	180.14	180.21	180.39	*****	180.24
ROW 2	180.16	180.41	180.63	180.27	180.37
ROW 3	179.05	179.43	179.27	179.04	179.20
ROW 4	176.96	177.13	177.12	176.84	177.01
ROW 5	174.67	174.84	174.72	174.35	174.65

NOTE: TEMPERATURES SHOWN ARE IN DEGREES FAHRENHEIT
AND ARE ARRANGED AS SEEN FROM WITHIN THE BED
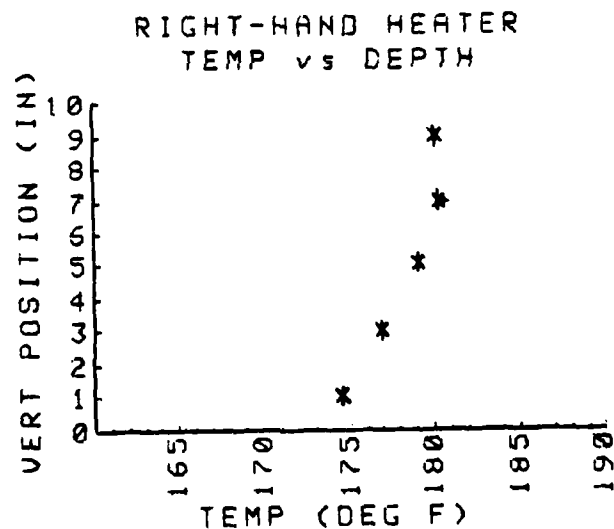
RIGHT-HAND HEATER
TEMP vs DEPTH

NOTE: PLOTTED TEMPERATURES ARE AVERAGES OF EACH
HORIZONTAL ROW

LEFT-HAND HEATER
TEMPERATURE PROFILE

	COL 1	COL 2	COL 3	COL 4	AVE
ROW 1	154.38	154.49	154.44	154.68	154.50
ROW 2	155.80	155.81	155.73	155.70	155.76
ROW 3	155.90	155.80	155.65	155.58	155.73
ROW 4	154.39	154.14	153.87	153.69	154.02
ROW 5	151.65	151.55	151.22	151.43	151.46

NOTE: TEMPERATURES SHOWN ARE IN DEGREES FAHRENHEIT
AND ARE ARRANGED AS SEEN FROM WITHIN THE BED

LEFT-HAND HEATER
TEMP vs DEPTH

NOTE: PLOTTED TEMPERATURES ARE AVERAGES OF EACH
HORIZONTAL ROW

162
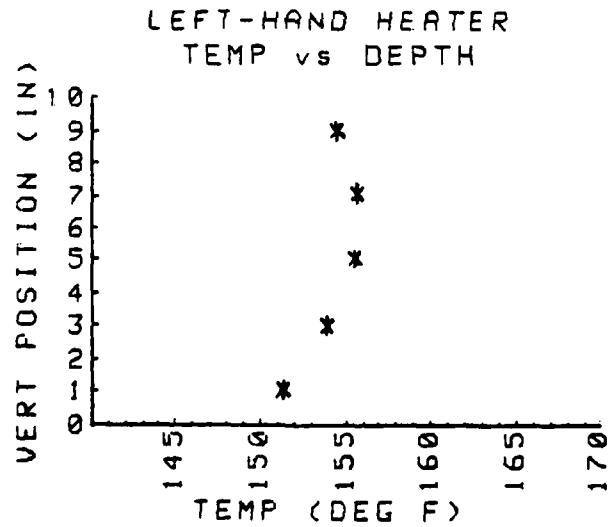
FLUIDIZED BED
TEMPERATURE PROFILE

85.01	81.79	81.67	76.94	80.65
81.87	82.01			82.84
81.82	81.90	81.79	81.33	79.41

NOTE: TEMPERATURES SHOWN ARE IN DEGREES FAHRENHEIT
AND ARE ARRANGED AS SEEN FROM ABOVE THE BED

CALCULATED RESULTS
RUN # 12B48E
06/17/82 - 0155

RIGHT-HAND HEATER

```
AVERAGE HEATER TEMPERATURE =            178.29 DEG F
AVERAGE PLATE SURFACE TEMPERATURE =     178.27 DEG F
AVERAGE BED TEMPERATURE =                81.46 DEG F
ELECTRICAL ENERGY INTO HEATER =         133.41 BTU/HR
LOSS FROM HTR BACKING TO ATM =           10.82 BTU/HR
h(HTR BACKING-ATM) =              .51 BTU/HR-FT^2-DEG F
LOSS FROM HTR PERIMETER TO BED =         16.12 BTU/HR
HEAT FLUX THRU PLATE =                  106.48 BTU/HR
h(PLATE-BED) =                   3.17 BTU/HR-FT^2-DEG F
```


LEFT-HAND HEATER

```
AVERAGE HEATER TEMPERATURE =            154.29 DEG F
AVERAGE PLATE SURFACE TEMPERATURE =     154.26 DEG F
AVERAGE BED TEMPERATURE =                81.46 DEG G
ELECTRICAL ENERGY INTO HEATER =         160.10 BTU/HR
LOSS FROM HTR BACKING TO ATM =            6.44 BTU/HR
h(HTR BACKING-ATM) =              .35 BTU/HR-FT^2-DEG F
LOSS FROM HTR PERIMETER TO BED =         24.67 BTU/HR
HEAT FLUX THRU PLATE =                  128.98 BTU/HR
h(PLATE-BED) =                   5.10 BTU/HR-FT^2-DEG F
```


ENERGY BALANCE

```
AVERAGE AIR INLET TEMPERATURE =          75.64 DEG F
AIR OUTLET TEMPERATURE =                 82.94 DEG F
AVERAGE BED TEMPERATURE =                81.46 DEG F
q(AIR OUT) =                            126.26 BTU/HR
q(LOSS F/R WALL) =                        0.00 BTU/HR
q(TOTAL OUT OF BED) =                   126.26 BTU/HR
q(TOTAL INTO BED) =                     276.25 BTU/HR
SUPERFICIAL VELOCITY =                     .55 FT/SEC
SUPERFICIAL MASS VELOCITY =             143.54 LBM/HR-FT^2
PARTICLE REYNOLDS NUMBER =                2.87
```

5. A typical data run. (Bed thermocouple probe #57 reads
   significantly higher than other bed thermocouples.
   Reading exceeds highest heater thermocouple reading.)

NOTE: ALL VALUES WERE RECALCULATED AFTER OMITTING
       THERMOCOUPLE NR. 57 READING. REVISED RESULTS
       ARE PRESENTED IN TABLES AND CURVES PREVIOUSLY
       SHOWN.

EXPERIMENTAL DATA
RUN # 06B36M
06/08/82 - 1630

RUN NUMBER =   06B36M

BED WIDTH =   6.25 INCHES

STATIC BED HEIGHT =   12.5 INCHES

AIR FLOW RATE =   12.48 CFM

AMBIENT TEMPERATURE =   74.50 DEG F

RIGHT HEATER VOLTAGE =   60.0 VOLTS

RIGHT HEATER CURRENT =   1.12 AMPS

LEFT HEATER VOLTAGE =   60.0 VOLTS

LEFT HEATER CURRENT =   1.28 AMPS

BED EXPANSION =   0.25 INCHES

COMMENTS: VIOLENT FLUIDIZATION AT CARRYOVER
LIMIT

EXPERIMENTAL DATA
RUN # 06B36M
06/08/82 - 1630

THERMOCOUPLE READINGS

TC#	OUTPUT (mV)	TEMP (DEG F)	TC#	OUTPUT (mV)	TEMP (DEG F)
1	1.930	117.46	41	1.773	110.81
2	1.936	117.68	42	1.774	110.85
3	1.951	118.31	43	1.726	108.83
4	.980	79.43	44	1.966	118.82
5	2.004	120.53	45	2.108	124.75
6	2.004	120.50	46	2.007	120.55
7	2.005	120.57	47	.936	74.62
8	2.000	120.34	48	.935	74.56
9	2.096	124.34	49	.935	74.57
10	2.089	124.06	50	1.631	104.85
11	2.081	123.72	51	1.592	103.22
12	2.088	123.96	52	1.621	104.49
13	2.180	127.75	53	1.608	103.89
14	2.185	127.92	54	1.609	103.90
15	2.164	127.07	55	1.579	102.38
16	2.166	127.11	56	1.629	104.75
17	2.209	128.88	57	2.260	131.38
18	2.219	129.27	68	1.582	102.44
19	2.214	129.09	69	1.658	105.70
20	2.208	128.96	70	1.942	117.78
21	1.936	117.53	71	2.025	121.28
22	1.948	118.03	72	1.565	101.71
23	1.947	117.96	73	1.626	104.32
24	1.944	117.82	74	1.313	90.81
25	2.005	120.38	75	1.497	98.78
26	1.987	119.65	76	1.768	110.39
27	1.997	.120.04	77	1.705	107.71
28	2.017	120.87	78	1.682	106.72
29	2.061	122.74	79	1.740	109.20
30	2.053	122.35			
31	2.051	122.30			
32	2.056	122.44			
33	2.071	123.09			
34	2.067	122.88			
35	2.075	123.21			
36	2.079	123.38			
37	2.080	123.42			
38	2.058	122.50			
39	2.055	122.37			
40	2.094	124.25			

RIGHT-HAND HEATER
TEMPERATURE PROFILE

	COL 1	COL 2	COL 3	COL 4	AVE
ROW 1	117.46	117.68	118.31	*****	117.82
ROW 2	120.53	120.50	120.57	120.34	120.48
ROW 3	124.34	124.06	123.72	123.96	124.02
ROW 4	127.75	127.92	127.07	127.11	127.46
ROW 5	128.88	129.27	129.09	128.96	129.05

NOTE: TEMPERATURES SHOWN ARE IN DEGREES FAHRENHEIT
AND ARE ARRANGED AS SEEN FROM WITHIN THE BED

RIGHT-HAND HEATER
TEMP vs DEPTH

NOTE: PLOTTED TEMPERATURES ARE AVERAGES OF EACH
HORIZONTAL ROW

167
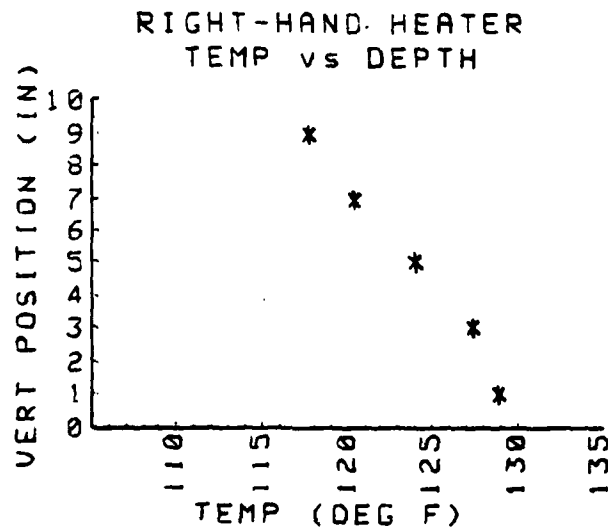
LEFT-HAND HEATER
TEMPERATURE PROFILE

	COL 1	COL 2	COL 3	COL 4	AVE
ROW 1	117.53	118.03	117.96	117.82	117.84
ROW 2	120.38	119.65	120.04	120.87	120.24
ROW 3	122.74	122.35	122.30	122.44	122.46
ROW 4	123.09	122.88	123.21	123.38	123.14
ROW 5	123.42	122.50	122.37	124.25	123.13

NOTE: TEMPERATURES SHOWN ARE IN DEGREES FAHRENHEIT
AND ARE ARRANGED AS SEEN FROM WITHIN THE BED

LEFT-HAND HEATER
TEMP vs DEPTH

NOTE: PLOTTED TEMPERATURES ARE AVERAGES OF EACH
HORIZONTAL ROW

168
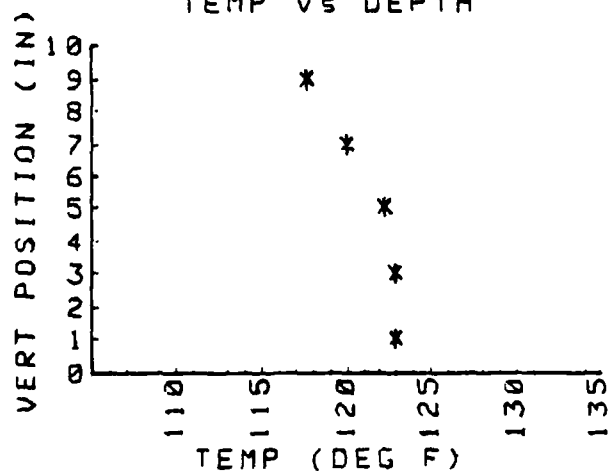
EXPERIMENTAL DATA
RUN# 06B36M
06/08/82 - 1630

FLUIDIZED BED
TEMPERATURE PROFILE

```
-----------------------------
|                           |
|  104.75  103.89  104.85   |
|                           |
|                  103.22   |
|                           |
|  131.38  103.90  104.49   |
|                           |
-----------------------------
```

NOTE: TEMPERATURES SHOWN ARE IN DEGREES FAHRENHEIT
AND ARE ARRANGED AS SEEN FROM ABOVE THE BED

```
                    **CALCULATED RESULTS**
                        RUN # 06B36M
                      06/08/82 - 1630


                      RIGHT-HAND HEATER


    AVERAGE HEATER TEMPERATURE =                123.77 DEG F
    AVERAGE PLATE SURFACE TEMPERATURE =         123.71 DEG F
    AVERAGE BED TEMPERATURE =                   108.07 DEG F
    ELECTRICAL ENERGY INTO HEATER =             229.29 BTU/HR
    LOSS FROM HTR BACKING TO ATM =                2.96 BTU/HR
    h(HTR BACKING-ATM) =                 .19 BTU/HR-FT^2-DEG F
    LOSS FROM HTR PERIMETER TO BED =             8.13  BTU/HR
    HEAT FLUX THRU PLATE =                      218.20  BTU/HR
    h(PLATE-BED) =                     40.18  BTU/HR-FT^2-DEG F


                      LEFT-HAND HEATER


    AVERAGE HEATER TEMPERATURE =                121.36 DEG F
    AVERAGE PLATE SURFACE TEMPERATURE =         121.29 DEG F
    AVERAGE BED TEMPERATURE =                   108.07 DEG G
    ELECTRICAL ENERGY INTO HEATER =             262.05 BTU/HR
    LOSS FROM HTR BACKING TO ATM =                 .00 BTU/HR
    h(HTR BACKING-ATM) =                 .00 BTU/HR-FT^2-DEG F
    LOSS FROM HTR PERIMETER TO BED =             4.41  BTU/HR
    HEAT FLUX THRU PLATE =                      257.64  BTU/HR
    h(PLATE-BED) =                     56.11  BTU/HR-FT^2-DEG F


                       ENERGY BALANCE


    AVERAGE AIR INLET TEMPERATURE =              74.58 DEG F
    AIR OUTLET TEMPERATURE =                    102.38 DEG F
    AVERAGE BED TEMPERATURE =                   108.07 DEG F
    q(AIR OUT) =                                353.81 BTU/HR
    q(LOSS F/R WALL) =                           22.30 BTU/HR
    q(TOTAL OUT OF BED) =                       376.11 BTU/HR
    q(TOTAL INTO BED) =                         488.38 BTU/HR
    SUPERFICIAL VELOCITY =                         .80 FT/SEC
    SUPERFICIAL MASS VELOCITY =         202.78 LBM/HR-FT^2
    PARTICLE REYNOLDS NUMBER =                     4.05
```

170

APPENDIX F.

EQUIPMENT LISTING

DEVICE	MANUFACTURER	MODEL #	SERIAL #
Axial Flow Turbo Compressor	Spencer Turbine	550 SCFM	
Rotometer	Fisher & Porter	34 SCFM	
30-Inch Water Manometer	Meriam	33KA35	A69513
Computer	Hewlett-Packard Company	HP 85	2151A50182
Data Acquisition System	Hewlett-Packard Company	HP 3497A	
Dual Flexible Disk Drive	Hewlett-Packard Company	HP 82901M	
Plotter	Hewlett-Packard Company	HP 7225A	
Printer	Hewlett-Packard Company	HP 82905B	2143J12965
Copper Constantan Thermocouples	Omega Engineering	10 Gauge	
Regulated DC Power Supply 60V, 2 A (Left)	Lambda	LK345A	C1821
Regulated DC Power Supply 60V, 2 A (Right)	Hewlett-Packard Company	6296A	1552A02618
Computating Bridge	Rosemount	920A	110
Calibration Bath	Rosemount	913A	
Strip Heaters 250 Watts	Watlo	250 Watts	8044

171

APPENDIX G.

EXPERIMENTAL UNCERTAINTY ANALYSIS

In order to arrive at an estimate of the difference between measured or calculated values and the true values of various parameters, the following uncertainty analysis was accomplished:

1. TEMPERATURE MEASUREMENTS

A. Thermocouple Readings - Since the thermocouple output voltage was measured automatically by the Data Acquisition System, human error in reading the output was avoided; however, the values arrived at by the System were still subject to random error as well as inaccuracies in the empirical correlation developed during the calibration of the thermocouples. Because of these effects, it is believed that the thermocouple readings are accurate to within $\pm^{o}F$.

B. Ambient Temperature Reading - This measurement was accomplished with a mercury-in-glass thermometer having minimum graduations of $1^{o}F$ and a range of $-20^{o}F$ to $+140^{o}F$. It is believed that the thermometer could be read correctly to within $\pm 0.5^{o}F$. Allowing for the error within the device, the uncertainty of the thermometer reading is considered to be $\pm 1^{o}F$.

2. PRESSURE MEASUREMENTS

A. Bed Pressure Drop - The minimum manometer scale reading was 0.1 inch with a total range of 30 inches. Readings of 0.05 inches were possible. For static measurements, the pressure readings are considered to be accurate within 0.2%; however, during conditions under which the water column was fluctuating, the uncertainty was increased to as much as 2% of the full scale reading.

B. Venturi Inlet Static Pressure - The minimum scale reading was 0.1 inch with a total range of 60 inches. Readings of 0.05 inches were possible. The pressure readings are considered to be accurate to within 0.1% of full scale.

C. Venturi Differential Pressure - The minimum scale reading was 0.001 inches over a range of 2 inches. The reading was considered to be accurate to within 0.1% of full scale.

D. Atmospheric Pressure - Minimum scale readings of 0.001 in. Hg over a range of approximately 32 inches were observed. As a consequence, the uncertainty of the reading was considered to be 0.1% of full scale.

3. DISTANCE/SIZE MEASUREMENTS

A. Bed Width/Depth - Measurements were considered accurate to within ±0.0625 in. or 0.5% of the apparatus depth.

B.   Bed Probe Depth - Due to the bending motion imparted
to the probes by the particle activity, the depth measure-
ments were considered accurate to within the 0.25 in. or
1.5% of the bed depth.

C.   Bed Expansion - Due to the rapidly fluctuating ex-
panded bed surface level, the bed depth is considered to
have an uncertainty of ±0.5 in. or 5% of bed depth.

D.   Venturi Inlet/Throat Diameter - These measurements
are considered accurate to within ±0.001 in. or 0.2% of
diameter.

E.   Particle Diameter - Determined by optical microscope
examination conducted by Morgan, [Ref. 2], D_p = 0.0122 (310
microns) ± 1%.

F.   Plate/Wall Thickness - Measurements were considered
accurate to within 0.02 in. or 5% of the wall thickness.

4.   VOLTAGE/CURRENT MEASUREMENTS

Minimum ammeter scale graduations were 0.1 Amp with a
total range of 2 Amps. Because the power supplies were not
calibrated or compared with a known standard an uncertainty
of ±10% of the full scale deflection is assigned to the
current reading. The minimum voltmeter scale reading was
1 volt with a range of 60 volts. Once again, due to the
lack of calibration, an uncertainty of 5% is assigned of
full scale deflection.

5. THERMAL CONDUCTIVITIES

Due to the variation in conductivities found in the literature, the following uncertainties are assigned:

A. k_c = 232 Btu/Hr-Ft-^{o}F ±0.5%

B. k_{mb} = 0.112 Btu/Hr-Ft-^{o}F ±10%

C. k_i = 0.025 Btu/Hr-Ft-^{o}F ±10%

D. k_{fr} = 0.112 But/Hr-Ft-^{o}F ±10%

6. DENSITY MEASUREMENTS

Particle Density - Established by Morgan to be 154.6 Lbm/Ft^2 ±3%.

APPENDIX H. ROTOMETER CALIBRATION COMPUTER PROGRAM LISTING

```
10 PRINTER IS 701.100
20 S=.634
30 CLEAR @ DISP "      ROTOMETER CALIBRATION"
40 DISP " "
50 DISP "THIS PROGRAM CONVERTS VENTURI PRESSURE DATA INTO ROTOMETER FLOW RATES"
60 PAUSE
70 CLEAR @ DISP "ENTER Patm(IN Hg)"
80 INPUT P
90 CLEAR @ DISP "ENTER Tin(DEG F)"
100 INPUT T
110 CLEAR @ DISP "ENTER Y"
120 INPUT Y
130 ! CALCULATE Patm(PSI)
140 P1=P*14.7/29.92
150 ! CALCULATE Tin(DEG R)
160 T1=T+459.69
170 CLEAR @ DISP "PRESS CONTINUE TO START PROCESSING"
180 PAUSE
190 CLEAR @ DISP "ENTER FLOWMETER READING"
200 INPUT F
210 CLEAR @ DISP "ENTER Pig(IN H2O)"
220 INPUT I2
230 CLEAR @ DISP "ENTER DELTA P(IN RO)"
240 INPUT I3
250 !  CALCULATE FLOWRATES
260 ! CALCULATE Pig(PSI)
270 P2=I2*14.7/33.91/12
280 ! CALCULATE Pi(PSI)
290 P3=P1-P2
300 ! CALCULATE DELTA P(PSI)
310 P4=I3*62.4*.834/12/144
320 ! CALCULATE X
330 X=P4/P3
340 ! CALCULATE RHOi
350 D=P3*144/53.34/T1
360 ! CALCULATE MASS FLOW(LBM/SEC)
370 CLEAR @ DISP "ENTER ASSUMED REYNOLDS NUMBER"
380 INPUT R
390 CLEAR @ DISP "ENTER DISCHARGE COEFFICIENT ASSOCIATED WITH ASSUMED REYNOLDS N
UMBER"
400 INPUT C
410 E=1.032796
420 K=C*E
430 M=K*3.56327/144*Y*SQR(2*32.174*D*P4*144)
440 ! CALCULATE VOLUME FLOW RATE(FT3/SEC)
450 V1=M/D
460 ! CALCULATE VOLUME FLOW RATE(FT3/MIN)
470 V2=V1*60
480 ! CALCULATE REYNOLDS NUMBER
490 R2=V1/14.25309*144*D*4.26/12/.000000379/32.174
500 CLEAR @ DISP "ASSUMED REYNOLDS NUMBER =",R
510 !
520 DISP "CALCULATED REYNOLDS NUMBER =",R2
530 !
540 DISP "DO YOU WISH TO REPEAT CALCULATION USING A DIFFERENT REASSUMED REYNOLDS
 NUMBER? (Y/N)"
550 INPUT W1$
560 IF W1$="Y" THEN 360
570 PRINT CHR$(12)
```

```
580 PRINT USING 590
590 IMAGE 2/,28X,"**ROTOMETER CALIBRATION**"
600 PRINT USING 610
610 IMAGE 28X,"ASME HERSCHEL-TYPE VENTURI"
620 PRINT USING 630
630 IMAGE 33X,"4.26/2.13 IN DIA"620 PRINT USING 630 ; F
640 PRINT USING 650 ; F
650 IMAGE /,32X,DD,X,"PERCENT READING"
660 PRINT USING 670
670 IMAGE 32X,"--------------------"
680 PRINT USING 690
690 IMAGE 2/,31X,"**EXPERIMENTAL DATA**"
700 PRINT USING 710 ; P
710 IMAGE 2/,15X,"ATMOSPHERIC PRESSURE =",14X,DD.DDDDD,X,"IN Hg"
720 PRINT USING 730 ; T
730 IMAGE 15X"VENTURI INLET TEMPERATURE =",13X,DD.D,X,"DEG F"
740 PRINT USING 750 ; I2
750 IMAGE 15X,"VENTURI INLET STATIC GAGE PRESSURE =",2X,DD.DD,X,"IN H20"
760 PRINT USING 770 ; I3
770 IMAGE 15X,"VENTURI DIFFERENTIAL PRESSURE =",3X,D.DDD,X,"IN RED OIL"
780 PRINT USING 790 ; S
790 IMAGE 15X,"SPECIFIC GRAVITY OF RED OIL =",16X,D.DDD
800 PRINT USING 810
810 IMAGE 2/,31X,"**CALCULATED VALUES**"
820 PRINT USING 830 ; P1
830 IMAGE 2/,15X,"ATMOSPHERIC PRESSURE =",17X,DD.DDDD,X,"PSI"
840 PRINT USING 850 ; P2
850 IMAGE 15X,"VENTURI INLET GAGE PRESSURE =",10X,D.DDDDD,X,"PSI"
860 PRINT USING 870 ; P3
870 IMAGE 15X,"VENTURI INLET ABSOLUTE PRESSURE =",5X,DD.DDDDD,X,"PSI"
880 PRINT USING 890 ; P4
890 IMAGE 15X,"VENTURI DIFFERENTIAL PRESSURE =",8X,D.DDDDD,X,"PSI"
900 PRINT USING 910 ; D
910 IMAGE 15X,"VENTURI INLET AIR DENSITY =",8X,D.DDDDD,X,"LBM/FT3"
920 PRINT USING 930 ; X
930 IMAGE 15X,"VENTURI PRESSURE DROP RATIO (X) =",10X,D.DDDDD
940 PRINT USING 950 ; Y
950 IMAGE 15X,"EXPANSION FACTOR (Y) =",24X,D.DD
960 PRINT USING 970 ; R
970 IMAGE 15X,"ASSUMED REYNOLDS NUMBER =",21X,DDDD
980 PRINT USING 990 ; C
990 IMAGE 15X,"DISCHARGE COEFFICIENT (C) =",18X,D.DDD
1000 PRINT USING 1010 ; E
1010 IMAGE 15X,"VELOCITY OF APPROACH FACTOR (E) =",10X,D.DDDDD
1020 PRINT USING 1030 ; K
1030 IMAGE 15X,"FLOW COEFFICIENT (K) =",21X,D.DDDDD
1040 PRINT USING 1050 ; M
1050 IMAGE 15X,"AIR MASS FLOW RATE =",15X,D.DDDDD,X,"LBM/SEC"
1060 PRINT USING 1070 ; V2
1070 IMAGE 15X,"AIR VOLUMETRIC FLOW RATE =",14X,DD.DDD,X,"CFM"
1080 PRINT USING 1090 ; R2
1090 IMAGE 15X,"VENTURI INLET REYNOLDS NUMBER ="15X,DDDD
1100 CLEAR @ DISP "DO YOU WISH TO PROCESS ANOTHER SET OF READINGS? (Y/N)"
1110 INPUT W2$
1120 IF W2$="Y" THEN 170
1130 END
```

APPENDIX I.

THERMOCOUPLE CALIBRATION COMPUTER PROGRAM LISTING

```
10 DISP " "
20 DISP "                DAVCAL"
30 DISP " "
40 DISP "THIS CALIBRATION PROGR
   AM IS FOR USE WITH THE HP-34
   97 DATA ACQUISITION SYSTEM"
50 DISP " "
60 DISP "UP TO 50 THERMOCOUPLES
    MAY BE CALIBRATED SIMULTANI
   OUSLY"
70 DISP " "
80 DISP "UP TO 20 DIFFERENT BAT
   H TEMPERATURE SETTINGS MAY B
   E USED"
90 DISP " "
100 DISP "THERMOCOUPLE NUMBERS S
    HOULD AGREE WITH CHANNEL NUM
    BERS"
110 PAUSE
120 DISP " "
130 OPTION BASE 1
140 MASS STORAGE IS ":D701"
150 SHORT R(20,50),M(20,2)
160 DIM T(20,2)
170 DISP " "
180 DISP "HOW MANY THERMOCOUPLES
     ARE BEING CALIBRATED?"
190 INPUT K
200 DISP " "
210 DISP "HOW MANY BATH TEMPERA
    TURE SETTINGS ARE BEING USED
    ?"
220 INPUT N
230 H$="AF"
240 DISP " "
250 DISP "WHAT IS FIRST CHANNEL
    NUMBER?"
260 DISP "(TWO DIGITS)"
270 INPUT Y$
280 H$[3]=Y$
290 C=VAL(Y$)
300 H$[5]="AL"
310 DISP " "
320 DISP "WHAT IS LAST CHANNEL N
    UMBER?"
330 DISP "(TWO DIGITS)"
340 INPUT H$[7]
350 H$[9]="VT1VR5"
360 C$=H$
```

```
370 DISP " "
380 DISP "WHAT DO YOU WISH TO CA
    LL YOUR DATA FILE?"
390 DISP "(SIX CHARACTERS MAX)"
400 INPUT D$
410 FOR I=1 TO N
420 DISP " "
430 DISP "    TEMPERATURE SETTING
    #";I
440 DISP " "
450 DISP "WHAT IS THE PLATINUM B
    ATH SENSOR RESISTANCE?"
460 INPUT T(I,1)
470 DISP " "
480 DISP "WHAT IS THE CORRESPOND
    ING BATH TEMPERATURE (C)?"
490 INPUT T(I,2)
500 DISP " "
510 DISP "TO START SAMPLING PRES
    S CONTINUE"
520 PAUSE
530 CLEAR 709
540 OUTPUT 709 ;C$
550 FOR J=1 TO K
560 OUTPUT 709 ;"AS"
570 ENTER 709 ; B
580 R(I,J)=B*1000
590 NEXT J
600 BEEP
610 NEXT I
620 DISP " "
630 CLEAR & DISP "       SAMPLING
     COMPLETE"
640 DISP " "
650 DISP "RESULTS WILL BE PRINTE
    D MOMENTARILY"
660 DISP " "
670 DISP "THERMOCOUPLE OUTPUT IS
     IN MILIVOLTS"
680 DISP " "
690 DISP "BATH TEMP.IS IN CELSIU
    S"
700 DISP " "
710 PRINT "DATA IS STORED IN FIL
    E NAMED "
720 PRINT USING 730 ; CHR$(34),D
    $,CHR$(34)
730 IMAGE 11X,A,6A,A
740 CREATE D$,1,16500
750 ASSIGN# 1 TO D$
760 E=C-1
770 FOR I=1 TO K
780 FOR J=1 TO N
```

179

```
790  M(J,1)=R(J,I)
800  M(J,2)=T(J,2)
810  PRINT# 1 ; M(J,1),M(J,2)
820  NEXT J
830  F=E+I
840  PRINT USING 850
850  IMAGE 2/,"*********************
     ************"
860  PRINT USING 870
870  IMAGE "**********************
     *********",/,X
880  PRINT USING 890 ; F
890  IMAGE /,6X,"THERMOCOUPLE #",
     X,2D
900  PRINT USING 910
910  IMAGE 6X,"******************"
     ,2/,X
920  PRINT USING 930
930  IMAGE "TEMP",4X,"PLAT",6X,"T
     C",5X,"BATH"
940  PRINT USING 950
950  IMAGE X,"SET",3X,"RESIST",3X
     ,"OUTPUT",3X,"TEMP"
960  PRINT USING 970
970  IMAGE "****",3X,"******",3X,
     "******",3X,"****",/
980  FOR L=1 TO N
990  PRINT USING 1000 ; L,T(L,1),
     M(L,1),M(L,2)
1000 IMAGE X,DD,4X,DD.DDDD,2X,DD
     .DCD,3X,DD.DD
1010 NEXT L
1020 CLEAR @ DISP "      THERMOCO
     UPLE #",F
1030 DISP "READY FOR LEAST SQUAR
     ES CURVE FITTING"
1040 DISP " "
1050 DISP "ENTER 0 FOR A POWER F
     UNCTION (Y=AX^B)"
1060 DISP " "
1070 DISP "ENTER 1 FOR AN EXPONE
     NTIAL FUNCTION (Y=Ae^BX)"
1080 DISP " "
1090 DISP "ENTER 2 THRU 10 FOR A
      POLYNOMIAL OF N TERMS (DEG
     REE = N-1)"
1100 DISP "(Y=C1+C2X+C3X^2+C4X^3
     +....C(N)X^(N-1))"
1110 DIM Y(20),X(20),A(10,10),B(
     10,10),C(10),D(10)
1120 MAT Y=ZER(N)
1130 MAT X=ZER(N)
1140 FOR J=1 TO N
```

180

```
1150 X(J)=M(J,1)
1160 Y(J)=M(J,2)
1170 NEXT J
1180 INPUT Q
1190 REM "CALCULATE LOGARITHMS O
     F X- AND Y-VALUES IF NECESS
     ARY"
1200 IF Q>=2 THEN 1280
1210 FOR J=1 TO N
1220 LET Y(J)=LOG(M(J,2))
1230 NEXT J
1240 IF Q=1 THEN 1280
1250 FOR J=1 TO N
1260 LET X(J)=LOG(M(J,1))
1270 NEXT J
1280 REM "CALCULATE ELEMENTS OF
     A-MATRIX AND D-VECTOR"
1290 LET N1=Q
1300 IF N1>=2 THEN 1320
1310 LET N1=2
1320 MAT A=ZER(N1,N1)
1330 MAT D=ZER(N1)
1340 FOR J=1 TO N1
1350 FOR K=1 TO N1
1360 IF J+K>2 THEN 1390
1370 LET A(J,K)=N
1380 GOTO 1420
1390 FOR L=1 TO N
1400 LET A(J,K)=A(J,K)+X(L)^(J+K
     -2)
1410 NEXT L
1420 NEXT K
1430 FOR L=1 TO N
1440 IF J>1 THEN 1470
1450 LET D(J)=D(J)+Y(L)
1460 GOTO 1480
1470 LET D(J)=D(J)+Y(L)*X(L)^(J-
     1)
1480 NEXT L
1490 NEXT J
1500 REM "SOLVE SIMULTANEOUS  LI
     NEAR EQUATIONS"
1510 MAT B=INV(A)
1520 MAT C=B*D
1530 REM "PRINT EQUATION FOR CUR
     VE FIT"
1540 PRINT USING 1550
1550 IMAGE /,"-------------------
     -----------"
1560 IF Q>1 THEN 1670
1570 LET C1=EXP(C(1))
1580 IF Q=1 THEN 1630
1590 PRINT USING 1600
1600 IMAGE 5X,"***POWER FUNCTION
     ***",/,X
```

181

```
1610 PRINT "Y=";C1;"*X^";C(2)
1620 GOTO 1860
1630 PRINT USING 1640
1640 IMAGE 3X,"***EXPONENTIAL FU
     NCTION***",/,X
1650 PRINT "Y=";C1;"*EXP(";C(2);
     "*X)"
1660 GOTO 1860
1670 IF C(2)>=0 THEN 1740
1680 PRINT USING 1690
1690 IMAGE 3X,"***POLYNOMIAL FUN
     CTION***"
1700 PRINT USING 1710 ; Q-1
1710 IMAGE 10X,"(ORDER =",0,")",
     /,X
1720 PRINT "Y=";C(1);C(2);"X";
1730 GOTO 1790
1740 PRINT USING 1750
1750 IMAGE 3X,"***POLYNOMIAL FUN
     CTION***"
1760 PRINT USING 1770 ; Q-1
1770 IMAGE 10X,"(ORDER =",0,")",
     /,X
1780 PRINT "Y=";C(1);"+";C(2);"*
     X";
1790 IF Q=2 THEN 1860
1800 FOR J=3 TO Q
1810 IF C(J)>=0 THEN 1840
1820 PRINT C(J);"*X^";J-1;
1830 GOTO 1850
1840 PRINT "+";C(J);"*X^";J-1;
1850 NEXT J
1860 REM "PRINT INPUT VALUES OF
     X AND Y AND CALCULATED VALU
     ES OFY"
1870 IF Q>=2 THEN 1950
1880 FOR J=1 TO N
1890 LET Y(J)=EXP(Y(J))
1900 NEXT J
1910 IF Q=1 THEN 1950
1920 FOR J=1 TO N
1930 LET X(J)=EXP(X(J))
1940 NEXT J
1950 PRINT
1960 PRINT USING 1970
1970 IMAGE /,4X,"X",6X,"Y (ACT)"
     ,5X,"Y (CALC)"
1980 PRINT USING 1990
1990 IMAGE 3X,"***",5X,"**.****",
     ,5X,"**.****"
2000 LET S=0
2010 FOR J=1 TO N
2020 IF Q>=2 THEN 2080
2030 IF Q=1 THEN 2060
2040 LET Y1=C1*X(J)^C(2)
```

182

```
2050 GOTO 2120
2060 LET Y1=C1*EXP(C(2)*X(J))
2070 GOTO 2120
2080 LET Y1=C(1)
2090 FOR K=2 TO Q
2100 LET Y1=Y1+C(K)*X(J)^(K-1)
2110 NEXT K
2120 LET S=S+(Y(J)-Y1)^2
2130 PRINT USING 2140 ; X(J),Y(J
     ),Y1
2140 IMAGE X.DD.DDD,5X,DD.DD,6X,
     DD.DDDD
2150 NEXT J
2160 PRINT
2170 PRINT "SUM OF SQUARE ERRORS
     =";S
2180 CLEAR @ DISP "DO YOU DESIRE
      A PLOT?"
2190 DISP "(ENTER Y OR N)"
2200 INPUT P$
2210 IF P$="N" THEN 3690
2220 GOSUB 2250
2230 PAUSE
2240 GOTO 3690
2250 DIM Y1(4),A1(5),M1(5)
2260 Y1(1),Y1(3)=INF @ Y1(2),Y1(
     4)=-INF @ A1(1),A1(2),A1(3)
     ,A1(4),A1(5)=0
2270 FOR J=1 TO N
2280 IF Y1(2)<X(J) THEN Y1(2)=X(
     J)
2290 IF Y1(1)>X(J) THEN Y1(1)=X(
     J)
2300 IF Y1(4)<Y(J) THEN Y1(4)=Y(
     J)
2310 IF Y1(3)>Y(J) THEN Y1(3)=Y(
     J)
2320 A1(1)=A1(1)+X(J) @ A1(2)=A1
     (2)+X(J)*X(J) @ A1(3)=A1(3)
     +Y(J)
2330 A1(4)=A1(4)+Y(J)*Y(J) @ A1(
     5)=A1(5)+X(J)*Y(J)
2340 NEXT J
2350 M1(1)=A1(1)/N @ M1(2)=(A1(2
     )-A1(1)*A1(1)/N)/(N-1) @ M1
     (3)=A1(3)/N
2360 M1(4)=(A1(4)-A1(3)*A1(3)/N)
     /(N-1) @ M1(5)=(A1(5)-A1(1)
     *A1(3)/N)/(A1(2)-A1(1)*A1(1
     )/N)
2370 R5=M1(3)-M1(1)*M1(5) @ D5=0
2380 CLEAR @ D5=1 @ DISP "AUTO X
     -SCALING?:Y/N"
```

183

```
2390 INPUT R$
2400 ON FNR GOTO 2380,2410,2420
2410 X1=Y1(1) @ X2=Y1(2) @ GOTO
     2470
2420 CLEAR @ DISP "ENTER MINIMUM
      VALUE FOR X-AXIS"
2430 INPUT X1
2440 CLEAR @ DISP "ENTER MAXIMUM
      VALUE FOR X-AXIS".
2450 INPUT X2
2460 IF X1>=X2 THEN BEEP @ GOTO
     2420
2470 CLEAR @ DISP "DO YOU WISH V
     ERTICAL OR HORIZONTAL LABEL
     S ON THE X-AXIS?:V/H"
2480 INPUT R$
2490 IF NOT LEN(R$) THEN BEEP @
     GOTO 2470
2500 S9=1 @ IF UPC$(R$[1,1])="V"
      THEN S9=0 @ GOTO 2520
2510 IF UPC$(R$[1,1])#"H" THEN B
     EEP @ GOTO 2470
2520 CLEAR @ DISP "DESIRED NUMBE
     R OF INTERVALS ON X-AXIS? (
     <=16)"
2530 INPUT L1
2540 IF L1<1 OR L1>16 OR L1#INT(
     L1) THEN BEEP @ GOTO 2520
2550 CLEAR @ DISP "DESIRED NUMBE
     R OF SUBDIVISIONS BETWEEN L
     ABELED INTERVALS?"
2560 INPUT L3
2570 S8=0 @ IF L3=0 THEN S8=1 @
     L3=1
2580 IF L3<1 OR L3>L1 THEN BEEP
     @ GOTO 2550
2590 CLEAR @ DISP "DO YOU DESIRE
      AUTOMATIC SCALING OF THE Y
     -AXIS?:Y/N"
2600 INPUT R$
2610 ON FNR GOTO 2590,2670,2620
2620 CLEAR @ DISP "ENTER MINIMUM
     DESIRED VALUE FOR Y-AXIS"
2630 INPUT Y1
2640 CLEAR @ DISP "ENTER MAXIMUM
     DESIRED VALUE FOR Y-AXIS"
2650 INPUT Y2
2660 IF Y1>Y2 THEN BEEP @ GOTO 2
     620 ELSE 2680
2670 Y1=Y1(3) @ Y2=Y1(4)
2680 CLEAR @ DISP "ENTER DESIRED
      NUMBER OF INTERVALS ON THE
      Y-AXIS (<=12)"
```

```
2690 INPUT L2
2700 IF L2<1 OR L2>12 OR L2#INT(
     L2) THEN BEEP @ GOTO 2680
2710 CLEAR @ DISP "ENTER DESIRED
      NUMBER OF SUBDIVISIONS BET
     WEEN LABELED INTERVALS"  .
2720 INPUT L4
2730 S7=0 @ IF L4=0 THEN S7=1 @
     L4=1
2740 IF L4<1 OR L4>12 THEN BEEP
     @ GOTO 2710
2750 Z1=X2-X1 @ Z3=INT(200/L1)*L
     1 @ Z2=Y2-Y1 @ Z4=INT(144/L
     2)*L2
2760 D1=Z1/Z3 @ D2=Z2/Z4 @ Z5=X2
     +(207-Z3)*D1 @ X0=X1-48*D1
     @ Y0=Y1-40*D2
2770 GCLEAR @ SCALE X0,Z5,Y0,Y2+
     (151-Z4)*D2
2780 XAXIS Y1,Z1/L1,X1,X2+D1
2790 YAXIS X1,Z2/L2,Y1,Y2+D2
2800 IF S8 THEN 2960
2810 W1=LGT(ABS(Z1/L1*L3))
2820 W=LGT(ABS(X1+(X1=0)))+1
2830 IF W>5-(SGN(X1)=-1) OR W1<-
     3 THEN 2920
2840 IF S9 THEN 3520
2850 LDIR 90
2860 FOR J=X1 TO X2+D1 STEP Z1/L
     1*L3
2870 MOVE J-4*D1,Y0
2880 GOSUB 3320  .
2890 LABEL V$[1,W]
2900 NEXT J
2910 GOTO 2960
2920 MOVE X0,Y0
2930 LDIR 0
2940 I1=X1 @ GOSUB 3450 @ I1=Z1/
     L1 @ Z$=V$ @ GOSUB 3450
2950 LABEL "XMIN="&Z$[1,10]&":TI
     CS="&V$[1,10]
2960 IF S7 THEN 3140
2970 W1=LGT(ABS(Z2/L2*L4))
2980 W=LGT(ABS(Y1+(Y1=0)))+1
2990 IF W>5-(SGN(Y1)=-1) OR W1<-
     3 THEN 3070
3000 LDIR 0
3010 FOR J=Y1 TO Y2+D2 STEP Z2/L
     2*L4
3020 MOVE X0,J-4*D2
3030 GOSUB 3320
```

185

```
3040 LABEL V$[1,V]
3050 NEXT J
3060 GOTO 3140
3070 LDIR 90
3080 I1=Y1 @ GOSUB 3450
3090 MOVE X0+12*D1,Y1
3100 LABEL "YMIN="&V$[1,10]
3110 MOVE X0+24*D1,Y1
3120 I1=Z2/L2 @ GOSUB 3450
3130 LABEL "TICS="&V$[1,10]
3140 PENUP @ LDIR 0
3150 MOVE X(1),Y(1)
3160 FOR J=1 TO N @ MOVE X(J)-2*
     D1,Y(J)-4*D2 @ LABEL "*" @
     NEXT J @ BEEP
3170 FOR L=0 TO 100
3180 X4=Y1(1)+L*((Y1(2)-Y1(1))/1
     00)
3190 IF Q>=2 THEN 3250
3200 IF Q=1 THEN 3230
3210 LET Y4=C1*X4^C(2)
3220 GOTO 3290
3230 LET Y4=C1*EXP(C(2)*X4)
3240 GOTO 3290
3250 LET Y4=C(1)
3260 FOR K=2 TO Q
3270 LET Y4=Y4+C(K)*X4^(K-1)
3280 NEXT K
3290 PLOT X4,Y4
3300 NEXT L
3310 BEEP @ GOTO 3390
3320 V$="" @ X=J
3330 V$=VAL$(X)
3340 IF POS(V$,"E") THEN 3400
3350 G9=LGT(ABS(X+(X=0)))
3360 IF LEN(V$)>5 AND ABS(G9)>4-
     (SGN(X)=-1) THEN V=5 @ V$="
     -----" @ RETURN
3370 IF LEN(V$)<5 THEN V=LEN(V$)
     @ RETURN
3380 V$[1,5]=VAL$(X) @ V=5
3390 GRAPH @ RETURN
3400 E0=POS(V$,"E")
3410 IF V$[1,1]="-" THEN V$[3]=V
     $[E0] @ GOTO 3430
3420 V$[2]=V$[E0]
3430 V=LEN(V$) @ IF V>5 THEN PRI
     NT USING 3560 ; J @ V=5 @ V
     $="-----"
3440 RETURN
3450 V$=""
3460 V$=VAL$(I1)
```

186

```
3470 IF POS(V$,"E") THEN 3500
3480 V$[1,10]=VAL$(I1)
3490 ·RETURN
3500 V$[6,10]=V$[POS(V$,"E")]
3510 RETURN
3520 LDIR 0 @ L9=-INF
3530 FOR J=X1 TO X2+D1 STEP Z1/L
     1*L3
3540 GOSUB 3320
3550 IF L9>J-(V*4+6)*D1 OR L9>Z5
     +(1-V*8)*D1 THEN PRINT USIN
     G 3560 @ GOTO 3610
3560 IMAGE "LABEL DELETED AT ",7
     D.4D
3570 MOVE J+(2-V*4)*D1,Y1-12*D2
3580 L9=J+(V*4+2)*D1
3590 IF L9>Z5 THEN MOVE Z5+(2-V*
     8)*D1,Y1-12*D2
3600 LABEL V$[1,V]
3610 NEXT J
3620 GOTO 2960
3630 DEF FNR
3640 IF NOT LEN(R$) THEN I1=1 @
     GOTO 3660
3650 I1=POS("YN",UPC$(R$[1.1]))+
     1
3660 IF I1=1 THEN BEEP
3670 FNR=I1
3680 FN END
3690 CLEAR @ DISP "DO YOU WISH T
     O FIT A DIFFERENT TYPE CURV
     E?(Y/N)"
3700 INPUT W$
3710 IF W$="Y" THEN 3730
3720 GOTO 3740
3730 GOTO 1020
3740 NEXT I
3750 ASSIGN# 1 TO *
3760 BEEP
3770 CLEAR @ DISP "      CALIBRAT
     ION COMPLETE"
3780 END
```

187

HEAT TRANSFER DATA ACQUISITION COMPUTER PROGRAM LISTING

```
10 MASS STORAGE IS ":D701"
20 SHORT V(80)
30 DIM C(5),T(80),R(5),L(5),O1$[100]
40 O1$=" "
50 CLEAR & DISP "            QUICK"
60 DISP " "
70 DISP "THIS PROGRAM IS FOR USE IN SAMPLING FOR FUTURE PROCESSING "
80 DISP "OPERATING PARAMETERS AND TC OUTPUTS ARE STORED ON DISK FOR FUTURE REDUC
TION"
90 PAUSE
100 CLEAR & DISP "WHAT IS THE DATE? (MO/DA/YR)"
110 INPUT D1$
120 CLEAR & DISP "WHAT IS THE TIME? (MILITARY)"
130 INPUT T1$
140 CLEAR & DISP "WHAT IS THE BED WIDTH? (INCHES)"
150 INPUT X
160 CLEAR & DISP "WHAT IS THE STATIC BED HIEGHT? (INCHES)"
170 INPUT S1$
180 CLEAR & DISP "WHAT WAS THE HIGHEST NUMBERED PROBE UTILIZED? (TWO DIGITS)"
190 INPUT L$
200 L=VAL(L$)
210 CLEAR & DISP "WHAT IS THE VOLTAGE TO THE RIGHT-HAND HEATER? (VOLTS)"
220 INPUT V1
230 CLEAR & DISP "WHAT IS THE CURRENT TO THE RIGHT-HAND HEATER? (AMPS)"
240 INPUT I1
250 CLEAR & DISP "WHAT IS THE VOLTAGE TO THE LEFT-HAND HEATER? (VOLTS)"
260 INPUT V2
270 CLEAR & DISP "WHAT IS THE CURRENT TO THE LEFT-HAND HEATER? (AMPS)"
280 INPUT I2
290 CLEAR & DISP "WHAT IS THE AMBIENT TEMPERATURE? (DEG F)"
300 INPUT A1
310 CLEAR & DISP "WHAT IS THE AIR FLOW-RATE? (%)"
320 INPUT F1
330 F2=F1*.373
340 CLEAR & DISP "WHAT IS THE BED EXPANSION? (INCHES)"
350 INPUT E1$
360 CLEAR & DISP "ENTER ANY COMMENTS YOU WISH RECORDED (MAX 100 CHARACTERS)"
370 INPUT O1$[1]
380 CLEAR & DISP "WHAT DO YOU WISH TO CALL YOUR DATA FILE? (SIX CHARACTERS MAX)"
390 INPUT F$
400 H$="AF01AL"
410 H$[7]="79"
420 H$[9]="VT1VR5TE0"
430 CLEAR 709
440 OUTPUT 709 ;H$
450 CREATE F$,1,1500
460 ASSIGN# 1 TO F$
470 ASSIGN# 2 TO "COEFF2:D700"
480 PRINT# 1 ; D1$,T1$,X,S1$,L$,L,V1,I1,V2,I2,A1,F1,F2,E1$,O1$
490 PRINT USING 500
500 IMAGE "$$$$$$$$$$$$$$$$$$$$$$$$$$$$$$$$$"
510 PRINT USING 520
520 IMAGE 3/,3X,"$$EXPERIMENTAL DATA$$"
530 PRINT USING 540 ; F$
540 IMAGE 8X,"RUN #",X,6A
550 PRINT USING 560 ; D1$,T1$
560 IMAGE 6X,8A,X,"-",X,4A
570 PRINT USING 580
580 IMAGE 2/,2X,"TC#",3X,"OUTPUT",5X,"TEMP"
```

```
590 PRINT USING 600
600 IMAGE 9X,"(mV)",5X,"(DEG F)"LIST400
610 PRINT USING 620
620 IMAGE 2X,"---",5X,"-------",5X,"----"
630 CLEAR @ DISP "PRESS  CONTINUE WHEN READY TO BEGIN SAMPLING"
640 PAUSE
650 OUTPUT 709 ;"TE2"
660 FOR I=1 TO 79
670 OUTPUT 709 ;"AS"
680 ENTER 709 ; R
690 V(I)=R*1000
700 NEXT I
710 OUTPUT 709 ;"TE1TE"
720 ENTER 709 ; S
730 BEEP
740 CLEAR @ DISP "SAMPLING COMPLETE"
750 DISP "RESULTS WILL BE PRINTED MOMENTARILY"
760 READ# 2,1
770 FOR I=1 TO 79
780 READ# 2 ; C(1),C(2),C(3),C(4),C(5)
790 IF I>L THEN 810
800 GOTO 820
810 IF I<=67 THEN 940
820 T(I)=C(1)+C(2)*V(I)+C(3)*V(I)*V(I)+C(4)*V(I)*V(I)*V(I)+C(5)*V(I)*V(I)*V(I)*V
(I)
830 T(I)=T(I)*9/5+32
840 PRINT# 1 ; V(I),T(I)
850 IF I#41 THEN 920
860 PRINT USING 870
870 IMAGE 3/,2X,"TC#",3X,"OUTPUT",5X,"TEMP"
880 PRINT USING 890
890 IMAGE 9X,"(mV)",5X,"(DEG F)"
900 PRINT USING 910
910 IMAGE 2X,"---",3X,"------",5X,"----"
920 PRINT USING 930 ; I,V(I),T(I)
930 IMAGE 2X,DD,3X,DD.DDD,4X,DDD.DDDD
940 NEXT I
950 ASSIGN# 1 TO *
960 ASSIGN# 2 TO *
970 R(1)=(T(1)+T(2)+T(3))/3
980 R(2)=(T(5)+T(6)+T(7)+T(8))/4
990 R(3)=(T(9)+T(10)+T(11)+T(12))/4
1000 R(4)=(T(13)+T(14)+T(15)+T(16))/4
1010 R(5)=(T(17)+T(18)+T(19)+T(20))/4
1020 L(1)=(T(21)+T(22)+T(23)+T(24))/4
1030 L(2)=(T(25)+T(26)+T(27)+T(28))/4
1040 L(3)=(T(29)+T(30)+T(31)+T(32))/4
1050 L(4)=(T(33)+T(34)+T(35)+T(36))/4
1060 L(5)=(T(37)+T(38)+T(39)+T(40))/4
1070 G1=(T(41)+T(42)+T(43))/3
1080 G2=(T(44)+T(45)+T(46))/3
1090 P1=(T(47)+T(48)+T(49))/3
1100 B1=0
1110 X1=0
1120 FOR I=50 TO L
1130 IF I=55 THEN 1150
1140 GOTO 1170
1150 X1=1
1160 GOTO 1260
1170 IF I=65 THEN 1190
```

```
1180 GOTO 1210
1190 X1=2
1200 GOTO 1260
1210 IF I=66 THEN 1230
1220 GOTO 1250
1230 Y1=3
1240 GOTO 1260
1250 B1=B1+T(I)
1260 NEXT I
1270 N1=L-50+1-X1
1280 H1=(R(1)+R(2)+R(3)+R(4)+R(5))/5
1290 H2=(L(1)+L(2)+L(3)+L(4)+L(5))/5
1300 B1=B1/N1
1310 E1=V1*I1*3.4121
1320 E2=V2*I2*3.4121
1330 IF X1>1 THEN 1360
1340 P2=T(55)
1350 GOTO 1400
1360 IF X1>2 THEN 1390
1370 P2=(T(55)+T(65))/2
1380 GOTO 1400
1390 P2=(T(55)+T(65)+T(66))/3
1400 PRINT USING 1410 ; X
1410 IMAGE 3/,"BED WIDTH = ",DD.DD,X,"IN"
1420 PRINT USING 1430 ; S1$
1430 IMAGE "STATIC BED HEIGHT = ",5A," IN"
1440 PRINT USING 1450 ; F2
1450 IMAGE "AIR FLOW RATE = ",DDD.DD," CFM"
1460 PRINT USING 1470 ; A1
1470 IMAGE "AMBIENT TEMPERATURE= ",DD.DD," DEG F"
1480 PRINT USING 1490 ; V1
1490 IMAGE "RIGHT HEATER VOLTAGE= ",DD.D," VOLTS"
1500 PRINT USING 1510 ; I1
1510 IMAGE "RIGHT HEATER CURRENT = ",D.DD," AMPS"
1520 PRINT USING 1530 ; V2
1530 IMAGE "LEFT HEATER VOLTAGE = ",DD.D," VOLTS"
1540 PRINT USING 1550 ; I2
1550 IMAGE "LEFT HEATER CURRENT = ",D.DD," AMPS"
1560 PRINT USING 1570 ; E1$
1570 IMAGE "BED EXPANSION = ",4A," INCHES"
1580 PRINT USING 1590 ; O1$
1590 IMAGE "COMMENTS: ",100A
6160 END
```

HEAT TRANSFER DATA REDUCTION COMPUTER PROGRAM LISTING

```
10 SHORT V(80)
20 PRINTER IS 701.100
21 PRINT CHR$(27)&"&l1L"
30 PRINT CHR$(27)&"&l6D"
40 DIM C(5),T(80),R(5),L(5),O1$[100]
50 O1$=" "
60 E9=0
70 B9=0
80 CLEAR @ DISP "            PROCESS"
90 DISP " "
100 DISP "THIS PROGRAM IS FOR USE IN PROCESSING DATA WHICH HAS BEEN PREVIOUSLY R
ECORDED."
110 DISP " "
120 DISP "HEAT TRANSFER COEFFICIENTS ARE CALCULATED, DISPLAYED, AND PRINTED."
130 PAUSE
140 CLEAR @ DISP "WHAT IS THE NAME OF THE DATA FILE? (SIX CHARACTERS MAX)"
150 INPUT F$
160 CLEAR @ DISP "PRESS CONTINUE TO BEGIN PROCESSING"
170 PAUSE
180 ASSIGN# 1 TO F$
190 READ# 1 ; D1$,T1$,X,S1$,L$,L,V1,I1,V2,I2,A1,F1,F2,E1$,O1$
200 F2=F1*.32454+.795155
210 CLEAR @ DISP "DO YOU WISH A PRINT OUT OF THE EXPERIMENTAL DATA? (Y/N)"
220 INPUT R8$
230 IF R8$="Y" THEN 260
240 B9=1
250 GOTO 1110
260 CLEAR @ DISP "         COMMENT STATEMENT:"
270 DISP " "
280 DISP O1$
290 DISP " "
300 DISP "DO YOU WISH TO MAKE ANY CORRECTIONS? (Y/N)"
310 INPUT R9$
320 IF R9$="N" THEN 360
330 DISP " "
340 DISP "ENTER CORRECTED COMMENT STATEMENT"
350 INPUT O1$
360 !
370 !
380 !     ***PRINT EXPERIMENTAL CONDITIONS***
390 !
400 PRINT CHR$(12)
410 PRINT USING 420
420 IMAGE 3/,30X,"**EXPERIMENTAL DATA**"
430 PRINT USING 440 ; F$
440 IMAGE 35X,"RUN #",X,6A
450 PRINT USING 460 ; D1$,T1$
460 IMAGE 35X,8A,X,"-",X,4A
470 IF E9=1 THEN 1030
480 PRINT USING 490 ; F$
490 IMAGE 5/,22X,"RUN NUMBER =",20X,6A
500 PRINT USING 510 ; X
510 IMAGE /,22X,"BED WIDTH =",14X,DD.DD,X,"INCHES"
520 PRINT USING 530 ; S1$
530 IMAGE /,22X,"STATIC BED HEIGHT =",6X,5A,X,"INCHES"
540 PRINT USING 550 ; F2
550 IMAGE /,22X,"AIR FLOW RATE =",12X,DDD.DD,X,"CFM"
560 PRINT USING 570 ; A1
```

END

FILMED

DTIC
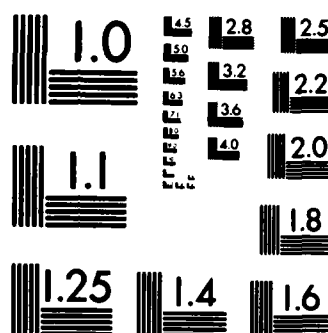
MICROCOPY RESOLUTION TEST CHART
NATIONAL BUREAU OF STANDARDS-1963-A

```
1170 IF B9=1 THEN 1390
1180 W1=0
1190 Z1=0
1200 FOR K=1 TO 40
1210 IF W1=1 THEN J=J+1 & GOTO 1230
1220 J=K+40
1230 IF J>L THEN 1250
1240 GOTO 1260
1250 IF J>=67 THEN 1340
1260 IF J>79 THEN Z1=1
1270 IF Z1=1 THEN 1310
1280 PRINT USING 1290 ; K,V(K),T(K),J,V(J),T(J)
1290 IMAGE 13X,DD,3X,DD.DDD,4X,DDD.DD,13X,DD,3X,DD.DDD,4X,DDD.DD
1300 GOTO 1330
1310 PRINT USING 1320 ; K,V(K),T(K)
1320 IMAGE 13X,DD,3X,DD.DDD,4X,DDD.DD
1330 GOTO 1360
1340 J=J+1 & W1=1
1350 GOTO 1250
1360 NEXT K
1370 ASSIGN# 1 TO *
1380 PRINT CHR$(12)
1390 R(1)=(T(1)+T(2)+T(3))/3
1400 R(2)=(T(5)+T(6)+T(7)+T(8))/4
1410 R(3)=(T(9)+T(10)+T(11)+T(12))/4
1420 R(4)=(T(13)+T(14)+T(15)+T(16))/4
1430 R(5)=(T(17)+T(18)+T(19)+T(20))/4
1440 L(1)=(T(21)+T(22)+T(23)+T(24))/4
1450 L(2)=(T(25)+T(26)+T(27)+T(28))/4
1460 L(3)=(T(29)+T(30)+T(31)+T(32))/4
1470 L(4)=(T(33)+T(34)+T(35)+T(36))/4
1480 L(5)=(T(37)+T(38)+T(39)+T(40))/4
1490 H1=(R(1)+R(2)+R(3)+R(4)+R(5))/5
1500 H2=(L(1)+L(2)+L(3)+L(4)+L(5))/5
1510 IF B9=1 THEN 3500
1520 !
1530 !         ***DISPLAY HEATER TEMP SNAPSHOT(R-H)***
1540 !
1550 PRINT USING 1560
1560 IMAGE 3/,30X,"**EXPERIMENTAL DATA**"
1570 PRINT USING 1580 ; F$
1580 IMAGE 35X,"RUN#",X,6A
1590 PRINT USING 1600 ; D1$,T1$
1600 IMAGE 33X,8A,X,"-",X,4A
1610 PRINT USING 1620
1620 IMAGE 3/,32X,"RIGHT-HAND HEATER"
1630 PRINT USING 1640
1640 IMAGE 31X,"TEMPERATURE PROFILE"
1650 PRINT USING 1660
1660 IMAGE /,25X,"COL 1",3X,"COL 2",3X,"COL 3",3X,"COL 4",7X,"AVE"
1670 PRINT USING 1680
1680 IMAGE 23X,"---------------------------------"
1690 PRINT USING 1700 ; T(1),T(2),T(3),R(1)
1700 IMAGE 17X,"ROW 1",X,"!",X,DDD.DD,2X,DDD.DD,2X,DDD.DD,2X,"******",2X,"!",2X,
DDD.DD
1710 PRINT USING 1720
1720 IMAGE 23X,"!",33X,"!"
1730 PRINT USING 1740 ; T(5),T(6),T(7),T(8),R(2)
1740 IMAGE 17X,"ROW 2",X,"!",X,DDD.DD,2X,DDD.DD,2X,DDD.DD,2X,DDD.DD,2X,"!",2X,DD
D.DD
```

193

```
570 IMAGE /,22X,"AMBIENT TEMPERATURE =",5X,DD.DD,X,"DEG F"
580 PRINT USING 590 : V1
590 IMAGE /,22X,"RIGHT HEATER VOLTAGE =",5X,DD.D,X,"VOLTS"
600 PRINT USING 610 : I1
610 IMAGE /,22X,"RIGHT HEATER CURRENT =",6X,D.DD,X,"AMPS"
620 PRINT USING 630 : V2
630 IMAGE /,22X,"LEFT HEATER VOLTAGE =",6X,DD.D,X,"VOLTS"
640 PRINT USING 650 : I2
650 IMAGE /,22X,"LEFT HEATER CURRENT =",7X,D.DD,X,"AMPS"
660 PRINT USING 670 : E1$
670 IMAGE /,22X,"BED EXPANSION =",11X,4A,X,"INCHES"
680 D9=LEN(O1$)
690 O1$[D9+1,100]=" "
700 IF D9>30 THEN 740
710 PRINT USING 720 : O1$[1,D9]
720 IMAGE /,22X,"COMMENTS:",X,30A
730 GOTO 970
740 K9=25
750 IF O1$[K9,K9]=" " THEN 780
760 K9=K9+1
770 GOTO 750
780 PRINT USING 790 : O1$[1,K9]
790 IMAGE /,22X,"COMMENTS:",X,40A
800 D2=K9+35
810 IF D9>D2 THEN 870
820 K8=K9+1
830 IF K8>D9 THEN 970
840 PRINT USING 850 : O1$[K9+1,D9]
850 IMAGE 22X,50A
860 GOTO 970
870 L9=D2
880 IF O1$[L9,L9]=" " THEN 910
890 L9=L9+1
900 GOTO 880
910 PRINT USING 920 : O1$[K9+1,L9]
920 IMAGE 22X,50A
930 L8=L9+1
940 IF L8>D9 THEN D9=L8
950 PRINT USING 960 : O1$[L9+1,D9]
960 IMAGE 22X,50A
970 PRINT CHR$(12)
980 E9=1
990 GOTO 360
1000 !
1010 !         ***PRINT THERMOCOUPLE READINGS***
1020 !
1030 PRINT USING 1040
1040 IMAGE /,30X,"THERMOCOUPLE READINGS"
1050 PRINT USING 1060
1060 IMAGE /,13X,"TC#",3X,"OUTPUT",4X,"TEMP",14X,"TC#",3X,"OUTPUT",4X,"TEMP"
1070 PRINT USING 1080
1080 IMAGE 20X,"(mV)",4X,"(DEG F)",19X,"(mV)",4X,"(DEG F)"
1090 PRINT USING 1100
1100 IMAGE 13X,"---",3X,"------",4X,"----",14X,"---",3X,"------",4X,"----"
1110 FOR I=1 TO 79
1120 IF I>L THEN 1140
1130 GOTO 1150
1140 IF I<=67 THEN 1160
1150 READ# 1 : V(I),T(I)
1160 NEXT I
```

192

```
1750 PRINT USING 1760
1760 IMAGE 23X," ",33X,"!"
1770 PRINT USING 1780 ; T(9),T(10),T(11),T(12),R(3)
1780 IMAGE 17X,"ROW 3",X,"!",X,DDD.DD,2X,DDD.DD,2X,DDD.DD,2X,DDD.DD,2X,"!",2X,DD
D.DD
1790 PRINT USING 1800
1800 IMAGE 23X,"!",33X,"!"
1810 PRINT USING 1820 ; T(13),T(14),T(15),T(16),R(4)
1820 IMAGE 17X,"ROW 4",X,"!",X,DDD.DD,2X,DDD.DD,2X,DDD.DD,2X,DDD.DD,2X,"!",2X,DD
D.DD
1830 PRINT USING 1840
1840 IMAGE 23X,"!",33X,"!"
1850 PRINT USING 1860 ; T(17),T(18),T(19),T(20),R(5)
1860 IMAGE 17X,"ROW 5",X,"!",X,DDD.DD,2X,DDD.DD,2X,DDD.DD,2X,DDD.DD,2X,"!",2X,DD
D.DD
1870 PRINT USING 1880
1880 IMAGE 23X,"-----------------------------------"
1890 PRINT USING 1900
1900 IMAGE /,16X,"NOTE: TEMPERATURES SHOWN ARE IN DEGREES FAHRENHEIT"
1910 PRINT USING 1920
1920 IMAGE 22X,"AND ARE ARRANGED AS SEEN FROM WITHIN THE BED"
1930 PRINT USING 1940
1940 IMAGE 21/,17X,"NOTE: PLOTTED TEMPERATURES ARE AVERAGES OF EACH"
1950 PRINT USING 1960
1960 IMAGE 23X,"HORIZONTAL ROW"
1970 PRINT CHR$(12)
1980 !
1990 !   ***PLOT TEMP GRAPH(R-H)**
2000 !
2010 PRINTER IS 2
2020 PRINT USING 2030 ; F$
2030 IMAGE 4/,10X,"RUN# ",X,6A
2040 PRINT USING 2050
2050 IMAGE 3/
2060 PRINTER IS 701,100
2070 Z9=IP(R(3))
2080 Z8=RMD(Z9,5)
2090 IF Z8=0 THEN 2120
2100 Z9=Z9-1
2110 GOTO 2080
2120 Z6=Z9-15
2130 Z7=Z9+15
2140 GCLEAR @ SETGU
2150 LOCATE 25,118,20,80
2160 ! FRAME
2170 SCALE Z6,Z7,0,10
2180 FXD 0
2190 LAXES 1,1,Z6,0,5,1
2200 Z5=Z7-16
2210 MOVE Z5,-3
2220 DEG
2230 LDIR 0 @ LORG 4
2240 LABEL "TEMP (DEG F)"
2250 Z4=Z6-3
2260 MOVE Z4,5
2270 LDIR 90 @ LORG 4
2280 LABEL "VERT POSITION (IN)"
2290 Z3=Z6+14
2300 MOVE Z3,12
2310 LDIR 0 @ LORG 4
```

```
2520 LABEL "RIGHT-HAND HEATER"
2530 Z2=Z6-14
2540 MOVE Z2,11
2550 LDIR 0 @ LORG 4
2560 LABEL "TEMP vs DEPTH"
2570 SETUU
2580 Y=9
2590 FOR I=1 TO 5
2400 MOVE R(I),Y
2410 Y=Y-2
2420 LORG 5
2430 LABEL "x"
2440 NEXT I
2450 COPY
2460 !    ***DISPLAY HEATER TEMP SNAPSHOT (L-H)***
2470 !
2480 PRINT USING 2490
2490 IMAGE 3/,30X,"**EXPERIMENTAL DATA**"
2500 PRINT USING 2510 ; F$
2510 IMAGE 35X,"RUN#",X,6A
2520 PRINT USING 2530 ; D1$,T1$
2530 IMAGE 33X,8A,X,"-",X,4A
2540 PRINT USING 2550
2550 IMAGE 3/,33X,"LEFT-HAND HEATER"
2560 PRINT USING 2570
2570 IMAGE 31X,"TEMPERATURE PROFILE"
2580 PRINT USING 2590
2590 IMAGE /,25X,"COL 1",3X,"COL 2",3X,"COL 3",3X,"COL 4",7X,"AVE"
2600 PRINT USING 2610
2610 IMAGE 23X,"————————————————————————"
2620 PRINT USING 2630 ; T(21),T(22),T(23),T(24),L(1)
2630 IMAGE 17X,"ROW 1",X,"|",X,DDD.DD,2X,DDD.DD,2X,DDD.DD,2X,DDD.DD,2X,"|",2X,DD
D.DD
2640 PRINT USING 2650
2650 IMAGE 23X,"|",33X,"|"
2660 PRINT USING 2670 ; T(25),T(26),T(27),T(28),L(2)
2670 IMAGE 17X,"ROW 2",X,"|",X,DDD.DD,2X,DDD.DD,2X,DDD.DD,2X,DDD.DD,2X,"|",2X,DD
D.DD
2680 PRINT USING 2690
2690 IMAGE 23X,"|",33X,"|"
2700 PRINT USING 2710 ; T(29),T(30),T(31),T(32),L(3)
2710 IMAGE 17X,"ROW 3",X,"|",X,DDD.DD,2X,DDD.DD,2X,DDD.DD,2X,DDD.DD,2X,"|",2X,DD
D.DD
2720 PRINT USING 2730
2730 IMAGE 23X,"|",33X,"|"
2740 PRINT USING 2750 ; T(33),T(34),T(35),T(36),L(4)
2750 IMAGE 17X,"ROW 4",X,"|",X,DDD.DD,2X,DDD.DD,2X,DDD.DD,2X,DDD.DD,2X,"|",2X,DD
D.DD
2760 PRINT USING 2770
2770 IMAGE 23X,"|",33X,"|"
2780 PRINT USING 2790 ; T(37),T(38),T(39),T(40),L(5)
2790 IMAGE 17X,"ROW 5",X,"|",X,DDD.DD,2X,DDD.DD,2X,DDD.DD,2X,DDD.DD,2X,"|",2X,DD
D.DD
2800 PRINT USING 2810
2810 IMAGE 23X,"————————————————————————"
2820 PRINT USING 2830
2830 IMAGE /,16X,"NOTE: TEMPERATURES SHOWN ARE IN DEGREES FAHRENHEIT"
2840 PRINT USING 2850
2850 IMAGE 22X,"AND ARE ARRANGED AS SEEN FROM WITHIN THE BED"
2860 PRINT USING 2870
```

195

```
2970 IMAGE 21/,17X,"NOTE: PLOTTED TEMPERATURES ARE AVERAGES OF EACH"
2980 PRINT USING 2990
2990 IMAGE 20X,"HORIZONTAL ROW"
3000 PRINT CHR$(12)
2910 !
2920 !     **PLOT TEMP GRAPH(L-H)**"
2930 !
2940 PRINTER IS 2
2950 PRINT USING 2960 ; F$
2960 IMAGE 4/,10X,"RUN# ",X,6A
2970 PRINT USING 2980
2980 IMAGE 3/
2990 PRINTER IS 701,100
3000 Z9=IP(L(3))
3010 Z8=RMD(Z9,5)
3020 IF Z8=0 THEN 3050
3030 Z9=Z9-1
3040 GOTO 3010
3050 Z6=Z9-15
3060 Z7=Z9+15
3070 GCLEAR @ SETGU
3080 LOCATE 25,118,20,80
3090 ! FRAME
3100 SCALE Z6,Z7,0,10
3110 FXD 0
3120 LAXES 1,1,Z6,0,5,1
3130 Z5=Z7-16
3140 MOVE Z5,-3
3150 DEG
3160 LDIR 0 @ LORG 4
3170 LABEL "TEMP (DEG F)"
3180 Z4=Z6-3
3190 MOVE Z4,5
3200 LDIR 90 @ LORG 4
3210 LABEL "VERT POSITION (IN)"
3220 Z3=Z6+14
3230 MOVE Z3,12
3240 LDIR 0 @ LORG 4
3250 LABEL "LEFT-HAND HEATER"
3260 Z2=Z6+14
3270 MOVE Z2,11
3280 LDIR 0 @ LORG 4
3290 LABEL "TEMP vs DEPTH"
3300 SETUU
3310 Y=9
3320 FOR I=1 TO 5
3330 MOVE L(I),Y
3340 Y=Y-2
3350 LORG 5
3360 LABEL "*"
3370 NEXT I
3380 COPY
3390 ! PRINT PAGE HEADING
3400 PRINT USING 3410
3410 IMAGE 3/,30X,"**EXPERIMENTAL DATA**"
3420 PRINT USING 3430 ; F$
3430 IMAGE 35X,"RUN#",X,6A
3440 PRINT USING 3450 ; D1$,T1$
3450 IMAGE 33X,8A,X,"-",X,4A
3460 PRINT USING 3470
```

```
3470 IMAGE 2/,34X,"FLUIDIZED BED"
3480 PRINT USING 3490
3490 IMAGE 31X,"TEMPERATURE PROFILE"
3500 !   READ BED SIZE
3510 Q1$=F$[1,2]
3520 IF Q1$="12" THEN 4590
3530 IF Q1$="10" THEN 4220
3540 IF Q1$="08" THEN 3890
3550 IF B9=1 THEN 3850
3560 !
3570 !    **DISPLAY 6 IN BED TEMP SNAPSHOT**
3580 !
3590 PRINT USING 3600
3600 IMAGE 2/,27X,"------------------------"
3610 PRINT USING 3620
3620 IMAGE 27X,"!",25X,"!"
3630 PRINT USING 3640
3640 IMAGE 27X,"!",25X,"!"
3650 PRINT USING 3660 ; T(56),T(53),T(50)
3660 IMAGE 27X,"!",X,DDD.DD,2X,DDD.DD,2X,DDD.DD,2X,"!"
3670 PRINT USING 3680
3680 IMAGE 27X,"!",25X,"!"
3690 PRINT USING 3700
3700 IMAGE 27X,"!",25X,"!"
3710 PRINT USING 3720 ; T(51)
3720 IMAGE 27X,"!",17X,DDD.DD,2X,"!"
3730 PRINT USING 3740
3740 IMAGE 27X,"!",25X,"!"
3750 PRINT USING 3760
3760 IMAGE 27X,"!",25X,"!"
3770 PRINT USING 3780 ; T(57),T(54),T(52)
3780 IMAGE 27X,"!",X,DDD.DD,2X,DDD.DD,2X,DDD.DD,2X,"!"
3790 PRINT USING 3800
3800 IMAGE 27X,"!",25X,"!"
3810 PRINT USING 3830
3820 PRINT USING 3840
3830 IMAGE 27X,"!",25X,"!"
3840 IMAGE 27X,"------------------------"
3850 ! CALCULATE AVERAGE BED TEMP
3860 B1=(T(50)+T(51)+T(52)+T(53)+T(54)+T(56)+T(57))/7
3870 GOTO 4900
3880 !
3890 !       **DISPLAY 8 IN BED TEMP SNAPSHOT**
3900 IF B9=1 THEN 4180
3910 !
3920 PRINT USING 3930
3930 IMAGE 2/,25X,"------------------------"
3940 PRINT USING 3950
3950 IMAGE 25X,"!",29X,"!"
3960 PRINT USING 3970
3970 IMAGE 25X,"!",29X,"!"
3980 PRINT USING 3990 ; T(56),T(53),T(50)
3990 IMAGE 25X,"!",5X,DDD.DD,2X,DDD.DD,2X,DDD.DD,2X,"!"
4000 PRINT USING 4010
4010 IMAGE 25X,"!",29X,"!"
4020 PRINT USING 4030
4030 IMAGE 25X,"!",29X,"!"
4040 PRINT USING 4050 ; T(51)
4050 IMAGE 25X,"!",21X,DDD.DD,2X,"!"
4060 PRINT USING 4070
```

```
4070 IMAGE 25X,"!",29X,"!"
4080 PRINT USING 4090
4090 IMAGE 25X,"!",29X,"!"
4100 PRINT USING 4110 ; T(57),T(54),T(52)
4110 IMAGE 25X,"!",5X,DDD.DD,2X,DDD.DD,2X,DDD.DD,2X,"!"
4120 PRINT USING 4130
4130 IMAGE 25X,"!",29X,"!"
4140 PRINT USING 4150
4150 IMAGE 25X,"!",29X,"!"
4160 PRINT USING 4170
4170 IMAGE 25X,"-------------------------------"
4180 ! CALCULATE AVERAGE BED TEMP
4190 B1=(T(50)+T(51)+T(52)+T(53)+T(54)+T(56)+T(57))/7
4200 GOTO 4900
4210 !
4220 !        ***DISPLAY 10 IN BED TEMP SNAPSHOT***
4230 IF B9=1 THEN 4550
4240 !
4250 PRINT USING 4260
4260 IMAGE 2/,23X,"-------------------------------"
4270 PRINT USING 4280
4280 IMAGE 23X,"!",33X,"!"
4290 PRINT USING 4300
4300 IMAGE 23X,"!",33X,"!"
4310 PRINT USING 4320 ; T(58),T(56),T(53),T(50)
4320 IMAGE 23X,"!",X,DDD.DD,2X,DDD.DD,2X,DDD.DD,2X,DDD.DD,2X,"!"
4330 PRINT USING 4340
4340 IMAGE 23X,"!",33X,"!"
4350 PRINT USING 4360
4360 IMAGE 23X,"!",33X,"!"
4370 PRINT USING 4380 ; T(59),T(51)
4380 IMAGE 23X,"!",X,DDD.DD,18X,DDD.DD,2X,"!"
4390 PRINT USING 4400
4400 IMAGE 23X,"!",33X,"!"
4410 PRINT USING 4420
4420 IMAGE 23X,"!",33X,"!"
4430 PRINT USING 4440 ; T(60),T(57),T(54),T(52)
4440 IMAGE 23X,"!",X,DDD.DD,2X,DDD.DD,2X,DDD.DD,2X,DDD.DD,2X,"!"
4450 PRINT USING 4460
4460 IMAGE 23X,"!",33X,"!"
4470 PRINT USING 4480
4480 IMAGE 23X,"!",33X,"!"
4490 PRINT USING 4500
4500 IMAGE 23X,"-------------------------------"
4510 PRINT USING 4520
4520 IMAGE /,15X,"NOTE:  TEMPERATURES SHOWN ARE IN DEGREES FAHRENHEIT"
4530 PRINT USING 4540
4540 IMAGE 21X,"AND ARE ARRANGED AS SEEN FROM ABOVE THE BED"
4550 ! CALCULATE AVERAGE BED TEMP
4560 B1=(T(50)+T(51)+T(52)+T(53)+T(54)+T(56)+T(57)+T(58)+T(59)+T(60))/10
4570 GOTO 4950
4580 !
4590 !     ***DISPLAY 12 IN BED TEMP SNAPSHOT***
4600 ! CALCULATE AVERAGE BED TEMP
4610 B1=(T(50)+T(51)+T(52)+T(53)+T(54)+T(56)+T(57)+T(58)+T(59)+T(60)+T(61)+T(62)+T(63))/13
4620 IF B9=1 THEN 4950
4630 !
4640 PRINT USING 4650
4650 IMAGE 2/,19X,"-------------------------------"
```

```
4660 PRINT USING 4670
4670 IMAGE 19X,":",41X,":"
4680 PRINT USING 4690
4690 IMAGE 19X," ",41X,":"
4700 PRINT USING 4710 : T(61),T(58),T(56),T(53),T(50)
4710 IMAGE 19X,":",X,DDD.DD,2X,DDD.DD,2X,DDD.DD,2X,DDD.DD,2X,DDD.DD,2X,":"
4720 PRINT USING 4730
4730 IMAGE 19X,":",41X,":"
4740 PRINT USING 4750
4750 IMAGE 19X,":",41X,":"
4760 PRINT USING 4770 : T(62),T(59),T(51)
4770 IMAGE 19X,":",X,DDD.DD,2X,DDD.DD,18X,DDD.DD,2X,":"
4780 PRINT USING 4790
4790 IMAGE 19X,":",41X,":"
4800 PRINT USING 4810
4810 IMAGE 19X,":",41X,":"
4820 PRINT USING 4830 : T(63),T(60),T(57),T(54),T(52)
4830 IMAGE 19X,":",X,DDD.DD,2X,DDD.DD,2X,DDD.DD,2X,DDD.DD,2X,DDD.DD,2X,":"
4840 PRINT USING 4850
4850 IMAGE 19X,":",41X,":"
4860 PRINT USING 4870
4870 IMAGE 19X,":",41X,":"
4880 PRINT USING 4890
4890 IMAGE 19X,"_____"
4900 IF B9=1 THEN 4960
4910 PRINT USING 4920
4920 IMAGE /,15X,"NOTE: TEMPERATURES SHOWN ARE IN DEGREES FAHRENHEIT"
4930 PRINT USING 4940
4940 IMAGE 21X,"AND ARE ARRANGED AS SEEN FROM ABOVE THE BED"
4950 !
4960 !      ***CALCULATE RESULTS**
4970 !
4980 ! CALCULATE AVERAGE AIR INLET TEMP
4990 P1=(T(47)+T(48)+T(49))/3
5000 ! CALCULATE AIR OUTLET TEMP
5010 P2=T(55)
5020 ! CALCULATE RH HEATER GUARD TEMP
5030 G1=(T(41)+T(42)+T(43))/3
5040 ! PRINT PAGE HEADING
5050 PRINT CHR$(12)
5060 PRINT USING 5070
5070 IMAGE 3/,30X,"**CALCULATED RESULTS**"
5080 PRINT USING 5090 ; F$
5090 IMAGE 35X,"RUN #",X,6A
5100 PRINT USING 5110 ; D1$,T1$
5110 IMAGE 33X,8A,X,"-",X,4A
5120 PRINT USING 5130
5130 IMAGE 2/,32X,"RIGHT-HAND HEATER"
5140 ! PRINT AVERAGE HEATER TEMPERATURE
5150 PRINT USING 5160 : H1
5160 IMAGE 2/,15X,"AVERAGE HEATER TEMPERATURE =",12X,DDD.DD,X,"DEG F"
5170 ! CALCULATE AND DISPLAY ELECTRICAL ENERGY INTO HEATER
5180 E1=V1*I1*3.4121
5190 ! CALCULATE AND DISPLAY LOSS OUT OF BACK OF HEATER
5200 G3=(H1-G1)*.1703163
5210 ! CALCULATE CONVECTION HEAT TRANSFER COEFFICIENT FROM GUARD TO ATMOSPHERE
5220 C1=G3/(.3472222*(G1-A1))
5230 ! CALCULATE LOSS FROM SIDES OF HEATER TO ATMOSPHERE
5240 S3=C1*.069444*(T(72)-A1)
5250 ! CALCULATE LOSS FROM TOP STRIP TO ATMOSPHERE
```

199

```
5250 U2=C1*.0208333*(T(68)-A1)
5260 ' CALCULATE LOSS FROM BOTTOM STRIP TO ATMOSPHERE
5270 S7=C1*.0208333*(T(71)-A1)
5280 ' CALCULATE TOTAL LOSSES TO ATMOSPHERE
5300 H4=G3+S3+U2+S7
5310 ' CALCULATE HEAT FLUX THRU RH PLATE
5320 P3=E1-H4
5330 V9=0
5340 ' CALCULATE SURFACE TEMPERATURE OF PLATE
5350 P5=H1-P3*.0208333/((232-.032*(H1-70))*.347222)
5360 ' CALCULATE HEAT TRANSFER COEFFICIENT FOR PLATE TO BED
5370 P7=P3/(.347222*(P5-B1))
5380 ' CALCULATE LOSS FROM SIDE STRIPS TO BED
5390 C3=P7*.069444*(T(73)-B1)
5400 ' CALCULATE LOSS FROM TOP STRIP TO BED
5410 S9=P7*.0208333*(T(69)-B1)
5420 ' CALCULATE LOSS FROM BOTTOM STRIP TO BED
5430 S5=P7*.0208333*(T(70)-B1)
5440 ' CALCULATE TOTAL LOSSES INTO BED
5450 H3=C3+S9+S5
5460 ' CALCULATE NEW HEAT FLUX THRU PLATE
5470 X9=E1-H4-H3
5480 V9=V9+1
5490 ! COMPARE NEW PLATE HEAT FLUX WITH OLD AND REPEAT CALCULATION IF DIFFERENCE
 EXCEEDS 0.01
5500 X8=ABS(P3-X9)
5510 IF X8>=.01 THEN P3=X9 @ GOTO 5340
5520 ' PRINT RESULTS
5530 PRINT USING 5540 ; P5
5540 IMAGE 15X,"AVERAGE PLATE SURFACE TEMPERATURE =",5X,DDD.DD,X,"DEG F"
5550 PRINT USING 5560 ; B1
5560 IMAGE 15X,"AVERAGE BED TEMPERATURE =",15X,DDD.DD,X,"DEG F"
5570 PRINT USING 5580 ; E1
5580 IMAGE 15X,"ELECTRICAL ENERGY INTO HEATER =",8X,DDD.DD,X,"BTU/HR"
5590 PRINT USING 5600 ; H4
5600 IMAGE 15X,"LOSS FROM HTR BACKING TO ATM =",9X,DDD.DD,X,"BTU/HR"
5610 PRINT USING 5620 ; C1
5620 IMAGE 15X,"h(HTR BACKING-ATM) =",8X,DDD.DD,X,"BTU/HR-FT^2-DEG F"
5630 PRINT USING 5640 ; H3
5640 IMAGE 15X,"LOSS FROM HTR PERIMETER TO BED =",7X,DDD.DD,X,"BTU/HR"
5650 PRINT USING 5660 ; P3
5660 IMAGE 15X,"HEAT FLUX THRU PLATE =",17X,DDD.DD,X,"BTU/HR"
5670 PRINT USING 5680 ; P7
5680 IMAGE 15X,"h(PLATE-BED) =",14X,DDD.DD,X,"BTU/HR-FT^2-DEG F"
5690 !
5700 !        CALCULATE AND DISPLAY RESULTS FOR LEFT-HAND HEATER
5710 !
5720 PRINT USING 5730
5730 IMAGE 2/,33X,"LEFT-HAND HEATER"
5740 ! CALCULATE LH HEATER GUARD TEMPERATURE AVE
5750 G2=(T(44)+T(45)+T(46))/3
5760 ! CALCULATE ELECTRICAL ENERGY INTO HEATER
5770 E2=V2*I2*3.4121
5780 ! CALCULATE LOSS FROM BACK OF HEATER TO ATMOSPHERE
5790 G4=(H2-G2)*.1703163
5800 ! CALCULATE CONVECTION HEAT TRANSFER COEFFICIENT FROM GUARD TO ATMOSHPERE
5810 C2=G4/(.347222*(G2-A1))
5820 ! CALCULATE LOSS FROM SIDES OF HEATER TO ATMOSPHERE
5830 S4=C2*.069444*(T(78)-A1)
5840 ! CALCULATE LOSS FROM TOP STRIP TO ATMOSPHERE
```

```
5850 U3=C2*.0208333*(T(78)-A1)
5860 ! CALCULATE LOSS FROM BOTTOM STRIP TO ATMOSPHERE
5870 S8=U3
5880 ! CALCULATE TOTAL LOSSES TO ATMOSPHERE
5890 H6=G4+S4+U3+S8
5900 ! CALCULATE HEAT FLUX THRU LH PLATE
5910 P4=E2-H6
5920 ! CALCULATE SURFACE TEMPERATURE OF PLATE
5930 P6=H2-P4*.0208333/((232-.032*(H2-70))*.347222)
5940 ! CALCULATE HEAT TRANSFER COEFFICIENT FOR PLATE TO BED
5950 P8=P4/(.347222*(P6-B1))
5960 ! CALCULATE LOSS FROM SIDE STRIPS TO BED
5970 C4=P8*.069444*(T(79)-B1)
5980 ! CALCULATE LOSS FROM TOP STRIP TO BED
5990 U1=P8*.0208333*(T(77)-B1)
6000 ! CALCULATE LOSS FROM BOTTOM STRIP TO BED
6010 S6=U1
6020 ! CALCULATE TOTAL LOSSES TO BED
6030 H5=C4+U1+S6
6040 ! CALCULATE NEW HEAT FLUX THRU PLATE
6050 X7=E2-H6-H5
6060 ! COMPARE NEW HEAT FLUX TO OLD AND REPEAT CALCULATION IF DIFFERENCE EXCEEDS
 0.01
6070 X6=ABS(P4-X7)
6080 IF X6>=.01 THEN P4=X7 @ GOTO 5920
6090 ! PRINT RESULTS
6100 PRINT USING 6110 ; H2
6110 IMAGE 2/.15X,"AVERAGE HEATER TEMPERATURE =",12X,DDD.DD,X,"DEG F"
6120 PRINT USING 6130 ; P6
6130 IMAGE 15X,"AVERAGE PLATE SURFACE TEMPERATURE =",5X,DDD.DD,X,"DEG F"
6140 PRINT USING 6150 ; B1
6150 IMAGE 15X,"AVERAGE BED TEMPERATURE =",15X,DDD.DD,X,"DEG G"
6160 PRINT USING 6170 ; E2
6170 IMAGE 15X,"ELECTRICAL ENERGY INTO HEATER =",8X,DDD.DD,X,"BTU/HR"
6180 PRINT USING 6190 ; H6
6190 IMAGE 15X,"LOSS FROM HTR BACKING TO ATM =",9X,DDD.DD,X,"BTU/HR"
6200 PRINT USING 6210 ; C2
6210 IMAGE 15X,"h(HTR BACKING-ATM) =",8X,DDD.DD,X,"BTU/HR-FT^2-DEG F"
6220 PRINT USING 6230 ; H5
6230 IMAGE 15X,"LOSS FROM HTR PERIMETER TO BED =",7X,DDD.DD,X,"BTU/HR"
6240 PRINT USING 6250 ; P4
6250 IMAGE 15X,"HEAT FLUX THRU PLATE =",17X,DDD.DD,X,"BTU/HR"
6260 PRINT USING 6270 ; P8
6270 IMAGE 15X,"h(PLATE-BED) =",14X,DDD.DD,X,"BTU/HR-FT^2-DEG F"
6280 !
6290 ! CALCULATE ENERGY BALANCE VALUES
6300 !
6310 ! CALCULATE AIR DENSITY
6320 X5=1.325*29.92/(P2+459.69)
6330 ! CALCULATE ENERGY CARRIED OUT OF BED BY AIR STREAM
6340 A5=F2*X5*60*.241*(P2-P1)
6350 ! CALCULATE LOSS THRU FRONT AND BACK FACES
6360 L6=.448*X*(T(75)-T(74))
6370 ! CALCULATE TOTAL ENERGY LEAVING BED
6380 A6=A5+L6
6390 ! CALCULATE TOTAL ENERGY INTO BED FROM RH HEATER
6400 B3=E1-H4
6410 ! CALCULATE TOTAL ENERGY INTO BED FROM LH HEATER
6420 B4=E2-H6
6430 ! CALCULATE TOTAL ENERGY INTO BED FROM ALL SOURCES
```

```
6440 A7=E3+B4
6450 ' CALCULATE CONVECTION HEAT TRANSFER COEFFICIENT F/B FACES-ATMOSPHERE
6460 D6=L6/(24*X)*(T(74)-41))
6470 ' CALCULATE CONVECTION HEAT TRANSFER COEFFICIENT F/B FACES-BED
6480 D7=L6/(24*X*(B1-T(75)))
6490 ' CALCULATE SUPERFICIAL VELOCITY
6500 U=F2/(6*X/144)/60
6510 ' CALCULATE SUPERFICIAL MASS VELOCITY
6520 G=U*X5*3600
6530 ' CALCULATE PARTICLE REYNOLDS NUMBER
6540 R=G/3600*.0009166667/.000000396/32.174
6550 ' PRINT RESULTS
6560 PRINT USING 6570
6570 IMAGE 2/,34X,"ENERGY BALANCE"
6580 PRINT USING 6590 ; P1
6590 IMAGE 2/,15X,"AVERAGE AIR INLET TEMPERATURE =",9X,DDD.DD,X,"DEG F"
6600 PRINT USING 6610 ; P2
6610 IMAGE 15X,"AIR OUTLET TEMPERATURE =",16X,DDD.DD,X,"DEG F"
6620 PRINT USING 6630 ; B1
6630 IMAGE 15X,"AVERAGE BED TEMPERATURE =",15X,DDD.DD,X,"DEG F"
6640 PRINT USING 6650 ; A5
6650 IMAGE 15X,"q(AIR OUT) =",27X,DDD.DD,X,"BTU/HR"
6660 PRINT USING 6670 ; L6
6670 IMAGE 15X,"q(LOSS F/R WALL) =",21X,DDD.DD,X,"BTU/HR"
6680 PRINT USING 6690 ; A6
6690 IMAGE 15X,"q(TOTAL OUT OF BED) =",18X,DDD.DD,X,"BTU/HR"
6700 PRINT USING 6710 ; A7
6710 IMAGE 15X,"q(TOTAL INTO BED) =",20X,DDD.DD,X,"BTU/HR"
6720 PRINT USING 6730 ; U
6730 IMAGE 15X,"SUPERFICIAL VELOCITY =",17X,DDD.DD,X,"FT/SEC"
6740 PRINT USING 6750 ; G
6750 IMAGE 15X,"SUPERFICIAL MASS VELOCITY =",7X,DDD.DD,X,"LBM/HR-FT^2"
6760 PRINT USING 6770 ; R
6770 IMAGE 15X,"PARTICLE REYNOLDS NUMBER =",20X,DDD.DD
6780 END
```

LIST OF REFERENCES

1. Othmer, D. F., *Fluidization*, Reinhold Publishing Corp., New York, 1956.

2. Morgan, M. C., *Particle Flow Cell Formation at Minimum Fluidization Flow Rates in a Rectangular Gas-Fluidized Bed*, M.S. Thesis, Naval Postgraduate School, Monterey, California, 1981.

3. Baerg, A., Klassen, J. and Gishler, P. E., "Heat Transfer in a Fluidized Solids Bed," *Canadian Journal of Research*, Volume 28, Sec. F, Nr. 8, August 1950.

4. Suo, M., "Calculated Methods for Performance of Heat Exchangers Enhanced with Fluidized Beds," *Letters in Heat and Mass Transfer*, Volume 3, pp. 555-564, 1976.

5. Beckwith, T. G., Buck, N. L., and Marangoni, R. D., *Mechanical Measurements 3rd Ed.*, Addison-Wesley Publishing Company, 1982.

6. Trivedi, R. C. and Rice, W. J., "Effect of Bed Depth, Air Velocity, and Distributor on Pressure Drop in an Air Fluidized Bed," *Chemical Engineering Progress Symposium Series Number 67*, Volume 62, pp. 57-63, 1966.

7. Filippovskii, N. F. and Baskakov, A. P., "Study of the Temperature Field Near a Hot Plate in a Fluidized Bed and of the Heat Transfer Between Them," *Inzhenerno-Fizichenskii Zhurnal*, Volume 22, No. 2, pp. 234-241, February 1972.

8. Depew, C. A. and Kramer, T. J., "Heat Transfer to Flowing Gas-Solid Mixtures," *Advances in Heat Transfer*, Volume 9, Academic Press, New York, pp. 113-180, 1973.

9. Sokolov, A. V., Baskakov, A. P., and Filippovskii, N. F., "Investigation of the Feasibility of Enhancing the Rate of Heat Transfer Between the Fluidized Bed and the Reactor Wall," *Fluid Mechanics-Soviet Research*, Volume 9, No. 5, September-October, 1980.

BIBLIOGRAPHY

Agarwal, O. P. and Storrow, J. A., "Pressure Drop in Fluidization Beds," Society of Chemical Industry, V. 15, pp. 278-286, April 1951.

Andeen, B. R. and Glicksman, L. R., Heat Transfer to Horizontal Tubes in Shallow Fluidized Beds, paper presented at ASME-AICHE Heat Transfer Conference, St. Louis, Missouri, 9-11 August 1976.

Baerg, A., Klassen, J. and Gishler, P. E., "Heat Transfer in Fluidized Solids Bed," Canadian Journal of Research Section F, V. 28, pp. 287-307, August 1950.

Bartholomew, R. N. and Katz, D. L., "Heat Transfer from Wall of Tube to Fluidized Bed," Chemical Engineering Progress Symposium Series Number 4, V. 48, pp. 3-10, 1952.

Baskakov, A. P., Berg, B. V., Vitt, O. K., Filippovskv, N. F., Kirakosyan, V. A., Goldobin, J. M., and Maskaev, V. K., "Heat Transfer to Objects Immersed in Fluidized Beds," Powder Technology, V. 8, No. 5/6, pp. 273-282, November/ December 1973.

Botterill, J. S. M., Fluid-Bed Heat Transfer, Academic Press, 1975.

Botterill, J. S. M. and Denloye, A. O. O., "Gas Convective Heat Transfer to Packed and Fluidized Beds," American Institute of Chemical Engineers Symposium Series Number 176, V. 74, pp. 194-202, 1978.

Botterill, J. S. M., Brundrett, G. W., Cain, G. L., and Elliot, D. E., "Heat Transfer to Gas Fluidized Beds," Chemical Engineering Progress Symposium Series Number 62, V. 62, pp. 1-6, 1966.

Botterill, J. S. M., Teoman, Y., and Yuregir, K. R., "Temperature Effects on the Heat Transfer Behavior of Gas Fluidized Beds," AICHE Symposium Series Number 208, V. 77, pp. 330-340, 1981.

Chen, J. C. and Withers, J. G., "An Experimental Study of Heat Transfer from Plain and Finned Tubes in Fluidized Beds," American Institute of Chemical Engineers Symposium Series Number 174, V. 74, pp. 327-333, 1978.

Chen, J. C., "Heat Transfer to Tubes in Fluidized Beds," American Society of Mechanical Engineers Paper Number 76-HT-75, 1976.

Davidson, J. F. and Harrison, D., Fluidized Particles, Cambridge University Press, 1963.

Decker, N. A. and Glicksman, L. R., "Conduction Heat Transfer at the Surface of Bodies immersed in Gas Fluidized Beds of Spherical Particles," AICHE Symposium Series Number 208, V. 77, pp. 341-349, 1981.

Dickey, B. R., Grimmett, E. S., and Kilian, D. C., "Waste Heat Disposal Via Fluidized Beds," Chemical Engineering Progress, V. 70, No. 1, pp. 60-64, January 1974.

Frantz, J. F., "Minimum Fluidization Velocities and Pressure Drop in Fluidized Beds," Chemical Engineering Progress Symposium Series Number 62, V. 62, pp. 21-31, 1966.

Gilliland, E. R. and Mason, E. A., "Gas and Solid Mixing in Fluidized Beds," Industrial and Engineering Chemistry, V. 41, No. 6, pp. 1191-1196, June 1949.

Gutfinger, C. and Abuaf, N., "Heat Transfer in Fluidized Beds," Advances in Heat Transfer, V. 10, pp. 167-218, Academic Press, 1974.

Huntsinger, R. C., "A Heat Transfer Correlation for Bed to Wall Heat Transfer in Gas-Solid Fluidized-Beds," Proceedings of South Dakota Academy of Science, V. 46, pp. 185-201, 1967.

Kato, K. and Wen, C. Y., "Gas-Particle Heat Transfer in Fixed and Fluidized Beds," Chemical Engineering Progress Symposium Series Number 105, V. 66, pp. 100-108, 1970.

Korolev, V. N. and Syromyatnikov, N. I., "The Fluid Mechanics and Structure of the Fluidized Beds in the Vicinity of a Plate Submerged in it," Heat Transfer-Soviet Research, V. 6, No. 4, July-August 1974.

Korolev, V. N. and Syromyatnikov, N. I., "Heat Transfer from a Surface with Artificial Roughness to a Fluidized Bed," Journal of Engineering Physics, V. 28, pp. 698-700, June 1975.

Kunii, D. and Levenspiel, O., <u>Fluidization Engineering</u>, Wiley, 1969.

Levenspiel, O. and Walton, J. S., "Bed-Wall Heat Transfer in Fluidized Systems, <u>Chemical Engineering Progress Symposium Series Number 9</u>, V. 50, pp. 1-13, 1954.

Maskayev, V. K. and Nosov, V. S., "Heat Transfer Between a Bed of Spherical Particles and the Fluidizing Gas Suspension," <u>Heat Transfer Soviet Research</u>, V. 7, No. 1, pp. 28-31, January/February 1975.

Mickley, H. S. and Fairbanks, D. F., "Mechanism of Heat Transfer to Fluidized Beds," <u>American Institute of Chemical Engineers Journal</u>; V. 1, pp. 374-384, September 1955.

Saxena, S. C., Grewal, N. S. and Gabor, J. D., "Heat Transfer Between a Gas Fluidized Bed and Immersed Tubes," <u>Advances in Heat Transfer</u>, V. 14, pp. 149-247, Academic Press, 1978.

Toomey, R. D. and Johnstone, H. F., "Heat Transfer Between Beds of Fluidized Solids and Walls of Container," <u>Chemical Engineering Progress Symposium Series Number 5</u>, V. 49, pp. 51-63, 1953.

Trivedi, R. C. and Rice, W. J., "Effect of Bed Depth, Air Velocity, and Distributor on Pressure Drop in an Air-Fluidized Bed," <u>Chemical Engineering Progress Symposium Series Number 67</u>, V. 62, pp. 57-63, 1966.

Vijayaraghavan, M. R. and Sastri, V. M. K., "Effect of Surface Roughness on Heat Transfer in Fluidized Beds," <u>Future Energy Production - Heat and Mass Transfer Processes</u>, V. 2, pp. 571-578, 1976.

INITIAL DISTRIBUTION LIST

No. Copies

1. Defense Technical Information Center   2
   Cameron Station
   Alexandria, Virginia 22314

2. Library, Code 0142   2
   Naval Postgraduate School
   Monterey, California 93943

3. Department Chairman, Code 69   1
   Department of Mechanical Engineering
   Naval Postgraduate School
   Monterey, California 93943

4. Professor P. F. Pucci, Code 69Pc   2
   Department of Mechanical Engineering
   Naval Postgraduate School
   Monterey, California 93943

5. Lieutenant David C. Neily, USN   1
   P. O. Box 247
   Bath, Maine 04530

END

FILMED

4-85

DTIC